

University of Groningen

Glucose metabolic patterns in neurodegenerative brain diseases

Teune, Laura

IMPORTANT NOTE: You are advised to consult the publisher's version (publisher's PDF) if you wish to cite from it. Please check the document version below.

Document Version

Publisher's PDF, also known as Version of record

Publication date:

2013

[Link to publication in University of Groningen/UMCG research database](#)

Citation for published version (APA):

Teune, L. K. (2013). Glucose metabolic patterns in neurodegenerative brain diseases Groningen: s.n.

Copyright

Other than for strictly personal use, it is not permitted to download or to forward/distribute the text or part of it without the consent of the author(s) and/or copyright holder(s), unless the work is under an open content license (like Creative Commons).

Take-down policy

If you believe that this document breaches copyright please contact us providing details, and we will remove access to the work immediately and investigate your claim.

Downloaded from the University of Groningen/UMCG research database (Pure): <http://www.rug.nl/research/portal>. For technical reasons the number of authors shown on this cover page is limited to 10 maximum.

Glucose Metabolic Patterns in Neurodegenerative Brain Diseases

This thesis was financially supported by the International Parkinson Foundation (IPF) and University Medical Center Groningen (UMCG).

Printing of this thesis was financially supported by the University of Groningen (RUG).

ISBN: 978-90-367-6121-5 (book)

ISBN: 978-90-367-6120-8 (e-pub)

© 2013, L.K. Teune

No parts of this thesis may be reproduced or transmitted in any forms or by any means, electronic or mechanical, including photocopying, recording or any information storage and retrieval system, without permission of the author

Lay-out: Peter van der Sijde, Groningen

Printed by: Telenga drukkerij, Groningen

RIJKSUNIVERSITEIT GRONINGEN

**Glucose Metabolic Patterns in
Neurodegenerative Brain Diseases**

Proefschrift

ter verkrijging van het doctoraat in de
Medische Wetenschappen
aan de Rijksuniversiteit Groningen
op gezag van de
Rector Magnificus, dr. E. Sterken,
in het openbaar te verdedigen op
woensdag 8 mei 2013
om 16.15 uur

door

Laura Klaaske Teune

geboren op 29 december 1981
te Amersfoort

Promotores: Prof. dr. K.L. Leenders
Prof. dr. R.A.J.O Dierckx

Copromotor: Dr. R.J. Renken

Beoordelingscommissie: Prof. dr. D. Eidelberg
Prof. dr. J. Booij
Prof. dr. J.B.T.M. Roerdink

Paranimfen:

Carolien Toxopeus
Jenny Teune

CONTENTS

CHAPTER 1: Introduction	9
CHAPTER 2: Molecular imaging in Parkinson's Disease <i>Neuromethods (2012): Molecular Imaging in the Neurosciences, Chapter 18: Parkinson's Disease</i>	11
CHAPTER 3: Typical cerebral metabolic brain patterns in neuro- degenerative brain diseases <i>Movement Disorders 2010; vol 25, No 14, pp 2395-2404</i>	25
CHAPTER 4: FDG-PET imaging in the differential diagnosis of neuro- degenerative brain diseases <i>Submitted</i>	37
CHAPTER 5: Validation of parkinsonian disease-related metabolic brain patterns <i>Movement Disorders, Epub ahead of print: 2013 Mar 11</i>	49
CHAPTER 6: The Alzheimer's Disease-related glucose metabolic brain pattern <i>Submitted</i>	57
CHAPTER 7: GLucose IMaging in ParkinsonismS	67
CHAPTER 8: Parkinson's Disease-related perfusion and glucose metabolic brain patterns identified with PCASL-MRI and FDG-PET imaging <i>Submitted</i>	75
CHAPTER 9: Discussion	83
Summary	95
References	99
Nederlandse Samenvatting	111
Dankwoord	117
Curriculum Vitae	121

CHAPTER 1

INTRODUCTION

INTRODUCTION

The differential diagnosis of neurodegenerative brain diseases may be difficult on clinical grounds only, especially at an early disease stage. Neurodegenerative brain diseases such as Parkinson's Disease (PD), multiple system atrophy (MSA), progressive supranuclear palsy (PSP), corticobasal degeneration (CBD), dementia with Lewy Bodies (DLB), Alzheimer's Disease (AD) and frontotemporal dementia (FTD) have overlapping features at presentation, while the typical clinical syndrome may become clear only at later disease stages. For this reason, there is increasing interest to use neuroimaging techniques in the hope to discover abnormal patterns of brain structure, energy consumption or network activity which are characteristic of such diseases. It is important to determine the relationship between biochemical brain activities and disease processes. Positron emission tomography (PET) tracer methods assess specific biochemical activities of the human brain and can be used to obtain insight in the pathophysiology of brain diseases.

In this thesis, the results of increasing possibilities of investigating resting brain activity in neurodegenerative brain diseases using [^{18}F]-fluorodeoxyglucose (FDG)-PET and magnetic resonance techniques imaging will be discussed.

The main objectives were to investigate differences in glucose metabolism and other image modalities in various neurodegenerative brain diseases using different analysis techniques. A general introduction and the results are presented in the following chapters.

OUTLINE OF THE THESIS

In chapter 2 an introduction on Parkinson's Disease and different molecular imaging techniques is given including the relevance for clinical practice.

In chapter 3 specific regional differences of brain metabolism applying [^{18}F]-fluoro- deoxyglucose positron emission tomography (FDG-PET), were identified in seven different neurodegenerative brain diseases when they were compared to a healthy control group using univariate methods. In chapter 4 the usefulness of FDG-PET in investigating different neurodegenerative brain diseases and applying more advanced multivariate analysis methods like the scaled subprofile model (SSM), principal component analysis (PCA) is reviewed.

In chapter 5 en 6 this SSM/PCA analysis technique is further investigated in our own population with parkinsonian syndromes in chapter 5 and in Alzheimer's Disease in chapter 6, suggesting that this method can assist in early differential diagnosis of neurodegenerative brain diseases. In chapter 7 the national database project GLucose IMaging in ParkinsonismS (GLIMPS) is introduced. The background, design and goal of the project will be outlined.

In chapter 8 a PD-related metabolic and perfusion covariance pattern is identified using perfusion-MRI and FDG-PET imaging and (dis)similarities in the disease-related pattern between perfusion and metabolism in PD patients is assessed.

Chapter 9 provides an overview, discussion and future perspectives of the disease-specific brain patterns presented in this thesis.

CHAPTER 2

MOLECULAR IMAGING IN PARKINSON'S DISEASE

L.K. TEUNE & K.L. LEENDERS

Department of Neurology, University Medical Center Groningen, the Netherlands

*Neuromethods (2012): Molecular Imaging in the Neurosciences,
Chapter 18: Parkinson's Disease*

ABSTRACT

Parkinson's disease (PD) is manifested clinically by bradykinesia, muscular rigidity and sometimes rest tremor. The pathological hallmark of PD is the degeneration of dopaminergic cells within the substantia nigra-pars compacta (SNc) and the subsequent dopamine depletion of the striatum. Besides disturbances in motor performance, other symptoms like REM sleep behavior disorder, autonomic dysfunction, depression and cognitive deficits can play a role in PD. It can be difficult to distinguish PD from other neurodegenerative brain diseases, but early diagnosis is important because prognosis and treatment options differ. Structural imaging is in general not helpful at early disease stages. However, nuclear imaging methods can display striatal dopaminergic activity in PD, but also visualize brain perfusion and glucose metabolism to show disease related changes in local brain function or identify cholinergic deficits associated with cognitive dysfunction. Presynaptic dopaminergic imaging either with PET or SPECT is the gold standard to differentiate between patients with parkinsonian features associated with and without a presynaptic dopaminergic deficit. In order to differentiate between PD and other neurodegenerative brain diseases, specific disease related metabolic patterns identified with FDG-PET imaging could be of great assistance in the individual clinical diagnosis.

1.1 INTRODUCTION

Parkinson's disease (PD) is the second most common neurodegenerative brain disease after Alzheimer's disease. The prevalence of PD in industrialized countries is generally estimated at 0.3% of the entire population and about 1% in people over 60 years of age. Reported standardized incidence rates of PD are 8-18 per 100000 person-years (de Lau and Breteler. 2006). PD is manifested clinically by bradykinesia, muscular rigidity and sometimes rest tremor. Supportive features of the diagnosis are a unilateral onset of motor symptoms, progressive disorder and a good and consistent levodopa response (Litvan, et al. 2003).

The basal ganglia, which consist of the striatum (putamen, caudate nucleus) together with globus pallidus pars interna and externa (GPI, GPe), substantia nigra pars reticulata and compacta (SNr, SNc) and subthalamic nucleus (STN) play a role in motor control, but they are also involved in various emotional and cognitive functions (Alexander, et al. 1986). The pathological hallmark of PD is the degeneration of dopaminergic neurons within the SNc and the subsequent dopamine depletion of the striatum, especially putamen. Via different types of dopamine receptors in the two populations of striatal output neurons, dopamine has an opposing effect on the basal ganglia output nuclei (GPI and SNr) and thus on the thalamic targets of these nuclei. Via the dopamine D1 receptor the activity of the direct pathway is facilitated. Activation of the direct pathway which projects directly to the GPI and SNr disinhibits the thalamus and thereby increases thalamocortical activity.

The indirect pathway passes first in a GABAergic way to the GPe and STN, and finally in an excitatory glutamatergic projection from the STN to the GPI, thereby inhibiting thalamocortical neurons.

The dopamine D2 receptor reduces transmission in the indirect pathway (DeLong and Wichmann. 2009, Groenewegen and van Dongen Y.C. 2008) (Figure 1). So although their synaptic actions are different, the dopaminergic inputs to the two pathways lead to the same effect, namely reducing inhibition of the thalamocortical neurons and thus facilitating movements initiated in the cortex. As mentioned before, in PD dopamine is depleted, which leads to reduced inhibition of the indirect pathway and reduced excitation of the direct pathway, with the net result of an excessive activation of the BG output nuclei and inhibition of thalamocortical and brainstem motor systems, leading to parkinsonian motor features (Bartels and Leenders. 2009, DeLong and Wichmann. 2007, Groenewegen. 2003).

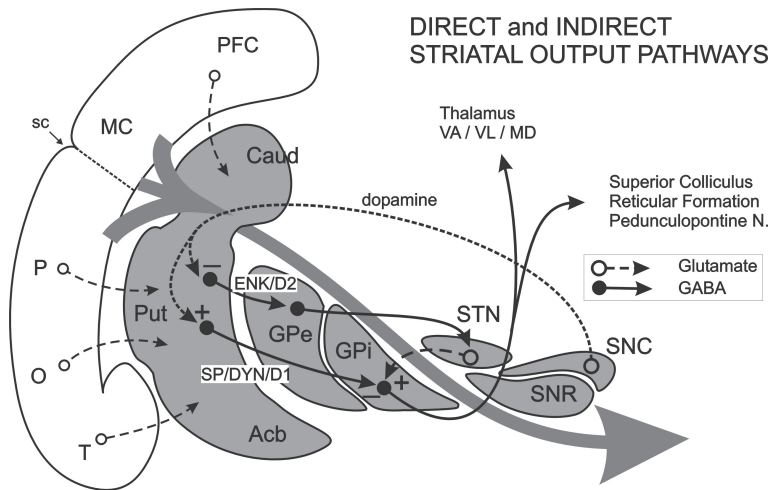


Figure 1: Direct and indirect striatal output pathways and the influence of dopamine on these routes, represented in a semi-sagittal scheme of the cerebral cortex and the basal ganglia. The direct pathway runs from the striatum to the internal segment of the globus pallidus and the substantia nigra pars reticulata. This pathway contains the peptides substance P (SP) and dynorphin (DYN) as well as the dopamine D1 receptor. The first link in the indirect striatal output pathway consists of the projections from the striatum to the external segment of the globus pallidus. These striatal neurons express the peptide enkephalin (ENK) and contain the dopamine D2 receptor. The subsequent steps in the indirect route are the pallido-subthalamic and the subthalamo-pallidal projections. Dopamine has opposite effects on the two striatal output routes, stimulating the direct pathway and inhibiting the indirect pathway. Abbreviations: Acb, nucleus accumbens; Caud, caudate nucleus; GPe, external segment of the globus pallidus; GPi, internal segment of the globus pallidus; MC, primary motor cortex; MD, mediodorsal thalamic nucleus; O, occipital cortex; P, parietal cortex; PFC, prefrontal cortex; Put, putamen; sc, central sulcus; SNC, substantia nigra pars compacta; SNR, substantia nigra pars reticulata; STN, subthalamic nucleus; T, temporal cortex; VA, ventral anterior thalamic nucleus; VL, ventral lateral thalamic nucleus. (Reproduced with permission: Wolters, van Laar, Berendse (eds.) Parkinsonism and Related Disorders. Amsterdam, VU University Press, 2008)

Especially at early disease stages in PD, levodopa administration is highly effective for improving motor symptoms. Long-term treatment is accompanied by fluctuations in motor performance and dyskinesias. As PD progresses, patients develop features which are difficult to treat, such as freezing episodes, autonomic dysfunction (orthostatic hypotension), depression and dementia (Horstink, et al. 2006). Deep brain stimulation (DBS) of the STN can be a highly effective and increasingly used treatment for selected patients in advanced disease stages. Reduction of motor fluctuations and disappearance of levodopa induced dyskinesias after dosage reduction of antiparkinsonian medication are the main features of this intervention (Asanuma, et al. 2006, Limousin, et al. 1998). Although the clinical progression and treatment response of PD is different from other parkinsonisms such as multiple system atrophy (MSA) and dementia with Lewy Bodies (DLB), they share the pathological feature of disturbed α -synuclein and are designated as α -synucleinopathies (Gilman, et al. 2008, McKeith. 2006). α -Synuclein is a structural protein localized primarily to synaptic terminals. In PD and DLB α -synuclein is a key component of the pathological hallmark Lewy Body and in MSA there are α -synuclein containing glial cytoplasmic inclusions (Galpern and Lang 2006). Other neurodegenerative brain diseases with parkinsonism like progressive supranuclear palsy (PSP) and corticobasal degeneration (CBD) show disturbances in tau protein handling and are designated as tauopathies (Galpern and Lang 2006, Litvan, et al. 1996, Mahapatra, et al. 2004). It can be difficult to distinguish PD from other neurodegenerative brain diseases, especially at early disease stages and on clinical grounds only. Structural imaging is in general not helpful at early disease stages. However, nuclear imaging methods can display striatal dopaminergic activity in PD, but also visualize brain perfusion and glucose metabolism to show disease related changes in local brain function or identify cholinergic deficits associated with cognitive dysfunction (Hilker, et al. 2005, Leenders, et al. 1984b). These techniques gain further insight in pathological mechanisms in PD and assist in the differential diagnosis of neurodegenerative brain diseases. In the next paragraphs, nuclear imaging methods which display different aspects of pathological mechanisms in PD will be further discussed.

2.2 STRIATAL DOPAMINERGIC IMAGING

Radiotracer neuroimaging techniques using positron emission tomography (PET) or single photon emission computed tomography (SPECT) can be helpful in visualizing and measuring striatal dopaminergic activity in patients with parkinsonism (Innis, et al. 1993, Leenders, et al. 1990). Dopamine synthesis takes place within the striatal nerve terminals of dopaminergic neurons (Figure 2). Radioactive tracers can bind to the dopamine transporter (DAT), the vesicular monoamine transporter 2 (VMAT2) and the enzyme aromatic-amino-acid decarboxylase (AADC). The dopaminergic system can be measured using different tracers (Piccini and Whone 2004).

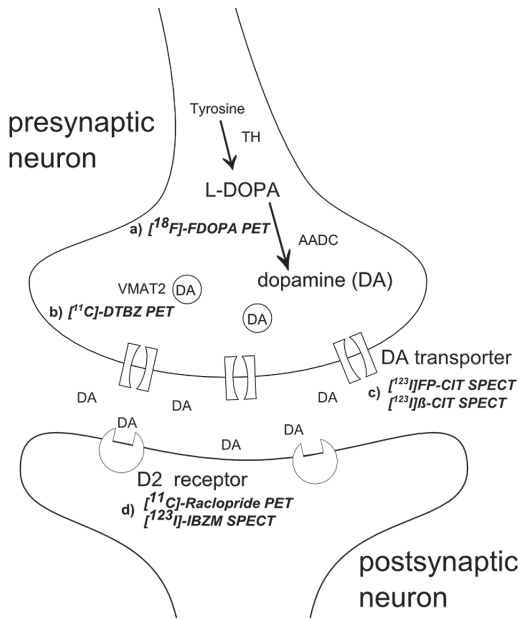


Figure 2: Schematic representation of dopamine synthesis within dopaminergic neurons, including sites of action of dopaminergic tracers (a,b,c,d). Dopamine (DA) synthesis takes place within the nerve terminals of dopaminergic neurons. Within the cytoplasm of dopaminergic terminals, tyrosine is first converted to L-3,4-dihydroxyphenylalanine (L-dopa) by the enzyme tyrosine hydroxylase (TH). L-dopa is then decarboxylated by aromatic amino acid decarboxylase (AADC) to DA. The synthesized DA enters the presynaptic vesicles via the vesicular monoamine transporter type 2 (VMAT 2). Following depolarization of nerve terminals, the stored DA is released into the synaptic cleft and interacts with pre- and postsynaptic DA receptors. a) The PET tracer $[^{18}\text{F}]$ FDOPA binds to AADC and estimates the rate of decarboxylation of FDOPA to $[^{18}\text{F}]$ -fluorodopamine by AADC which represents a function of striatal levodopa decarboxylase activity b) the PET tracer $[^{11}\text{C}]$ -DTBZ binds to VMAT2 and blocks the uptake of monoamines into the vesicles which

represents the integrity of striatal monoaminergic nerve terminal density. c) The SPECT tracers $[^{123}\text{I}]$ FP-CIT and $[^{123}\text{I}]$ β-CIT bind to the DA transporter which represents a marker of the integrity of presynaptic nigrostriatal dopamine terminals. d) The PET tracer $[^{11}\text{C}]$ -raclopride and the SPECT tracer $[^{123}\text{I}]$ -IBZM bind to the postsynaptic dopamine D2 receptor which allows the visualization of striatal dopamine D2 receptor binding.

2.2.1 Presynaptic dopaminergic imaging

The most widely used PET tracer to study the presynaptic dopaminergic system in PD is 6- $[^{18}\text{F}]$ fluoro-L-3, 4-dihydroxyphenylalanine (FDOPA). It estimates the rate of decarboxylation of FDOPA to $[^{18}\text{F}]$ -fluorodopamine by AADC, a function of striatal levodopa decarboxylase activity (Figure 2). $[^{18}\text{F}]$ FDOPA striatal uptake rate is correlated to cellular density of substantia nigra dopaminergic neurons and to striatal dopamine concentrations (Garnett, et al. 1983, Leenders, et al. 1986). In early PD patients, FDOPA uptake is diminished primarily in the posterior putamen and relatively preserved in the anterior putamen and caudate (Leenders, et al. 1990). In healthy controls the ratio of posterior putamen to caudate nucleus is about 1, whereas in early PD this ratio is around 0.6. In MSA patients, this gradient is not present and FDOPA uptake is reduced in both caudate and putamen (Otsuka, et al. 1996, Piccini and Whone. 2004). Nonetheless, subsequent studies have shown that caudate/putamen differences are not sufficiently reliable to categorize individual cases. Another method to distinguish healthy controls from PD patients is to look for asymmetrical uptake between the left and right putamen. In healthy controls there is no asymmetry and in early PD the putamen contralateral to the most affected diseased body side is more decreased (Leenders, et al. 1990)

Using SPECT and PET, the uptake of tracers with a high affinity for the dopamine transporter (DAT) can be measured (Booij, et al. 1997, Rinne, et al. 1995, Rinne, et al. 1999, Volkow, et al. 1995).

However, in clinical practice mostly SPECT is used, because this is more widely available. DATs are located on dopaminergic nerve endings and facilitate the release and reabsorption of dopamine in the presynaptic terminals and are modulated by the concentration of endogenous dopamine (Innis, et al. 1993). Striatal DAT binding represents a marker of the integrity of presynaptic nigrostriatal dopamine terminals and can be assessed with a variety of radio labeled cocaine derivatives, including [123 I]FP-CIT and [123 I] β -CIT-SPECT (Figure 2). Several studies have demonstrated that striatal β -CIT and FP-CIT uptake is reduced in patients with PD compared to controls (Booij, et al. 1997, Innis, et al. 1993, Rinne, et al. 1995, Tissingh, et al. 1998). Eshuis et al. demonstrated that both FP-CIT SPECT and F-DOPA-PET are equally able to distinguish patients with parkinsonian syndromes from healthy controls (Eshuis, et al. 2009)

Since the mid-1990s [11 C]-dihydrotetrabenazine (DTBZ)-PET has been used in humans to monitor the integrity of striatal monoaminergic nerve terminal density. However, nowadays it is only used in a few research centers in the world. Tetrabenazine binds to VMAT2 (a protein responsible for the uptake of monoamines into the synaptic vesicles) and blocks the uptake of monoamines into the vesicles (Figure 2) (Lee, et al. 2000). DTBZ has an advantage over FDOPA and DAT ligands in the sense that it has limited peripheral metabolism and is not subject to pharmacological regulation. However, the main disadvantage is the non-specificity for dopamine (Au, et al. 2005).

Presynaptic dopaminergic imaging can also be used to distinguish between PD patients and vascular parkinsonism or essential tremor, (Figure 3) (Gerschlager, et al. 2002, Marshall, et al. 2006) but not between PD and other parkinsonisms such as MSA and PSP (Piccini and Whone. 2004)

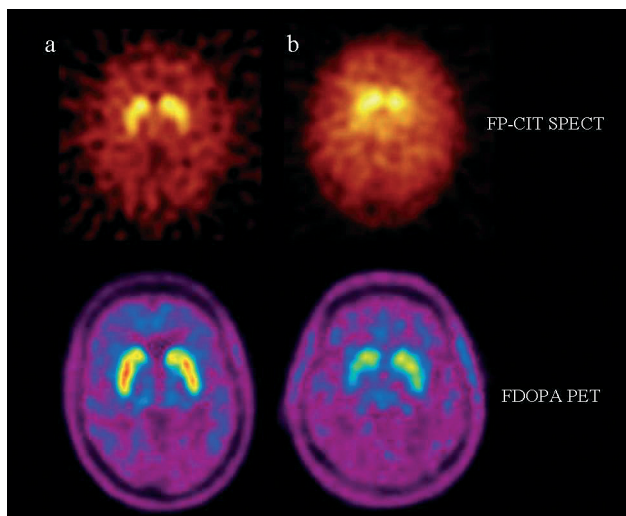


Figure 3: Example of individual patients with and without a presynaptic dopaminergic deficit using two different tracers. Above examples of a FP-CIT-SPECT scan and below examples of an FDOPA-PET scan. a) individual without a presynaptic dopaminergic deficit (essential tremor) and b) individual with a presynaptic dopaminergic deficit (patient with Parkinson's Disease).

Functional imaging of the presynaptic nigrostriatal dopaminergic system has been used to assess the rate of disease progression in PD (Brooks, et al. 2003, Hilker, et al. 2005, Pavese, et al. 2009, Pirker, et al. 2003, Rinne, et al. 1995, Volkow, et al. 1998). Using FDOPA-PET in PD, a more rapid decline in the putamen was observed than in the caudate nucleus, giving an overall annual rate of decline of 5.3% in the total striatum of FDOPA uptake (Morrish, et al. 1998).

There are also a number of longitudinal SPECT studies which report annual rates of progression between 5-8% of baseline in the striatum. However, DAT-SPECT does not have the anatomical resolution to detect subregional differences in rate of progression (Au, et al. 2005, Pirker, et al. 2003). Now that there is a marker of disease progression, it is also possible to study treatment interventions that may have an effect on disease progression. The CALM-PD study compared the early use of pramipexole with levodopa, using β -CIT-SPECT as an imaging modality, (Parkinson Study Group 2000) the REAL-PET study compared ropinirole vs levodopa in *de novo* PD patients and used FDOPA-PET as a marker to assess disease progression (Whone, et al. 2003) and in the ELLDOPA trial the effects of levodopa on clinical progression were studied using β -CIT-SPECT as an imaging modality (Fahn 2005). Furthermore, a few studies have been conducted to assess the effects of human embryonic dopaminergic tissue transplantation and they used FDOPA-PET to monitor imaging changes (Ma, et al. 2010b). Overall the results of these studies show no clear effect of dopamine agonist treatment on disease progression as indicated by striatal dopaminergic features. The radiotracer methods applied in these studies are adequate, but simply an effective influence of the drug treatment on neuronal degeneration has been absent. On the other hand, if indeed a change of local striatal dopaminergic activity takes place as is the case after implantation of embryonic dopaminergic cells, then the applied radiotracer methods do indeed reflect these changes.

Also it has been investigated whether DBS treatment of parkinsonian patients would halt or slow further progression of the disease since STN-DBS is expected to reduce the glutamatergic firing of the STN. One study investigated this but did not see an alteration of striatal FDOPA uptake in PD patients after implantation (Hilker, et al. 2005).

2.2.2 Postsynaptic dopaminergic imaging

One difference in striatal pathology between PD and other diseases like MSA and PSP can be evaluated by investigation of the postsynaptic dopamine D2 receptor. Examples of receptor binding ligands include [^{11}C]-raclopride for PET imaging and [^{123}I] iodobenzamide (IBZM) for SPECT imaging (Figure 2) (Farde, et al. 1985, Kung, et al. 1990). Several studies have shown that D2 receptors may be up-regulated in early untreated PD patients, but in later disease stages there is a reduction in striatal D2 receptor binding (Antonini, et al. 1997, Brooks, et al. 1992). Neurons containing dopamine 2 receptors are especially affected in patients with MSA and PSP (Brooks, et al. 1992, Schwarz, et al. 1993, Schwarz, et al. 1994). The differential diagnosis between PD and MSA or PSP using postsynaptic dopaminergic imaging is difficult because D2 receptor binding also declines in PD at later disease stages. Therefore [^{11}C]-raclopride-PET and IBZM-SPECT are not recommended

to use for this indication. In more recent studies [11C]-raclopride is used to study medication effects in PD (Pavese, et al. 2006)

2.3 REGIONAL BLOOD FLOW AND GLUCOSE METABOLISM

In addition to changes in striatal dopaminergic activity, nuclear imaging techniques can be used to visualize disease-related changes in local brain function using tracers for regional brain perfusion and glucose metabolism. Sokoloff et al. were the first to report that under physiological steady state conditions, cerebral blood flow (CBF) is coupled to the level of cerebral oxygen (CMRO₂) and glucose consumption (CMR_{glc}) (Sokoloff, et al. 1977). Furthermore, they established that functional activity in specific components of the central nervous system, is closely coupled to the local rate of energy metabolism. Stimulation of functional activity increases the local rate of glucose utilization and reduced functional activity lowers it (Sokoloff. 1977). There are different PET and SPECT tracers to visualize blood flow, oxygen and glucose consumption which will be discussed.

2.3.1 Brain perfusion

The distribution for regional cerebral blood flow (rCBF) and regional oxygen metabolism (rCMRO₂) is related to neuronal and synaptic functional activity. PET provides the opportunity to make regional measurements of rCBF and rCMRO₂. Frackowiak et al. applied the PET tracers which were labeled with ¹⁵O to measure regional blood flow and oxygen metabolism (Frackowiak, et al. 1980) Since then, this tracer has been used to study brain perfusion in different clinical conditions. Leenders et al. measured rCBF and rCMRO₂ in PD patients. They showed an increase of regional blood flow and oxygen metabolism in the basal ganglia of the affected hemisphere in PD patients with predominantly unilateral disease (Leenders, et al. 1984a). Furthermore, they studied the effect of levodopa administration on cerebral blood flow and they found a diffuse increase in rCBF after levodopa administration without stimulation of regional oxygen utilization. The effect of levodopa on rCBF did not correlate with the degree of clinical improvement and they suggest that the rise in rCBF is caused by vasodilatation due to a direct effect of levodopa on blood vessels (Leenders, et al. 1985). In the 80's, a SPECT tracer, ⁹⁹Tcm-hexamethylpropyleneamine oxime (⁹⁹Tcm-HM-PAO), was also developed to detect cerebral blood flow with SPECT-imaging (Holmes, et al. 1985, Leonard, et al. 1986). Nowadays, measurements of rCBF with PET or SPECT are not used in clinical practice, because it is a demanding and time-consuming procedure. For research purposes, the upcoming of functional magnetical resonance imaging (fMRI) in the 1990s, which measures the hemodynamic response function has made it easier to study changes in cerebral blood flow for example in task specific activation studies. Changes in Blood Oxygen Level Dependence (BOLD), which is the MRI contrast of blood deoxyhemoglobin, are well correlated to changes in blood flow (Kwong, et al. 1992). Since blood flow and brain metabolism are closely coupled, brain metabolism is measured with FDG-PET imaging in clinical practice to study regional differences in metabolism between diseases (see below).

2.3.2 Brain glucose metabolism

The PET tracer [18F]-fluorodeoxyglucose (FDG) allows the measurement of cerebral metabolic rate of glucose (CMRglc). FDG is a glucose analogue with physiological aspects almost identical to glucose. It is transported from the blood to the brain by a carrier-mediated diffusion mechanism. Glucose is then phosphorylated to glucose-6-PO₄, and FDG to FDG-6-PO₄, catalyzed by hexokinase. While glucose phosphate is metabolized further to carbon dioxide and water, FDG phosphate is not a substrate for any enzyme known to be present in brain tissue and is trapped for some longer time and therefore a useful imaging marker. Reivich et al. were the first to study FDG-PET in man (Reivich, et al. 1979)

Since then, FDG-PET imaging has been used to identify characteristic disease-related patterns of regional glucose metabolism in patients with parkinsonism (Eckert, et al. 2005, Juh, et al. 2004, Teune, et al. 2010) (Figure 4).



Figure 4: SPM (t) maps of decreased metabolic activity were overlaid on a T1 MR template thresholded at $P < 0.001$ with cluster cutoff of 20 voxels. Patient groups are indicated on the vertical axis and on the horizontal axis, seven transversal slices through the brain are shown. PD = Parkinson's Disease: Decreased metabolic activity in the contralateral to the most affected body side parieto-occipital and frontal regions; MSA = Multiple system atrophy: Decreased metabolic activity in bilateral putamen and cerebellum; PSP = progressive supranuclear palsy: decreased metabolic activity in the prefrontal cortex, caudate nucleus, thalamus and mesencephalon; CBD = corticobasal degeneration: Decreased metabolic activity in the contralateral to the most affected body side cortical regions; DLB = dementia with Lewy Bodies: Decreased metabolic activity in the occipital and parieto-temporal regions. Adapted from: Teune LK et al. Typical Cerebral Metabolic Patterns, Movement Disorders. (2010) 25, 2395-2404

A characteristic metabolic pattern is identified in PD patients using principal component analysis showing regionally relatively increased metabolism in the globus pallidus and putamen, thalamus, pons and cerebellum and relatively decreased metabolism in the lateral frontal, premotor and parietal association areas. Ma et al. reproduced this Parkinson disease-related covariance pattern (PDRP) using H215O PET scanning (Eidelberg, et al. 1994, Ma, et al. 2007a). Increased striatal FDG uptake in PD patients is explained by loss of inhibitory nigrostriatal dopaminergic input, leading to functional overactivation of the putamen (Eggers, et al. 2009). Network expression in Parkinson's disease also increases linearly with disease progression (Huang, et al. 2007c). FDG-PET studies have also been performed to study effects of treatment and their relations with neural network pathophysiology. A study using an automated approach for quantifying network activity in single scans, found that both STN DBS and levodopa therapy were associated with downward modulation of the PDRP. Furthermore, brain regions like the premotor cortex and post parietal areas which are reduced in untreated PD, rise after treatment with levodopa or STN DBS, presumably by increasing excitatory afferent activity from the thalamus (Asanuma, et al. 2006). Furthermore, STN DBS was found to activate glucose metabolism in the frontal limbic and associative territory (Hilker, et al. 2004). Hilker et al. investigated the metabolic effects of high frequency DBS of the STN and they conclude that STN-DBS excites the subthalamic area and the directly connected pallidum via an increased neuronal output originating from the stimulation site (Hilker, et al. 2008). Recently, newly developed high resolution PET scanners with a FWHM of 2.5 mm permits the determination of regional FDG uptake in small subcortical nuclei, showing a significantly higher CMRGlC in PD patients compared to controls bilaterally in the basal ganglia output nuclei (pallidum and substantia nigra) and unilateral in the caudate and putamen (Eggers, et al. 2009).

Several studies have used FDG-PET imaging to differentiate PD from other diseases (Eckert and Eidelberg. 2004, Klein, et al. 2010, Klein, et al. 2005, Otsuka, et al. 1997, Yong, et al. 2007). Eckert et al. demonstrated disease-related metabolic patterns for MSA and PSP. The MSA-related pattern was characterized by decreased metabolism in putamen and cerebellum and the PSP-related pattern consisted of mediofrontal hypometabolism and hypometabolism of the brainstem (Eckert, et al. 2008). Using an automated image-based classification procedure, individual patients could be differentiated in PD, MSA and PSP categories with high specificity (Tang, et al. 2010b). In contrast to the cognitive problems that are related to PD itself, in PD patients with dementia (PDD), and DLB patients compared to controls, decreased metabolism was found in parietal, frontal, anterior cingulate and in occipital areas. The metabolic deficits were more extensive in DLB than in PDD. In comparison with PD patients, those with DLB and PDD showed greater metabolic deficits in parietal and frontal regions (Yong, et al. 2007).

For clinical practice disease specific patterns as found in PD and other neurodegenerative diseases with parkinsonism can be a valuable aid in the differential diagnosis. One should realize that the patterns show relative metabolic increases and decreases and not absolute values of glucose consumption. In PD however, mostly cortical decreases are not clear on visual inspection

and sometimes an accentuated striatum is shown. In contrast, metabolic decreases in other parkinsonisms can be detected with visual inspection (Figure 5).

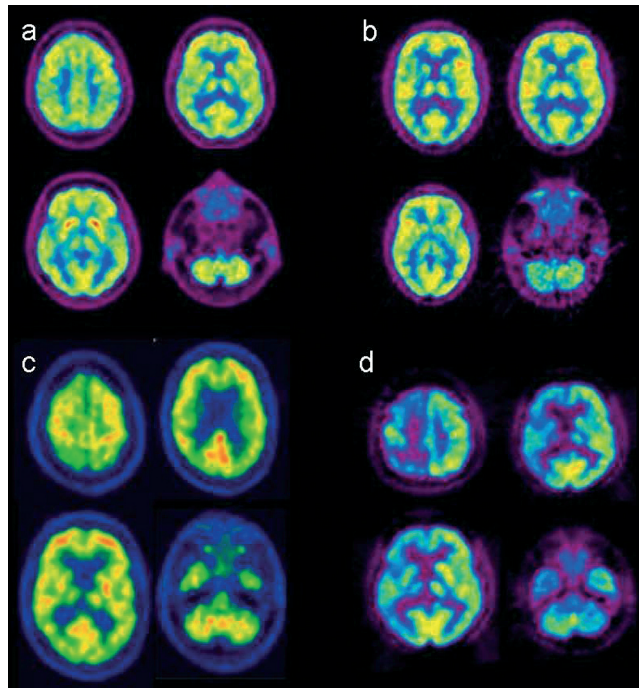


Figure 5: Individual FDG-PET scans of 4 patients. a) Patient with Parkinson's Disease: normal FDG uptake in the cortical regions, normal or slightly elevated uptake in the putamen; b) patient with multiple system atrophy: decreased FDG uptake in the cerebellum and striatum; c) patient with progressive supranuclear palsy: decreased FDG uptake in the mediofrontal regions; d) patient with corticobasal degeneration: contralateral to the most affected body side, decreased FDG uptake in the all cortical regions and in the striatum and thalamus, cerebellar diaschisis.

2.4 OTHER TRACERS

2.4.1 Cholinergic system

Many patients with PD develop mental dysfunction ranging from subtle cognitive deficits to severe dementia (PDD). Cholinergic deficits probably play an important role in the pathogenesis of PD-associated dementia. N-[¹¹C]-methyl-4-piperidyl acetate (MP4a) is an established radiotracer for quantification of cerebral acetylcholinesterase activity. It has been used to assess deficiency of cholinergic innervation in AD, PSP but also in PD, PDD and DLB, and for the assessment of the pharmacological effect of cholinesterase inhibitors. Hilker et al. (Hilker, et al. 2005) studied patients with PD and PDD with combined PET [¹¹C]-MP4A and [¹⁸F]-fluorodopa (FDOPA)-PET for evaluation of cholinergic and dopaminergic transmitter changes. They conclude that while non-demented PD patients had a moderate cholinergic dysfunction, patients with PDD presented with a severe

cholinergic deficit in various cortical regions. In a recent study of Klein et al. (Klein, et al. 2010), PDD and DLB patients were compared with PD patients without dementia and they found in PDD as well as DLB a marked MP4A and FDG reduction in cortical areas compared to PD. Both studies did not find a significant difference in cortical and striatal FDOPA uptake between PD and PDD/DLB patients suggesting that cholinergic dysfunction seems to be crucial for the development of dementia in addition to the dopamine system related motor symptoms. Clinically, these data support the notion that cognitive function deteriorates in some predisposed patients with PD after administration of anticholinergic drugs (Ehrt, et al. 2010). Furthermore, they support the effect of cholinesterase inhibitors in PDD on cognition as has been shown in a placebo controlled trial with rivastigmine (Emre, et al. 2007). Recently, an 18F-labeled derivative of 11CMP4A, [18F] fluoroethylpiperidin-4ylmethyl acetate ([18F] FEP-4MA) showed desirable properties for quantification of cerebral AChE activity by PET. This could potentially make measurement of AChE more widely applicable because of the longer half life of 18F than 11C, making it possible to transport the tracer from a center equipped with a cyclotron to other PET centers (Kikuchi, et al. 2010).

2.4.2 Neuroinflammation

[11C]-PK11195 PET, a peripheral benzodiazepine receptor has been used for *in vivo* brain imaging of microglia activation in PD patients. An increased number of activated microglia has been found in the SN of PD brains and animal studies have suggested the relevance of microglia activation to cell death (Teismann, et al. 2003). Ouchi et al. studied microglial activation using [11C]-PK11195 PET in PD patients and found increases in midbrain binding potential of PK11195 correlated inversely with a dopamine transporter marker in putamen and correlated positively with clinical motor scores (Ouchi, et al. 2005). In contrast, Gerhard et al. found increased PK binding in the pons, basal ganglia and frontal, temporal cortical regions in PD patients which did not correlate with clinical severity of putamen 18FDOPA uptake. They suggested that microglia are activated early in the disease course and levels then remain relatively static (Gerhard, et al. 2006). This increased inflammation in basal ganglia and midbrain could not be reproduced by Bartels et al. (Bartels, et al. 2010). They found variable results with different methods of analysis. Therefore they conclude that tracers with higher levels of specific binding in brain and better capacity to quantify peripheral benzodiazepine receptor expression should be developed, because radiotracer studies that can monitor neuroinflammatory processes within the brain will be of great value for the translation of potentially effective treatments.

2.4.3 Adenosine system

Adenosine is an endogenous inhibitory neurotransmitter and modulates functions within the central nervous system. Adenosine A1 receptors (A1Rs) are widely distributed throughout the brain but adenosine A2A receptors (A2ARs) are highly concentrated within the basal ganglia (Fredholm and Svenningsson. 2003, Jarvis, et al. 1989). Adenosine A2A receptors have a selective localization to the basal ganglia and specifically to the GABAergic neurons of the indirect pathway which also

expresses the D2 dopamine receptor. This offers an opportunity to modulate the output from the striatum and A2a antagonists could influence motor function in experimental models in PD suggesting that it might be effective as a symptomatic treatment in humans without provoking marked dyskinesias (Jenner, et al. 2009). Mishina et al. investigated the distribution of the A2Rs in humans using PET and [7-methyl-11C (E)-8-(3, 4, 5-trimethoxystyryl)-1, 3, 7-trimethylxanthine ([11C] TMSX). The binding potential was largest in anterior and posterior putamen and next largest in caudate nucleus and thalamus and small in cerebral cortex (Mishina, et al. 2007). [11C] TMSX-PET is a promising PET ligand which can be used to detect differences in striatal adenosine receptor binding in PD patients compared to controls.

2.4.4 Cardiac sympathetic denervation

Orthostatic hypotension is an early indicator of MSA, but may also occur in advanced stages of PD. The underlying pathology of orthostatic hypotension is different in both diseases. In PD, orthostatic hypotension is caused primarily by postganglionic sympathetic dysfunction. In MSA there is predominantly central and preganglionic degeneration. [123I]-metaiodobenzylguanidine (MIBG) binding in SPECT scanning visualizes catecholaminergic terminals and can be used to detect cardiac sympathetic degeneration. Reduced uptake of MIBG binding represents postganglionic cardiac sympathetic dysfunction which is the case in PD (Nakajima, et al. 2008). Sympathetic cardiac uptake in MSA patients is unaffected (Braune, et al. 1999). However, studies are not consistent in all cases. Some studies report that not all of the parameters of MIBG uptake could discriminate PD from MSA and is therefore in early PD patients of limited value (Chung, et al. 2009, Ishibashi, et al. 2010)

CONCLUSIONS

Presynaptic dopaminergic imaging either with PET or SPECT is the gold standard to differentiate between patients with parkinsonian features associated with and without a presynaptic dopaminergic deficit. In addition, in order to differentiate between PD and other neurodegenerative brain diseases, specific disease related metabolic patterns identified with FDG-PET imaging could be of great assistance in the individual clinical diagnosis. Furthermore there are some promising nuclear imaging techniques identifying the cholinergic and adenosine system which in the future can assist in gaining further insight in pathophysiological mechanisms in PD.

CHAPTER 3

TYPICAL CEREBRAL METABOLIC BRAIN PATTERNS IN NEURODEGENERATIVE BRAIN DISEASES

L.K. TEUNE¹, A.L. BARTELS¹, B.M. DE JONG¹, A.T.M. WILLEMSSEN², S.A. ESHUIS²,
J.J. DE VRIES¹, J.C.H. VAN OOSTROM¹ AND K.L. LEENDERS¹

*¹Department of Neurology and ²Nuclear Medicine & Molecular Imaging,
University Medical Center Groningen, the Netherlands*

ABSTRACT

The differential diagnosis of neurodegenerative brain diseases on clinical grounds is difficult, especially at an early disease stage. Several studies have found specific regional differences of brain metabolism applying [¹⁸F]-fluoro-deoxyglucose positron emission tomography (FDG-PET), suggesting that this method can assist in early differential diagnosis of neurodegenerative brain diseases.

We have studied patients who had an FDG-PET scan on clinical grounds at an early disease stage and included those with a retrospectively confirmed diagnosis according to strictly defined clinical research criteria. 96 patients could be included of which 20 patients with Parkinson's disease (PD), 21 multiple system atrophy (MSA), 17 progressive supranuclear palsy (PSP), 10 corticobasal degeneration (CBD), 6 dementia with lewy bodies (DLB), 15 Alzheimer's disease (AD) and 7 frontotemporal dementia (FTD). FDG PET images of each patient group were analysed and compared to 18 healthy controls using Statistical Parametric Mapping (SPM5).

Disease-specific patterns of relatively decreased metabolic activity were found in PD (contralateral parieto-occipital and frontal regions), MSA (bilateral putamen and cerebellar hemispheres), PSP (prefrontal cortex and nucleus caudatus, thalamus and mesencephalon), CBD (contralateral cortical regions), DLB (occipital and parieto-temporal regions), AD (parieto-temporal regions), and FTD (fronto-temporal regions).

The integrated method addressing a spectrum of various neurodegenerative brain diseases provided means to discriminate patient groups also at early disease stages. Clinical follow up enabled appropriate patient inclusion. This implies that an early diagnosis in individual patients can be made by comparing each subject's metabolic findings with a complete database of specific disease-related patterns.

3.1 INTRODUCTION

The differential diagnosis of neurodegenerative brain diseases may be difficult on clinical grounds only. It is important to diagnose these patients early, because prognosis and treatment options differ between neurodegenerative brain diseases. Moreover, accurate differential diagnosis is important to reduce heterogeneity in pharmacological trials (Litvan et al. 2003). Several neurodegenerative diseases have overlapping features at presentation, while the typical clinical syndrome may become clear only at later disease stages.

Neurodegenerative brain diseases that present with parkinsonian features are Parkinson's disease (PD) (Litvan et al. 2003), multiple system atrophy (MSA) (Gilman et al. 2008), progressive supranuclear palsy (PSP) (Litvan et al. 1996), corticobasal degeneration (CBD) (Mahapatra et al. 2004) and dementia with Lewy Bodies (DLB) (McKeith et al. 2005). Although the pathophysiology and clinical progression of these diseases are different, PD, MSA and DLB share the pathological feature of disturbed α -synuclein and are designated as α -synucleinopathies (Galpern and Lang. 2006, Gilman et al. 2008). Other neurodegenerative brain diseases with parkinsonism show disturbances in tau protein handling. PSP and CBD are tauopathies, which points at similarities with frontotemporal dementia (FTD) (McKhann et al. 2001) and also overlap in pathology with Alzheimer's disease (AD) (Galpern and Lang. 2006, McKhann et al. 1984).

The establishment of an exact diagnosis of neurodegenerative brain diseases would benefit from additional tests. Structural imaging is in general not helpful, although specific abnormalities can be identified at later disease stages. Functional imaging of cerebral glucose metabolism with [18 F]-fluorodeoxyglucose positron emission tomography (FDG-PET) provides an index for regional neuronal activity. This method has shown differences in regional distribution of cerebral glucose metabolism for each neurodegenerative brain disease, suggesting that it can assist in early differential diagnosis (Diehl-Schmid et al. 2007, Eckert et al. 2005, Eckert et al. 2008, Foster et al. 2007, Herholz et al. 2002, Jeong et al. 2005, Juh et al. 2004, Klein et al. 2005, Ma et al. 2007a, Minoshima et al. 2001, Mosconi et al. 2008, Silverman et al. 2001, Yong et al. 2007). A problem with the general assessment of these results is, however, the use of different analysing techniques of regional cerebral FDG uptake and inclusion of patients with a more advanced clinical disease stage. Before a generic approach and diagnostic consensus for all neurodegenerative brain diseases can be determined, an overview of specific disease-related metabolic patterns for parkinsonisms and dementias analysed using the same image statistical method needs first to be established. The application of disease-specific metabolic patterns as a reference array for comparison with a single patient dataset will in the end be helpful in clinical practice to diagnose individual patients at early disease stages.

The objective of the present study was to identify distinctive cerebral metabolic patterns at early disease stages, in patients with retrospectively confirmed diagnosis of PD, MSA, PSP, CBD, DLB, AD and FTD as compared to healthy controls. Statistical Parametric Mapping (SPM5) and global mean normalization was used for all comparisons.

3.2 METHODS

Patients

All medical records of patients over the past ten years (Jan 1998 till Dec 2008) who were referred for FDG-PET imaging to assist in clinical diagnosis of a neurodegenerative brain disease were reviewed. At the time of referral for imaging, clinical diagnosis of most patients was uncertain. Disease progression over time, after the FDG-PET scan had been performed, allowed an exact diagnosis at a later stage. We were able to include patients with a clear retrospective diagnosis according to established clinical research criteria which were applied by the investigators LT and KL with a follow up time in PD (Litvan et al. 2003) of 4 ± 3 (mean \pm SD in years), MSA (Gilman et al. 2008) (2 ± 1), PSP (Litvan et al. 1996) (3 ± 2), CBD (Mahapatra et al. 2004) (3 ± 1), DLB (McKeith et al. 2005) (2 ± 1), AD (McKhann et al. 1984) (3 ± 2) and FTD (McKhann et al. 2001) (3 ± 1). In total 96 patients were included, of which 20 patients with PD (age 63 ± 9 y) with a Disease Duration (DD) at scanning of 3 ± 2 years. Of the 20 PD patients, 6 were predominantly affected on the right body side (R) and 14 were left body sided affected (L). 13 probable MSA-P, one probable MSA-C and 7 possible MSA-P patients (age 64 ± 10 ; DD 4 ± 2) could be included. Furthermore, 13 probable and 4 possible PSP patients (age 68 ± 8 ; DD 2 ± 1), 10 CBD patients of whom 7 were right body sided affected and 3 left body sided (age 69 ± 9 ; DD 2 ± 1 , 7R/3L) and 6 DLB patients (age 71 ± 7 ; DD 3 ± 2) were included. The diagnosis of all 15 included AD patients (age 65 ± 10 ; DD 3 ± 2) was corroborated by neuropsychological examination. At last 7 FTD patients were included (61 ± 10 ; DD 3 ± 2). As a control group, 18 healthy controls out of an existing database (age 56 ± 14) were included in the study.

FDG PET data acquisition and image analysis

Patients underwent a static FDG PET scan under standard resting conditions with the eyes closed. FDG-PET scans were acquired in a 3D mode after injection of approximately 200 MBq FDG using a Siemens ECAT HR+ PET scanner. Patient groups were analysed using SPM5 (Statistical Parametric Mapping; Functional Imaging Laboratory (FIL), Wellcome Department of Imaging Neuroscience, London, UK) running on Matlab 7.1 (R14, Mathworks Inc.) All reconstructed FDG-PET images were spatially normalised onto the dimensions of a standard brain (Montreal Neurological Institute; MNI) with voxel sizes of the written normalised images of $1\times 1\times 1$ mm and default estimation and writing options. The normalized images were smoothed using a 10 mm full width at half-maximum (FWHM) isotropic Gaussian kernel. Images of the 6 predominantly right body side affected PD patients and 7 right body side affected CBD patients were flipped so that all PD and CBD patients had the right side of the brain as most affected side.

FDG-PET statistical analysis

Images of each of the seven patient groups were separately compared to controls using a two-sample t test. The image data were proportionally scaled to the cerebral global mean (the image

global mean is calculated as the arithmetical mean of voxels above the threshold of $1/8^{\text{th}}$ of the grand mean followed by grand mean scaling to 100) (Yakushev, et al. 2008). Threshold masking was set at 0.8 and an explicit mask in MNI space, supplied with SPM5, was added to remove emission counts outside the brain. SPM (t) maps were created and regions with a cluster-corrected threshold ($P < 0.05$) and voxels within each cluster ($P < 0.001$) above a Z score of 3.4 will be reported. If clusters were adjacent to each other, statistical significance of a cluster was assessed by examining its survival at a higher initial voxel threshold.

3.3 RESULTS

SPM (t) maps were created and overlaid onto a single subject T1 MR template (MNI, SPM5). Figure 1 shows regions with decreased metabolic activity, relative to the global mean, in patient groups compared to controls and figure 2 displays regionally increased metabolic activity, relative to the global mean, of patient groups compared to controls. In table 1 and 2 regions with a cluster-

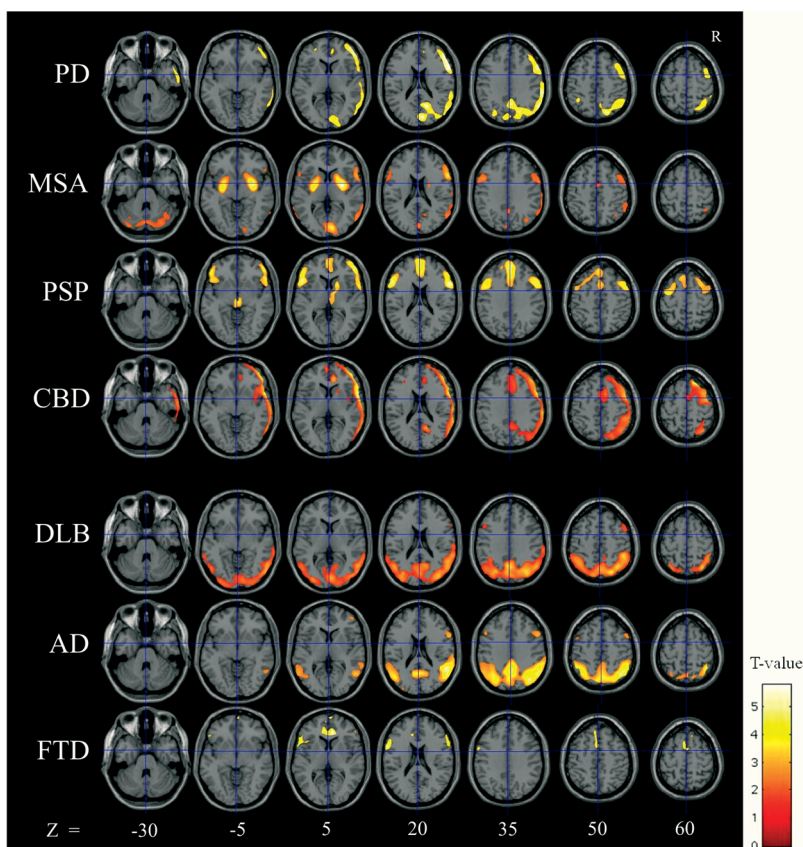


Figure 1: SPM (t) maps of decreased metabolic activity were thresholded at $P < 0.001$ with cluster cutoff of 20 voxels. Patient groups are indicated on the vertical axis and on the horizontal axis, seven transversal slices through the brain are shown.

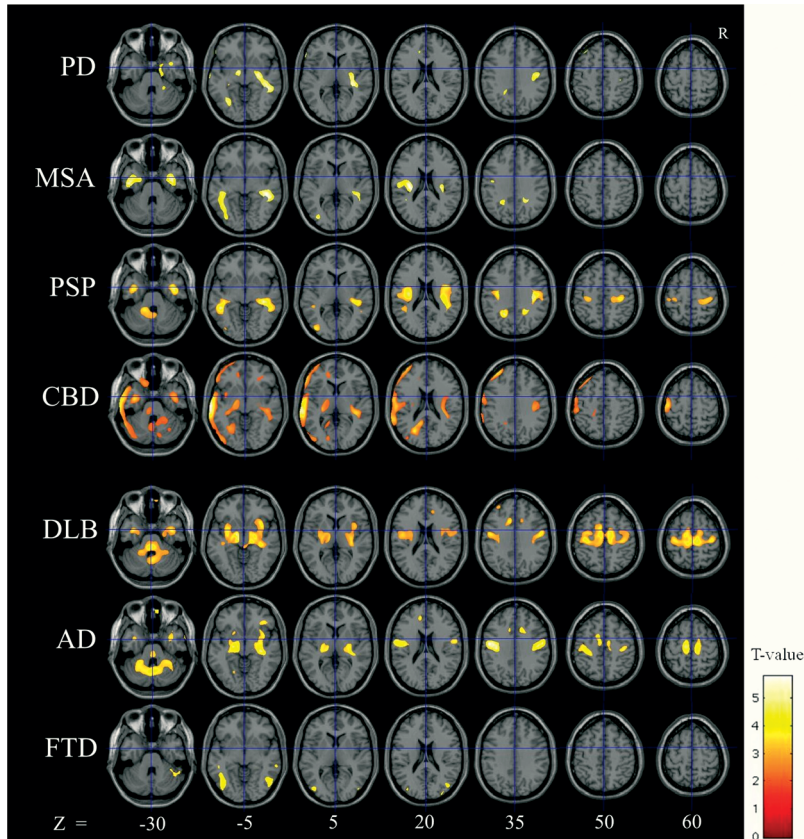


Figure 2: SPM (t) maps of increased metabolic activity were thresholded at $P < 0.001$ with cluster cutoff of 20 voxels. Patient groups are indicated on the vertical axis and on the horizontal axis, seven transversal slices through the brain are shown.

corrected threshold ($P < 0.05$) and voxels within each cluster ($P < 0.001$) above a Z score of 3.4 are reported. In table 1, each statistical significant region of relatively decreased metabolism in the brain is reported for each patient group. Table 2 reports regions with relatively increased metabolism.

Parkinson's disease

In PD patients, decreased metabolic activity was seen almost entirely contralateral to the affected body side, distributed over the prefrontal cortex, anterior cingulate gyrus and a few parietal-occipital regions. Relatively increased metabolic activity was seen predominantly in a few white matter regions including the posterior limb of the internal capsule bilaterally, extending at a relaxed threshold ($P < 0.05$ uncorrected) to the pallidum and posterior putamen contralateral to the affected body side. Furthermore, increased metabolic activity was seen in cerebellum, pons, contralateral hippocampal area and sensorimotor area.

Table 1: Regions with relatively decreased metabolic activity

Regions	Patient groups						
	PD MMNI (Z-score)	MSA MMNI (Z-score)	PSP MMNI (Z-score)	CBD MMNI (Z-score)	DLB MMNI (Z-score)	AD MMNI (Z-score)	FTD MMNI (Z-score)
Sup. frontal g.	33 6 66 (4.0)*		-2 50 32 (5.1)	17 29 61 (6.5) -3 58 7 (4.4)*			5 67 0 (3.8)* -3 39 46 (3.5)*
Mid. frontal g.	-27 46 13 (3.5)*			47 49 6 (6.4)	50 15 45 (3.8)*	46 50 80 (3.5)*	
Inf. frontal g.	58 15 22 (5.0)	60 15 20 (5.2)	58 14 21 (5.6) -53 18 10 (5.6)	59 10 3 (7.4)	-49 18 32 (3.5)*	52 15 40 (4.5)*	61 17 20 (3.6)* -58 14 13 (4.2)
Insula				41 1 0 (4.3)*			
Ant. cingulate g.	9 45 12 (3.9)*		0 9 42 (4.0)	12 39 8 (5.6)			10 39 6 (4.5) -8 43 6 (4.0)*
Mid. cingulate g.			0 2 73 (4.3)*	10 9 44 (4.8)			-4 -3 74 (4.2)*
SMA		59 1 44 (4.1)* -49 10 34 (3.9)*	-36 -4 60 (5.6)	55 3 43 (6.0)			
Precentral g.							
Postcentral g.							
Sup. parietal l.	35 62 55 (4.3)*			33 50 66 (5.1)	23 73 52 (5.6) -29 67 57 (4.7) 48 41 49 (5.5) -38 52 43 (5.7)		-58 -6 42 (3.5)*
Inf. parietal l.	-37 51 45 (4.1)*			67 23 25 (6.1)			
Supramarg.	63 33 33 (4.9)			41 63 44 (5.6)		43 52 59 (5.4)	
Angular g.	57 61 33 (4.5)	38 64 44 (4.4)*			40 62 45 (6.9)	41 65 45 (6.1) -45 64 29 (4.5)	
Precuneus	6 58 29 (4.6)				-2 62 36 (5.5)	-7 60 28 (5.8)	
Sup. temporal g.							
Mid. temporal g.		58 64 9 (4.0)*		59 64 17 (5.1)	54 54 23 (5.1) 56 64 15 (5.2) -48 64 15 (5.1)	53 52 23 (6.1)	42 20 38 (3.4)*
Inf. temporal g.	57 7 36 (4.1)*			64 55 3 (5.1)			
Sup. occipital g.	25 67 30 (4.9)			23 77 47 (4.6)			
Mid. occipital g.	36 75 30 (4.7)						
Cuneus	16 61 21 (4.9)			14 57 22 (5.0)			
Calcarine	13 86 13 (4.7)	9 85 7 (5.3)				5 86 6 (4.9)	
Caudate nucleus			19 11 6 (4.0)*	20 14 8 (3.6)*			
Putamen		30 3 2 (7.0) -28 9 0 (6.0)					
Thalamus			14 6 12 (4.2)*	17 9 12 (3.7)*			
Mesencephalon			3 24 4 (4.0)*				
Cerebellum		37 84 37 (4.4) -32 85 35 (4.8)					

MMNI coordinates (x y z (mm)) = right hemisphere; -x y z = left hemisphere) and Z scores of each statistically significant region are reported for each patient group. * = region is not cluster-corrected; sup. = superior; mid. = middle inf. = inferior g. = gyrus; ant. = anterior; SMA = supplementary motor area; l. = lobule; supramarg. = supramarginal.

Table 2: Regions with relatively increased metabolic activity

Regions	PD		MSA		PSP		CBD		DLB		AD		FTD	
	MMNI (Z-score)	MMNI (Z-score)	MMNI (Z-score)	MMNI (Z-score)	MMNI (Z-score)	MMNI (Z-score)	MMNI (Z-score)	MMNI (Z-score)	MMNI (Z-score)	MMNI (Z-score)	MMNI (Z-score)	MMNI (Z-score)	MMNI (Z-score)	MMNI (Z-score)
Sup. frontal g.	-33	34	49 (3.5)*											
Mid. frontal g.														
Inf. frontal g.														
Insula														
Ant. cingulate g.														
Mid. cingulate g.														
SMA														
Paracentral lob.														
Precentral g.														
Postcentral g.	44	-15	38 (4.7)*	-51	-15	17 (3.9)*	-42	-27	65 (3.6)*					
Supramarg. g														
Precuneus														
Sup. temporal g.														
Mid. temporal g.	-68	-14	-3 (3.5)*	-51	-21	-12 (4.2)*	-48	-18	-11 (4.2)*					
Inf. temporal g.														
Hippocampus	27	-15	-10 (4.3)	45	-23	-20 (4.4)	-40	-20	-17 (4.2)*					
Parahip. g.	22	-14	-23 (4.1)*											
Mid. occipital g.														
Inf. occipital g.														
Calcarine														
Fusiform g.														
Lingual g.														
White matter	36	-30	0 (4.4)	43	-33	-3 (4.4)	42	-4	-28 (5.1)					
Thalamus	-11	-9	-7 (4.2)	-30	-21	21 (4.4)	-47	-41	-9 (5.5)					
Pons														
Vermis														
Cerebellum	21	-41	-40 (3.6)*											

MMNI coordinates (x y z (mm)) = right hemisphere; -x y z = left hemisphere) and Z scores of each statistically significant region are reported for each patient group. * = region is not cluster-corrected; sup. = superior; mid. = middle inf. = inferior g. = gyrus; ant. = anterior; SMA = supplementary motor area; parahip. = parahippocampal; lob. = lobule; supramarg. = supramarginal.

Multiple system atrophy

In MSA patients, most prominent decreases in metabolic activity were seen in bilateral putamen and cerebellar hemispheres. Furthermore, a decrease was found in the right inferior frontal gyrus, primary motor cortex, right angular gyrus, right middle temporal gyrus and calcarine. Relatively increased metabolic activity was seen in a few white matter regions, temporal regions, left sensorimotor area and middle occipital gyrus.

Progressive supranuclear palsy

In PSP patients, a clear pattern of decreased metabolic activity was seen in the whole prefrontal cortex, including superior and inferior frontal gyrus, supplementary motor area (SMA), primary motor cortex and middle cingulate gyrus. Furthermore, decreased metabolism was found in the right caudate nucleus, thalamus and mesencephalon. Relatively increased metabolic activity was seen in a few white matter regions, cerebellum, insula, temporo-occipital regions and left sensorimotor area.

Corticobasal degeneration

In the CBD patient group, a strictly unilaterally decreased metabolism was seen in cortical regions, contralateral to the affected body side, including parieto-temporal regions, prefrontal cortex and motor cortex. Furthermore, a decrease was found in the anterior and middle cingulate gyrus and a little in the contralateral caudate nucleus and thalamus. Interestingly, relatively increased metabolic activity was seen in cortical areas ipsilateral to the affected body side, including motor- and sensorimotor cortex. In addition, an increased metabolism was found bilaterally in a few white matter regions and cerebellar hemispheres.

Dementia with Lewy Bodies

DLB patients had a marked decrease in metabolic activity in the occipital lobe. In addition, decreases were found in parieto-temporal and frontal regions. Relatively increased metabolic activity was seen in some white matter regions, thalamus, hippocampus and pons. Such relative increases were also seen in the sensorimotor and primary motor cortex, SMA, paracentral lobule and both anterior and middle cingulate gyrus.

Alzheimer's Disease

In AD patients, most prominent decreases in metabolic activity were found in the angular gyrus and other parieto-temporal regions including precuneus extending to the posterior- and middle cingulate gyrus. Furthermore, decreases were found in the right middle and inferior frontal gyrus. Relatively increased metabolic activity was seen in some white matter regions, cerebellum and pons, SMA and sensorimotor cortex.

Frontotemporal Dementia

In FTD patients, decreased metabolic activity was seen in the superior and inferior frontal gyrus, anterior cingulate gyrus, SMA, sensorimotor area and middle temporal gyrus. Relatively increased metabolic activity was seen a little in occipital, cerebellar and white matter regions.

3.4 DISCUSSION

The present study demonstrates a series of typical cerebral metabolic patterns of patients with various neurodegenerative brain diseases in a relatively early disease stage using the same statistical image analysis for each group. The general features of differences in each of the patient groups, compared to controls, are consistent with previous studies. However, some interesting differences can be noted. In Parkinson's disease, we found a disease-specific contralateral cortical decrease of metabolic activity, which to our knowledge has not been described before, probably because previous studies did not correct for most affected body side (Huang et al. 2007a, Ma et al. 2007a). One study of Eckert (Eckert et al. 2005) did flip the data according to the most affected body side, in a small group of early and advanced stage PD. We included 20 PD patients at an early disease stage, and this disease-specific contralateral cortical decrease could hypothetically be an early marker of disease.

We found a distinct disease-specific metabolic pattern for MSA, PSP and CBD which is similar to the metabolic patterns found for these diseases by the Eidelberg group (Eckert et al. 2005, 2008). In neuropathological studies in MSA (Wenning et al. 1997), PSP (Hauw et al. 1994) and CBD (Dickson et al. 2002) the areas described in our study show neuronal degeneration. Another difference which explains the decreased striatal metabolic activity in MSA, PSP and CBD and distinguishes these diseases from PD is that a postsynaptic striatal neuronal loss is detected post mortem in MSA, PSP and CBD and not in PD (Stacy and Jankovic. 1992).

Decreased metabolic activity in occipital regions was the most defining feature in DLB patients, especially in comparison with AD patients and is consistent with previous imaging studies (Lobotesis et al. 2001, Minoshima et al. 2001, Yong et al. 2007). This could be related to the presence of complex visual hallucinations which are thought to be useful in distinguishing DLB from other dementias (McKeith et al. 2005).

In AD patients, we found expected decreased metabolic activity in parieto-temporal regions, corroborating a meta-analysis of 9 studies (AD patients versus controls) which showed sensitivity and specificity of 86% (Patwardhan et al. 2004).

More limited metabolic decreases were found in FTD patients in accordance with previous reports (Diehl-Schmid et al. 2007, Jeong et al. 2005). The clinical manifestation of FTD can comprise different neuropathological diagnoses at autopsy and if patients die at an early disease stage the brain may be unremarkable (Cairns et al. 2007, McKhann et al. 2001).

In our study, global normalisation was applied to improve pattern recognition in the comparisons between patient groups. Recently, a discussion was started whether increases of metabolic activity

in PD are absolute or only relative i.e. artefactual due to the use of global mean normalization (Borghammer et al. 2009b, Grunder et al. 2009, Ma et al. 2009). The use of normalization to the global mean is valid if there is no difference in global mean values between groups (Grunder et al. 2009). Borghammer showed in simulated (^{15}O)-PET images of disease states in control subjects that lower global values, even when not statistically significant, led to localized subcortical increases in activity following normalization of the data to the global mean. They concluded that subcortical hyperactivity emerges as a general phenomenon of global mean normalized studies in which increases are then relative to cortical decreases (Borghammer et al. 2009b). Areas that show increased metabolic activity may in fact be regarded as most preserved brain regions. However, the question remains if this also holds for PD, especially because increased metabolic activity is seen in the pallidothalamic regions, which are proposed to be overactive in an absolute sense in PD (Eggers et al. 2009, Ma et al. 2009).

Absolute quantification of FDG-PET data may be the best method to overcome the global mean normalization problem. However, that is a time-consuming and demanding procedure, which is not feasible in clinical practice. As an alternative for normalization to the global mean, some studies have applied normalization to the white matter, pons, cerebellum or sensorimotor cortex (Foster et al. 2007, Minoshima et al. 2001, Yakushev et al. 2008). In these regions, we generally found increased activity in most of our patient groups, which may provide an argument that these areas are preserved and can be used as reference region for normalization. On the other hand, normalization to white matter may be not valid because it is not precisely known, whether and how metabolic changes occur in white matter in neurodegenerative brain diseases. The pons region is not an optimal reference region either, because it is very small and the sensorimotor area is hard to demarcate exactly from other brain regions. Cerebellar areas have been used in AD and FTD as reference region. However, the use is limited because for example in MSA patients a decreased cerebellar metabolic activity can be seen. Recently, Yakushev presented the reference cluster method as alternative for global mean normalization (Yakushev et al. 2009). The proposed algorithm normalizes not by structure/anatomical region, but rather by the metabolically most preserved part (reference cluster) and thus ensures the most effective count normalization (Borghammer et al. 2009a, Yakushev et al. 2009). This method can only be used if metabolic differences are expected in one direction. In PD, a larger (cortical) reference cluster should then be chosen instead of subcortical or cerebellar, possibly hyperactive structures.

Our study was designed to detect distinctive metabolic brain patterns in different typical patient groups at early disease stages. These patterns of relatively decreased and relatively increased metabolism can help in the differential diagnosis. A limitation of the present study is that, despite data acquisition of FDG-PET scans over the past ten years, some group samples are still small. Nevertheless, it is remarkable that the expected patterns were indeed present in the clinical scans of our appropriate patient groups and were clearly distinguishable. Furthermore, healthy controls had a younger mean age than some patient groups. An age-dependent global metabolic decrease is

well-known (comparing young and elderly subjects with a larger age difference) but this is cancelled out in the normalization procedure in this study. A major advantage is that typical metabolic brain patterns could be determined at early stages of a specific disease because we had access to long-term follow up data of clinical disease progression. At last, statistical analysis of FDG-PET scans using SPM5 and global mean normalization is relatively easy. It can be implemented in each center, and could therefore be useful in clinical practice.

Future perspectives

The build up of a database with disease-specific patterns, as shown in our study, can be used to prospectively compare patients who are clinically still without a clear diagnosis and improve early diagnosis in neurodegenerative brain diseases. Furthermore, the newer high resolution PET cameras will permit more reliable absolute quantification of FDG uptake as a marker of neuronal activity in small subcortical nuclei which are involved in the pathophysiology of PD (Yakushev et al. 2009).

3.5 CONCLUSION

This study reports an overview of specific patterns of cerebral metabolic activity with the same statistical image analysis technique for conditions with parkinsonism or dementia. Statistical analysis of FDG-PET scans using SPM5 and global mean normalization is relatively easy and therefore useful in clinical practice. It can assist in early diagnosis of individual patients when each subject's metabolic findings are compared with a database of specific disease-related patterns.

Acknowledgments

We would like to thank the department of nuclear medicine (especially the medical nuclear workers) for providing the FDG-PET scans and Ms. Renée Staal for database management.

CHAPTER 4

FDG-PET IMAGING IN THE DIFFERENTIAL DIAGNOSIS OF NEURODEGENERATIVE BRAIN DISEASES

L.K. TEUNE, A.L. BARTELS AND K.L. LEENDERS

Department of Neurology, University Medical Center Groningen, the Netherlands

Submitted

ABSTRACT

The differential diagnosis of neurodegenerative brain diseases may be difficult on clinical grounds only, especially at an early disease stage. Neurodegenerative brain diseases such as Parkinson's disease (PD), multiple system atrophy (MSA), progressive supranuclear palsy (PSP), corticobasal degeneration (CBD), dementia with Lewy Bodies (DLB), Alzheimer's disease (AD) and frontotemporal dementia (FTD) have overlapping features at presentation, while the typical clinical syndrome may become clear only at later disease stages. It is important to diagnose a neurodegenerative disease at an early disease stage, because treatment and also the expectancy of future motor or cognitive problems differ between the diseases. It is increasingly recognised that positron emission tomography (PET) tracer methods can be used for the measurement of biochemical processes of the human brain, to obtain insight in the pathophysiology of brain diseases and to assist in an early diagnosis.

Neurodegenerative brain diseases are characterised by cellular malfunction and biochemical alterations that occur in early disease stages, before structural brain alterations may become clear. Increases and decreases of synaptic activity in the brain are accompanied by proportional changes in capillary perfusion and local glucose consumption. Loss of neurons may result in decreased glucose consumption in distant brain regions by deafferentiation, while also increased regional glucose consumption by increased activation of afferent neurons can occur.

The PET tracer [^{18}F]-fluorodeoxyglucose (FDG) allows the measurement of glucose consumption. FDG is a glucose analog with physiological aspects almost identical to glucose.

FDG-PET imaging has been used intensively to study glucose metabolism and to identify disease-specific cerebral metabolic patterns in several neurodegenerative brain diseases.

Disease-specific regional differences of brain glucose metabolism have been found in various neurodegenerative brain diseases, including parkinsonian syndromes and dementia. This has improved our understanding of the pathophysiology of these diseases as well as our ability to diagnose patients at an earlier disease stage. Reviewed here are the results of increasing possibilities of investigating brain energy metabolism in neurodegenerative brain diseases using FDG-PET with univariate and multivariate analysis methods. An overview of specific metabolic patterns in several neurodegenerative diseases will be given and the usefulness of FDG-PET in clinical practice will be discussed.

4.1 CEREBRAL GLUCOSE METABOLISM

Increases and decreases of synaptic activity in the brain are accompanied by proportional changes in capillary perfusion and local glucose consumption. These changes in glucose consumption are the effect of changed activity or density of the afferent nerve terminals in that region. Loss of neurons may result in decreased glucose consumption in distant brain regions by deafferentation, while also increased regional glucose consumption by increased activation of afferent neurons can occur. The PET tracer [^{18}F]fluorodeoxyglucose (FDG) allows the measurement of glucose consumption. FDG is a glucose analog with physiological aspects almost identical to glucose. It is transported from the blood to the brain by a carrier-mediated diffusion mechanism. FDG and glucose are phosphorylated by hexokinase as the first step of the glycolytic process. FDG differs from glucose in that a hydrogen atom replaced the hydroxyl group at the second carbon atom of the molecule. Glucose is then phosphorylated to glucose-6- PO_4 , and continues along the glycolytic pathway for energy production. However, FDG is phosphorylated to FDG-6- PO_4 , which is not a substrate for further metabolism and trapped in tissues. As glucose is the only source of energy for the brain it reflects the neuronal integrity of underlying brain pathology. Since FDG is a competitive substrate with glucose for both transport and phosphorylation, it is important for tracer uptake to avoid high blood glucose levels during an FDG-PET scan in subjects with diabetes.

In neurodegenerative brain diseases, specific brain regions degenerate and specific patterns of metabolic brain activity develop. This happens before clear structural changes can be detected with imaging techniques. Measurement of glucose consumption with FDG-PET imaging thus allows us to identify disease-specific cerebral metabolic brain patterns in several neurodegenerative brain diseases at an early disease stage. Since the first FDG-PET study in man in 1979 (Reivich et al. 1979) regional differences in cerebral glucose metabolism have been reported in various neurodegenerative brain diseases including parkinsonian syndromes.

4.2 DISEASE-SPECIFIC METABOLIC BRAIN PATTERNS: METHODS

Univariate methods like voxel-based statistical parametric mapping (SPM) analyses have been used to identify group differences between patients with neurodegenerative brain diseases and controls (Eckert et al. 2005, Juh et al. 2004, Yong et al. 2007).

At the University Medical Center Groningen, The Netherlands, we have performed a retrospective study (Teune et al. 2010) selecting typical patients with 7 different neurodegenerative brain diseases who had had a clinical FDG brain scan at a time point when their diagnosis was not sure yet. These patients developed in the following years the mentioned typical disease states. Images of each of the seven patient groups were separately compared to controls using a two-sample t test. At those early scans, already typical differences between patient groups and healthy controls were found for each disease.

However, Scaled Subprofile modelling/principal component analysis (SSM/PCA), a multivariate method, not only identifies group differences, but is also able to identify relationships in relatively

increased and decreased metabolic activity between different brain regions in combined samples of patients and control scans (Eidelberg 2009, Moeller et al. 1987). Covariance analysis techniques are considered appropriate methods to explore network activity. In the SSM, a threshold of the whole-brain maximum can be applied to remove out-of-brain voxels, followed by a log transformation. A threshold of 35% is used by the Eidelberg research group resulting in a mask of mainly grey matter (Spetsieris and Eidelberg 2010). After removing between-subject and between-region averages, a principal component analysis (PCA) can be applied. PCA transforms a set of correlated variables into a new set of orthogonal uncorrelated variables that are called the principal components. Voxels participating in each principal component (PC) may have either a positive or a negative loading. The loadings express the covariance structure (i.e. the strength of the interaction) between the voxels that participate in the PC. They are ordered in terms of the variability they represent. That is, the first principal components represents for a single dimension (variable) the greatest amount of variability in the original dataset. Each succeeding orthogonal component accounts for as much of the remaining variability as possible. They can be very helpful in determining how many of the components are really significant and how much the data can be reduced.

In most studies, the components that together describe at least 50% of the variance are used for further analysis, but this is an arbitrary limit. To identify a covariance pattern that best discriminates a patient group from a control group, each subject's expression of the selected principal components with the lowest AIC (Akaike information criterion) value (Akaike 1974) are entered into a stepwise regression procedure. This regression results in a linear combination of the PCs that best discriminated the two groups and is designated as the disease-specific metabolic covariance pattern.

Important for its use in clinical practice is that this metabolic covariance pattern can then be applied to individual patients to test whether they express the pattern or not. Every voxel value in a subject scan is multiplied by the corresponding voxel weight in the covariance pattern, with a subsequent summation over the whole brain volume. The resulting subject score captures to what extent a subject expresses the covariance pattern.

4.3 DISEASE-SPECIFIC METABOLIC BRAIN PATTERNS IN PATIENTS WITH PARKINSONISM.

4.3.1 Parkinson's Disease

Parkinson's disease (PD) is characterized by bradykinesia, rigidity, sometimes rest tremor and postural instability. A disturbed α -synuclein protein forming so-called Lewy bodies seems to play a causal role, which was a reason to designate PD as a α -synucleinopathy. The main pathophysiological changes result from degeneration of catecholaminergic, especially dopaminergic cells in brainstem regions.

A characteristic metabolic covariance pattern has been identified in PD patients (PD-related pattern, PDRP) showing regionally relatively increased metabolism in the globus pallidus and

putamen, thalamus, pons and cerebellum and relatively decreased metabolism in the lateral frontal, premotor and parietal association areas (Ma, et al. 2007b) Network expression in PD patients also increases linearly with disease progression (Huang, et al. 2007c). Tang tried to study network changes in the PD-related motor pattern before symptom onset by studying 15 hemiparkinsonian patients and focusing mainly on the “presymptomatic” hemisphere. They conclude that abnormal PDRP activity antecedes the appearance of motor signs by approximately 2 years (Tang et al. 2010a). However, this needs to be proven in future research in true presymptomatic patients.

Parkinson’s Disease and metabolic brain patterns related to specific symptoms

In addition to motor symptoms, cognitive dysfunction is also common in PD, especially executive and visuospatial dysfunction. FDG-PET studies have been performed to study these specific symptoms and their relations with neural network pathophysiology. The Eidelberg research group has shown PD subclassifications related to specific symptoms. Network analysis with the SSM/PCA approach detected a significant covariance pattern in non-demented PD patients that correlated with memory and executive functioning tasks. The expression of this PD-related cognitive pattern (PDCP) in individual patients correlated with severity of cognitive dysfunction (Huang et al. 2007b). Alterations in neuropsychological test results in advanced PD were found to correlate with decreases in glucose metabolism in the dorsolateral prefrontal cortex, lateral orbitofrontal cortex ventral and dorsal cingulum and in Broca area (Kalbe et al. 2009). In the study of Kalbe, PD patients with deep brain stimulation in the subthalamic nucleus (STN-DBS) showed cognitive decline that correlated with decrease in glucose metabolism in these areas. In another study in STN-DBS treated patients, STN-DBS was found to activate glucose metabolism in the frontal limbic and associative territory (Hilker et al. 2004). Interestingly, cortical areas that show hypometabolism in patients with depression (Mayberg HS. 1994) are similar to the regions that show restored glucose metabolism after STN-DBS. This finding agrees with the clinical observation that PD-related depression tends to improve after STN-DBS.

Mure identified a spatial covariance pattern associated with Parkinson tremor which was characterized by covarying increases in the cerebellum/dentate nucleus and primary cortex and to a minor degree in the caudate/putamen (Mure et al. 2011).

Hallucinations in PD have been related to relative frontal hypermetabolism compared to PD patients without hallucinations (Nagano-Saito et al. 2004). However, another study showed hypometabolism in occipitotemporoparietal regions in PD patients with hallucinations, sparing the occipital pole, while no significant increase in regional glucose metabolism was detected (Boecker et al. 2007). Interestingly, in patients with dementia with Lewy bodies (DLB), who also suffer from hallucinations, glucose metabolism was also decreased in occipitoparietal regions, however without sparing of the occipital pole (see DLB section).

4.3.2 Multiple system atrophy

Multiple system atrophy is a sporadic neurodegenerative brain disease which affects both men and women and generally starts in the sixth decade of life. The main clinical features are parkinsonism, autonomic failure, cerebellar ataxia, and pyramidal signs in any combination. However, two major motor presentations can be distinguished. Parkinsonian features predominate in 80% of patients (MSA-P subtype) and cerebellar ataxia is the main motor feature in 20% of patients (MSA-C subtype) (Gilman et al. 2008, Wenning et al. 1997).

In MSA-P the striatonigral system is the main site of pathology but less severe degeneration can be widespread and normally includes the olivopontocerebellar system. In MSA-C pathological changes are mainly seen in the olivopontocerebellar system and involvement of striatum and substantia nigra are less severe (Wenning et al. 1997). The discovery of glial cytoplasmic inclusions in MSA brains highlighted the unique glial pathology as biological hallmark of the disease. Their distribution selectively involves basal ganglia, supplementary and primary motor cortex, the reticular formation and pontocerebellar system. Glial cytoplasmic inclusions contain besides classical cytoskeletal antigens also α -synuclein, which is a presynaptic protein present in Lewy Bodies, and this accumulation seems to play a central part not only in MSA but also in other α -synucleinopathies such as PD and DLB.

Disease-related metabolic patterns were also present in MSA consisting of hypometabolism in putamen and cerebellum in MSA (Eckert et al. 2008). Poston found that differences in expression of the MSA-related pattern correlated with clinical disability (Poston et al. 2012).

4.3.3 Progressive supranuclear palsy

The clinical picture of progressive supranuclear palsy (PSP) has been first described by Steele, Richardson and Olszewski (Steele JC, Richardson J, Olszewski J. 1964) and is characterized by progressive parkinsonism, early gait and balance impairment, vertical gaze palsy and more profound frontal cognitive disturbances. PSP is one of several neurodegenerative diseases characterised by accumulation of hyperphosphorylated tau (tauopathy), forming abnormal filamentous inclusions in neurons and glia in the precentral and postcentral cortical areas but also in the thalamus, subthalamic nucleus, red nucleus and substantia nigra. Other neurodegenerative brain diseases which show disturbances in tau protein handling are corticobasal degeneration (CBD) and frontotemporal dementia (FTD) but there is also overlap in pathology with Alzheimer's disease (AD).

However, the metabolic brain patterns in these tauopathies are quite different. The covariance pattern of PSP consists of decreased metabolism in the prefrontal cortex, frontal eye fields, caudate nuclei, medial thalamus and upper brainstem (Eckert et al. 2008). Brain stem atrophy and atrophy of the medial frontal cortical regions have also been reported in histopathological studies (Hauw et al. 1994).

4.3.4 Corticobasal Degeneration

The most striking features of patients with corticobasal degeneration (CBD) include marked asymmetrical parkinsonism and apraxia but also postural instability, limb dystonia, cortical sensory loss, dementia and the alien limb phenomenon. CBD is one of the tauopathies and clinical diagnosis is complicated by both the variability of presentation of true CBD and the syndromes that look alike but are caused by other tauopathies with parkinsonism like PSP or FTD (Josephs et al. 2006). However with functional neuroimaging a clear distinction can be made. In CBD, a typical pattern of hypometabolism is seen in cortical regions contralateral to the affected body side, including parieto-temporal regions, prefrontal cortex and motor cortex. Furthermore, a decrease can be found in the contralateral caudate nucleus, putamen and thalamus (Eckert et al. 2005, Teune et al. 2010). No covariance pattern has been described using the SSM/PCA technique in CBD.

4.4 DISEASE-SPECIFIC METABOLIC BRAIN PATTERNS IN THE DIFFERENTIAL DIAGNOSIS OF INDIVIDUAL PATIENTS WITH PARKINSONISM.

Interestingly, Tang and co-workers studied the potential role of FDG PET in the individual diagnosis of 167 patients who had parkinsonian features but uncertain clinical diagnosis (Tang et al. 2010b) After FDG-PET imaging, patients were assessed by blinded movement disorders specialists for a mean of 2.6 years before a final clinical diagnosis was made (gold standard). SSM/PCA analysis can quantify the expression of an obtained covariance pattern in each subject which allows assessing the expression of a given pattern on a single case basis. Using this automated image-based classification procedure and the previously defined disease-related covariance patterns in PD, MSA and PSP, individual patients were differentiated with high specificity.

However, blinded, prospective imaging studies (ideally involving multiple centers, a larger validation group, repeat imaging, and more extensive post-mortem confirmation) are needed to establish the accuracy and precision of this pattern-based categorisation procedure. These studies are currently undertaken.

For routine clinical practice, this knowledge of disease-specific patterns of regional metabolic activity in neurodegenerative brain diseases can be a valuable aid in the differential diagnosis of individual patients, especially at an early disease stage.

4.5 DISEASE-SPECIFIC METABOLIC BRAIN PATTERNS IN DEMENTIA.

4.5.1 Alzheimer's Disease

Alzheimer's disease (AD) is a progressive neurodegenerative brain disease accounting for 50-60% of cases of dementia. AD is characterized by a severe decline in episodic memory together with general cognitive symptoms such as impaired judgement, decision making and orientation

(McKhann et al. 1984). A correct clinical diagnosis can be difficult, especially in early disease stages or in patients with for example comorbid depression, high education or young age (Bohnen et al. 2012). FDG-PET imaging can be used to assist in the differential diagnosis, because for different dementia syndromes, a separate pattern of hypometabolism can be found. In Alzheimer's disease (AD), decline of FDG uptake in posterior cingulate, temporoparietal and prefrontal association cortex was related to dementia severity (Herholz et al. 2002). Foster used visual interpretation of an automated three-dimensional stereotactic surface projection technique of patients with AD and FTD. They showed that visual interpretation of FDG-PET scans after training is more reliable and accurate in distinguishing FTD from AD than clinical methods alone (Foster et al. 2007).

Although multivariate analytical techniques might identify diagnostic patterns that are not captured by univariate methods, they have rarely been used to study neural correlates of Alzheimer's Disease or cognitive impairment. Because cognitive processes are the result of integrated activity in networks rather than activity of any one area in isolation, functional connectivity can be better captured by multivariate methods. A study from Habeck examined the efficacy of multivariate and univariate analytical methods and concluded that multivariate analysis might be more sensitive than univariate analysis for the diagnosis of early Alzheimer's disease (Habeck et al. 2008).

Scarmeas et al were the first to derive an AD-related covariance pattern using $H_2^{15}O$ to measure brain perfusion (Scarmeas et al. 2004). It consisted of relatively increased perfusion in the bilateral insula, lingual gyri and cuneus with bilaterally decreased flow in bilateral inferior parietal lobule and cingulate in AD patients. However, using this PET tracer they found a sensitivity of 76-94% and a specificity of 63-81% with considerable overlap in pattern expression among AD patients and controls. Therefore they concluded that the derived $H_2^{15}O$ pattern cannot be used as a sufficient diagnostic test in clinical settings. Specific FDG covariance patterns to distinguish early AD-related cognitive decline using multivariate methods have yet to be specified.

4.5.2 Frontotemporal dementia

Frontotemporal dementia (FTD) is one of the neurodegenerative diseases commonly mistaken for AD. FTD patients do not have a true amnesic syndrome but can present with either gradual and progressive changes in behaviour, or gradual and progressive language dysfunction. Gross examination of the post-mortem brain from a patient with FTD usually reveals frontal or temporal lobar atrophy or both, but the distribution or severity of brain atrophy are not specific for a particular neurodegenerative brain disease. Jeong and Diehl-Schmid analysed FDG-PET scans of FTD patients on a voxel-by-voxel basis using Statistical Parametric Mapping (SPM). They found hypometabolism depending on disease stage in the frontal lobe, parietal and temporal cortices (Diehl-Schmid et al. 2007, Jeong et al. 2005).

4.5.3 Dementia with Lewy Bodies

The clinical overlap of dementia and parkinsonism is highlighted in Dementia with Lewy Bodies

(DLB). These patients show besides dementia extrapyramidal motor symptoms and marked neuropsychiatric disturbances including visual hallucinations, depression, variability in arousal and attention (McKeith 2006). Consistent observation of a metabolic reduction in the medial occipital cortex in DLB patients (Minoshima et al. 2001, Teune et al. 2010) using FDG-PET imaging suggests the use of FDG-PET in the differential diagnosis of AD and DLB and of PD and DLB. Minoshima found that the presence of occipital hypometabolism distinguished DLB from AD with 90% sensitivity and 80% specificity when using post-mortem diagnosis as the gold standard diagnosis (Minoshima et al. 2001).

4.6 DISEASE-SPECIFIC METABOLIC BRAIN PATTERNS IN HYPERKINETIC MOVEMENT DISORDERS

4.6.1 Huntington's disease

Huntington's disease (HD) is characterized by progressive dementia and chorea, starting around 30-40 years of age. HD is caused by a dominantly inherited CAG repeat expansion mutation that generates lengthening of the protein huntingtin, with size-dependent neurotoxicity. Several PET studies have shown hypometabolism in the caudate nucleus, both in symptomatic and asymptomatic mutation carriers (Grafton et al. 1992) (Antonini et al. 1996) In asymptomatic carriers, metabolic decreases were also significantly associated with the CAG repeat number (Antonini et al. 1996). Furthermore, it was found that FDG uptake in the caudate nucleus provided a predictive measure for time of onset of the disease, in addition to the mutation size (Ciarmiello et al. 2012).

Another study applied network analysis of FDG-PET scans in presymptomatic mutation carriers (Feigin et al. 2001). They found a HD-related metabolic covariance pattern (HDRP) characterized by caudate and putaminal hypometabolism, but also including mediotemporal reductions as well as relative increases in occipital regions. Disturbances of these striatotemporal projections may underlie aspects of the psychiatric and cognitive abnormalities that occur in the earliest stages of HD, before the onset of motor signs (Cummings. 1995).

4.6.2 Dystonia

Dystonia is a movement disorder characterized by involuntary, sustained muscle contractions causing twisting movements and abnormal postures. The most common forms of primary torsion dystonia (PTD) are DYT1 and DYT6, both caused by autosomal inherited mutations with a reduced penetrance.

Functional neuroimaging techniques have been applied in different dystonic disorders including primary generalized dystonia, mainly DYT1 and DYT6 and dopa-responsive dystonia, as well as focal dystonic syndromes such as torticollis, writer's cramp and blepharospasm. A common finding is abnormality of the basal ganglia, cerebellum and associated outflow pathways to sensorimotor cortex and other regions involved with motor performance. However, controversial results have

been found in imaging dystonias, partly attributed to methodological differences but also to the heterogeneity of the dystonias. Using the SSM/PCA approach a reproducible pattern of abnormal regional glucose utilization in two independent cohorts of DYT1 carriers have been found (Eidelberg 1998, Trost et al. 2002). This torsion-dystonia related metabolic pattern is characterized by increases in the posterior putamen/globus pallidus, cerebellum and SMA. Interestingly, also in clinically non-manifesting mutation carriers this pattern was found, suggesting a cerebral “vulnerability to develop dystonia” network change. Also in manifesting and non-manifesting DYT 6 carriers abnormal network activity has been identified. A difference between DYT1 and DYT6 metabolic patterns can be seen in the putamen, where glucose metabolism is increased in DYT1 and decreased in DYT6, possibly due to cell loss in DYT6. Furthermore, the cerebellum shows increased activity in DYT1 and normal activity in DYT6 (Carbon et al. 2004).

The TDRP network is not expressed in patients with Dopa-responsive dystonia (DRD) (Trost et al. 2002).

DRD is characterized by an early onset of dystonic symptoms and later appearance of parkinsonian symptoms. A defining feature is a marked and sustained response to low doses of levodopa, suggesting that the lesion may be functional in the presynaptic dopaminergic system rather than anatomical. The DRD-related metabolic pattern is characterized by relative increases in the dorsal midbrain, cerebellar vermis and SMA, associated with covarying decreases in putamen, lateral premotor and motor cortical regions (Asanuma et al. 2005). This DRD-related pattern is not apparent in DYT 1 and 6 carriers supporting the hypothesis that the pathophysiology of DRD differs from that of other forms of dystonia. They also found that the Parkinson-related metabolic pattern is not apparent in DRD patients. Thus FDG-PET can be useful to distinguish PD-related dystonia from dopa-responsive dystonia with parkinsonism (Asanuma et al. 2005).

4.6.3 Gilles de la Tourette

Tourette syndrome is characterized by the presence of chronic motor and vocal tics that develop before the age of 18. Comorbid behavioural abnormalities are common in Tourette syndrome, most notably obsessive-compulsive disorder and attention deficit/hyperactivity disorder (Lebowitz et al. 2012). The neurophysiology remains poorly understood with varying and inconsistent neuropathological and neuroimaging findings, possibly due to the clinical heterogeneity of the disorder. Pourfar identified a Tourette syndrome related pattern characterized by reduced metabolic activity of the striatum and orbitofrontal cortex associated with relatively increased metabolic activity in the premotor cortex and cerebellum (Pourfar et al. 2011). A second metabolic brain pattern was found in patients with Tourette syndrome and obsessive compulsive disorder characterized by reduced activity in the anterior cingulate and dorsolateral prefrontal cortex and relative increases in primary motor cortex and precuneus. Subject expression correlated with symptom severity. These findings suggest that the different clinical manifestations of the Tourette syndrome are associated with different abnormal brain networks (Pourfar, et al. 2011).

4.7 CONCLUSION

FDG-PET imaging is increasingly available for routine clinical practice and has remained the only available radiotracer to detect accurately and reliably the cerebral glucose metabolism. As glucose is the only source of energy for the brain it reflects the energy needs of underlying brain neuronal systems. The SSM/PCA method can identify relationships in relatively increased and decreased metabolic activity between different brain regions in combined samples of patients and controls. The expression of a covariance pattern can be quantified in an individual patient. The obtained subject score indicates to what extent that patient expresses the disease-related pattern. These metabolic brain patterns can therefore be a valuable aid in the differential diagnosis of individual patients with neurodegenerative brain diseases.

CHAPTER 5

VALIDATION OF PARKINSONIAN DISEASE-RELATED METABOLIC BRAIN PATTERNS

L.K. TEUNE¹, R.J. RENKEN², D. MUDALI³, B.M. DE JONG¹, R.A. DIERCKX⁴,
J.B.T.M. ROERDINK³, AND K.L. LEENDERS¹

¹Department of Neurology, University Medical Center Groningen, ²NeuroImaging Center, University Medical Center Groningen, ³Johann Bernoulli Institute for Mathematics and Computer Science, University of Groningen, ⁴Nuclear Medicine & Molecular Imaging, University Medical Center Groningen, the Netherlands

ABSTRACT

Objective: To validate disease-related metabolic brain patterns for Parkinson's Disease, multiple system atrophy and progressive supranuclear palsy.

Methods: The study included twenty Parkinson's Disease, twenty one with multiple system atrophy and seventeen progressive supranuclear palsy: all of whom had undergone a clinically motivated [18F]-fluoro-deoxyglucose positron emission tomography scan at an early stage of their disease. At a follow up time after the scan of 2-4 years, a clinical diagnosis was made according to established clinical research criteria. Patient groups were compared to eighteen healthy controls using a multivariate covariance image analysis technique called scaled subprofile model/principal component analysis (SSM/PCA).

Results: Disease-related metabolic brain patterns for these parkinsonian disorders were identified. Validation showed that these patterns were highly discriminative of the three disorders.

Conclusion: Early diagnosis of parkinsonian disorders is feasible when the expression of disease-related metabolic brain patterns is quantified at single-subject level.

5.1 INTRODUCTION

Visual examination of [^{18}F]-fluoro-deoxyglucose positron emission tomography (FDG-PET) scans may guide the differential diagnosis of parkinsonian syndromes. Nevertheless, interpretation of both clinical symptoms and FDG-PET scans can be difficult. Previously, univariate methods like statistical parametric mapping (SPM) have been used to identify group differences between parkinsonian patients and controls (Eckert et al. 2005, Juh et al. 2004, Teune et al. 2010). However, scaled subprofile modelling/principal component analysis (SSM/PCA), a multivariate method, not only identifies group differences, but also relationships in metabolic activity between different brain regions in combined samples of patients and control scans (Moeller and Strother. 1991, Spetsieris et al. 2009). A Parkinson's disease-related metabolic pattern was characterized by relative increases in pallidothalamic, pontine and cerebellar metabolism and relative decreases in the premotor and posterior parietal areas while typical disease-related metabolic patterns have also been identified for multiple system atrophy (MSA) and progressive supranuclear palsy (PSP) (Eckert et al. 2008, Ma et al. 2007b, Poston et al. 2012). SSM/PCA additionally enables quantifying the magnitude of the expression of a network for individual subjects (subject score) thus facilitating clinical investigation at single-subject level (Spetsieris and Eidelberg. 2010).

Recently, Tang highlighted the diagnostic value of FDG PET in parkinsonian patients with diagnostic uncertainty, by discriminating between Parkinson's disease (PD), MSA and PSP with high specificity using an automated image-based classification procedure (Tang et al. 2010b). Since all previously mentioned papers on SSM/PCA-processed FDG-PET data originate from one research group, the present study aimed to validate these patterns in other cohorts, which is an essential prerequisite before routine clinical application. Therefore, specificity and sensitivity of disease-related metabolic patterns for PD, MSA and PSP were assessed in our own patient population.

5.2 METHODS

Patients

FDG-PET scans selected from a previous study (Teune, et al. 2010) describing 18 healthy controls and 20 PD, 21 MSA, 17 PSP patients were included for the present analysis. At the time of referral for imaging, the clinical diagnosis of most patients was uncertain. The final clinical diagnoses according to established clinical research criteria (Gilman, et al. 2008, Litvan, et al. 1996, Litvan, et al. 2003) were made after a follow up time after scanning of 4 ± 3 years (y) in PD, 2 ± 1 y in MSA and 3 ± 2 y in PSP. Included PD patients were 9 male (M), 11 female (F), 6 right body-side affected, 14 left-side affected, with mean age of 63 ± 9 y and Disease Duration (DD) at scanning of 3 ± 2 years. Fourteen probable MSA, 7 possible MSA patients (10M, 11F, age 64 ± 10 y; DD 4 ± 2 y) and 13 probable, 4 possible PSP patients (9M, 8F, age 68 ± 8 y; DD 2 ± 1 y) were included.

FDG-PET data acquisition and statistical analysis

Patients were scanned on a Siemens ECAT HR+ PET scanner in a 3D mode under standard resting conditions (eyes closed) after injection of approximately 200 MBq FDG in 4ml saline. Reconstructed FDG-PET images were spatially normalised to a standard brain PET template (Montreal Neurological Institute; MNI) using SPM8 (Functional Imaging Laboratory, running in Matlab 7.10.0 (R2010a, Mathworks)) and smoothed with a 10mm full width at half-maximum isotropic Gaussian kernel. SSM/PCA was applied using software written in-house, based on the methods of Spetsieris and Eidelberg (Eidelberg. 2009, Spetsieris and Eidelberg. 2010). A 35% threshold of the whole-brain maximum was applied to remove out-of-brain voxels which results in a mask of mainly grey matter, followed by a log transformation. After removing between-subject and between-region averages, a principal component analysis (PCA) was applied. All components that together described at least 50% of the variance were used for further analysis. A disease-related metabolic covariance pattern was determined by a linear combination of the selected principal components with the lowest AIC (Akaike information criterion) value (Akaike. 1974) in a stepwise regression procedure. The correctness of the in-house written script was verified by performing the analysis both with the Eidelberg software and our own software, which provided identical results.

Without a second patient group for pattern validation (Spetsieris et al. 2010), a leave-one-out cross validation procedure was performed, resulting in subject scores independent from the pattern identification step. Subject scores were transformed into z-scores with respect to the healthy control population and displayed, for each comparison separately, in a scatter plot.

Receiving-operating-characteristic (ROC) curves were determined for the probability values of PD, MSA and PSP. Optimum cut-off probability values for classifying individual patients were calculated by identifying an inflection point on each ROC curve that corresponds to the best combination of sensitivity and specificity. Patients were classified as correctly diagnosed if their probability value was higher than the cut-off value. Thereafter, we calculated for each comparison sensitivity, specificity, and positive- and negative predictive value (PPV and NPV respectively).

In addition to obtaining valid subject scores, the leave-one-out procedure provides an estimate of the disease-related metabolic brain patterns and their variances. Dividing the estimate by its variance a T-score is obtained. Resulting patterns are thresholded at $T > 3.7$ (corresponding to $p < 0.001$, assuming normality of data) and overlaid onto a T1 MR template using MRIcron.

5.3 RESULTS

Spatial covariance analysis was performed on FDG-PET scans from PD, MSA and PSP patients. The model with the lowest AIC value (Akaike. 1974) was determined by a linear combination of PC (principal component) number 1,4,5 with variance accounted for (VAF) of 26.73% for PD; PC 1,2,4 (33.91% VAF) for MSA and PC 1 and 5 (26.30% VAF) for PSP. A leave-one-out cross validation procedure was subsequently performed, generating disease-related metabolic patterns (Figure.1) and scatter plots with corresponding ROC curves (Figure.2).

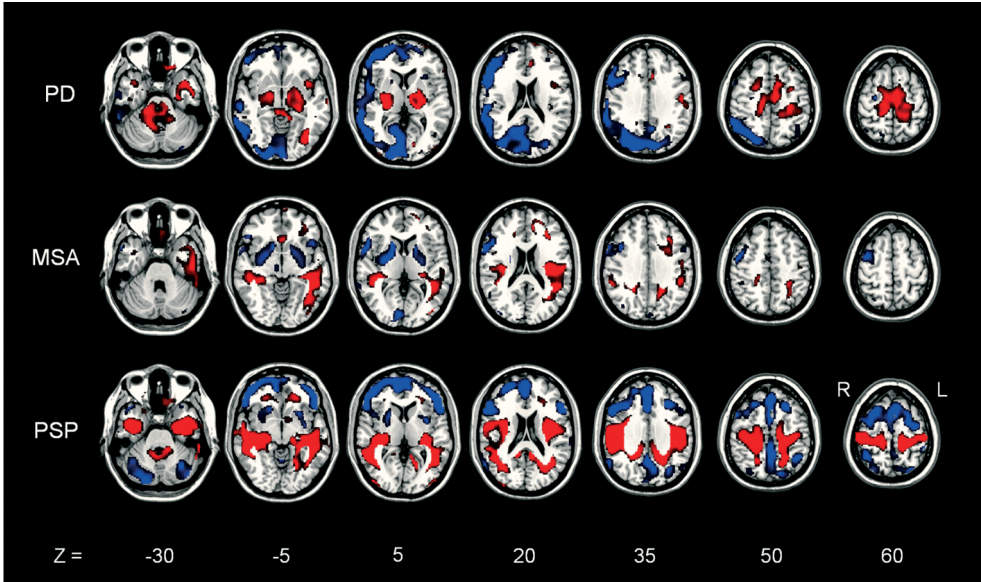


Figure 1: (T) maps of metabolic brain patterns were overlaid on a T1 MR template. Relative metabolic decreases (blue) and increases (red) compared to the control group are thresholded at $T=3.7-6.7$ ($P < 0.001$). Patient groups are indicated on the vertical axis and on the horizontal axis seven transversal slices through the brain are shown.

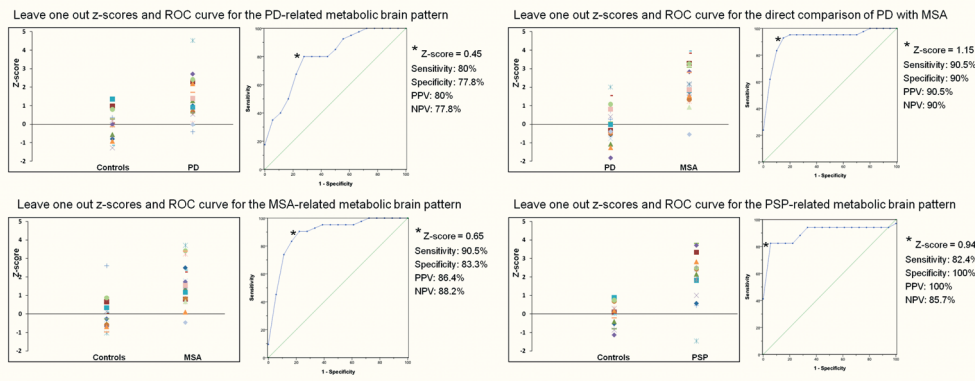


Figure 2: Scatter plot and ROC curves for each comparison. On the Y-axis the leave-one-out z-scores are displayed and on the X-axis the group comparisons. Receiving-operating-characteristic (ROC) curves were plotted for each comparison separately. * = inflection point (z-score); Y-axis= sensitivity, X-axis= 1-specificity; PPV = positive predictive value; NPV = negative predictive value.

The PD-related metabolic covariance pattern was characterized by relative metabolic decreases, especially contralateral to the affected body side in most patients, comprising the (posterior) parietal association cortex, visual cortex, lateral premotor and prefrontal association cortex. Relative increases were seen in the pons, bilateral thalamus, pallidum, dorsal putamen, primary motor cortex and supplementary MSA-related area. Their corresponding z-scores showed an overlap between the patients and healthy controls using the PD-related metabolic pattern. A cut-off value of $z=0.45$

resulted in a sensitivity of 80% and specificity of 77.8% for correct PD classification of an individual patient.

The MSA-related metabolic covariance pattern was characterized by relative metabolic decreases bilaterally in the putamen and caudate nucleus with minor decreases in the premotor and primary visual cortex on the right side. At a lower threshold ($p < 0.05$) metabolic decreases were seen in the cerebellum (data not shown). Relative increases were seen in the subcortical white matter and mid-temporal cortex. Their corresponding z-scores showed less overlap between the patients and healthy controls and at a cut-off value of $z = 0.65$, the MSA-related metabolic pattern had a sensitivity of 90.5% and specificity of 83.3%. A direct comparison between PD and MSA patients, which is clinically relevant, improved specificity to 90%.

The PSP-related metabolic covariance pattern was characterized by relative metabolic decreases bilaterally in prefrontal cortex regions, cingulate cortex, frontal eye fields and minor decreases in the posterior parietal association cortex, caudate nucleus, ventral putamen and cerebellum crus. At a lower threshold ($p < 0.05$) metabolic decreases were seen in thalamus and mesencephalon (data not shown). Relative increases were seen in the inferior- and mid-temporal cortex, subcortical white matter, sensorimotor cortex, pons and vermis.

The PSP-corresponding z-scores showed virtually no overlap with healthy controls. Using the PSP-related metabolic pattern at a cut-off value of $z = 0.94$, sensitivity was 82.4% and specificity of 100% (Figure.2).

5.4 DISCUSSION

Metabolic covariance patterns for PD, MSA and PSP obtained by SSM/PCA and leave-one-out cross validation in our patients were in agreement with previous studies (Eckert et al. 2008, Ma et al. 2007a). These patterns showed high sensitivity and specificity, supporting that these image-based classifications may improve clinical practice concerning diagnosing individual parkinsonian patients.

High stability and reproducibility of these metabolic covariance patterns was previously suggested by respectively a region-defined approach (Moeller et al. 1999), a test-retest design (Ma et al. 2007a) and in a cross-validation approach (Spetsieris et al. 2010), all by the same research group. This is now confirmed by the present study.

The next step is to prove the value in clinical practice. Tang et al have already demonstrated an image-based classification routine with high specificity to distinguish between parkinsonian patients (Tang et al. 2010b). In our present study we showed that the "simple" comparison between healthy controls and patient groups already yielded a high sensitivity and specificity for correctly classifying PD, MSA or PSP patients. Especially specificity increased by directly comparing PD and MSA, which is relevant because the clinical motivation for a FDG-PET originates from doubts between PD or MSA, not between healthy or PD.

The current clinical diagnosis is made by expert movement disorder specialists, although

neuropathological confirmation is considered to be more accurate. However, Hughes concluded that in case of a thorough examination made by expert movement disorder specialist using clinical research criteria and a sufficient follow up period, a sensitivity of 91.1% for PD, 88.2% for MSA and 84.2% for PSP compared to neuropathological examination can be found (Hughes et al. 2002). In general neurological practice, diagnostic accuracy is around 76% (Hughes et al. 1992). Therefore, the metabolic brain pattern results, obtained at early disease stage, represent high values of specificity and sensitivity and are especially beneficial in the early differential diagnosis of parkinsonian patients.

Further data inclusion will increase sensitivity and specificity of the listed metabolic brain patterns and will enable subclassifications in for example left/right body-side affected patients. The Eidelberg research group has already shown PD subclassifications related to specific symptoms (tremor, cognition) (Huang et al. 2007a, Mure et al. 2011, Poston and Eidelberg. 2009). Application of this method may also be useful for other parkinsonian and dementia syndromes to enhance diagnostic precision. This puts forward a research challenge to improve the SSM/PCA method. Regarding previous suggestions to select components used for creating a disease-related metabolic pattern (Spetsieris and Eidelberg. 2010), one might consider machine learning approaches like decision-tree methods to improve sensitivity and specificity (Quinlan. 1993).

5.6 CONCLUSION

The applied image-based classifications imply that an early diagnosis is feasible by quantifying the magnitude of the expression of different disease-related metabolic brain patterns through subject scores for individual parkinsonian patients.

CHAPTER 6

THE ALZHEIMER'S DISEASE-RELATED GLUCOSE METABOLIC BRAIN PATTERN

L.K. TEUNE¹, F. STRUKERT², R.J. RENKEN³, G.J. IZAKS^{2,4}, J.J. DE VRIES^{1,4},
M. SEGBERS⁵, J.B.T.M. ROERDINK⁶, R.A. DIERCKX⁵ AND K.L. LEENDERS¹

¹Department of Neurology, University Medical Center Groningen, ²University Center for Geriatric Medicine, University Medical Center Groningen, ³NeuroImaging Center, University Medical Center Groningen, ⁴Alzheimer Center Groningen, University Medical Center Groningen, ⁵Nuclear Medicine & Molecular Imaging, University Medical Center Groningen, Johann ⁶Bernoulli Institute for Mathematics and Computer Science, University of Groningen, the Netherlands

Submitted

ABSTRACT

Introduction: [^{18}F]fluorodeoxyglucose (FDG) PET imaging of the brain can be used to assist in the differential diagnosis of dementia. Group differences in regional cerebral glucose utilisation of patients with dementia compared to controls are well-known. However, multivariate analysis techniques aiming at identifying diagnostic neural networks in diseases, have been applied less frequently. The aim of this study was to present and validate an Alzheimer's disease-related (AD) glucose metabolic brain pattern and to apply it prospectively in a second cohort of individual patients with memory complaints.

Methods: As a first step, we used a multivariate analysis technique (scaled subprofile model, principal component analysis (SSM/PCA)) to identify an AD-related glucose metabolic covariance pattern in 18 healthy controls and 15 AD patients (identification cohort). The stability of the results was evaluated by a leave-one-out cross validation.

Next, we investigated the ability of the identified AD-related metabolic covariance pattern to discriminate between probable AD and non-probable AD (possible AD, mild cognitive impairment (MCI) or subjective complaints) and the association of the metabolic patterns with neuropsychological tests. This part of the study was done in an independent cohort of 15 patients referred to our memory clinic (confirmation cohort). Pattern expression was quantified as a z-score calculated on a single-case basis.

Results: The AD-related metabolic covariance pattern was calculated on the identification cohort and was characterized by relatively decreased metabolic activity in the temporal and parietal regions and relatively increased metabolic activity in the subcortical white matter, cerebellum and sensorimotor cortex. Receiver-operating characteristic (ROC) curves were determined in cohort identification cohort. At a cut-off value of $z=0.65$, a sensitivity of 93% and a specificity of 94% for correct AD classification were determined. In the confirmation cohort, all the subjects with clinically probable AD diagnosis showed a high expression of the AD-related pattern whereas in all the subjects with a non-probable AD diagnosis a low expression was found. The mean Z-scores between probable and non-probable AD patients differed significantly (Mann-Whitney U-test, $p<0.000$) and correlated significantly with neuropsychological tests.

Conclusion: The Alzheimer's disease-related cerebral glucose metabolic covariance pattern identified by SSM/PCA analysis was highly sensitive and specific for Alzheimer's disease. This method is expected to be helpful in the early diagnosis of Alzheimer's disease in clinical practice.

6.1 INTRODUCTION

Alzheimer's disease (AD) is a progressive neurodegenerative brain disease accounting for 50-60% of cases of dementia. AD is characterized by a severe decline in episodic memory together with general cognitive symptoms such as impaired judgement, decision making and orientation (McKhann et al. 1984). Other types of dementia are dementia with Lewy Bodies (DLB) and frontotemporal dementia (FTD) which together account for 15-25% of dementia cases (Gauthier et al. 2006). A correct clinical diagnosis may be difficult, especially in early disease stages or in patients with for example comorbid depression, higher education or younger age (Bohnen et al. 2012).

[¹⁸F]fluorodeoxyglucose (FDG) PET imaging of the brain can be used to assist in the differential diagnosis of dementia (Bohnen et al. 2012). In AD, a decline of FDG uptake in posterior cingulate, temporoparietal and prefrontal association cortex - representing a reduction of the first step of the glycolysis and thus the energy consumption in those brain regions - has been related to dementia severity (Herholz et al. 2002). Foster used visual interpretation of FDG-PET scans and statistical maps of patients with AD and FTD (Foster, et al. 2007). They showed that visual interpretation of regional brain glucose consumption is more reliable and accurate in distinguishing FTD from AD than clinical methods alone. Minoshima examined brain glucose metabolism of autopsy proven dementia with Lewy Bodies (DLB) and AD using an automated three-dimensional stereotactic surface projection technique (Minoshima et al. 2001). A significant metabolic reduction in the occipital cortex, including the primary visual cortex, in patients suffering from DLB compared to AD was found. We performed a retrospective study (Teune et al. 2010) selecting typical patients with parkinsonian and dementia syndromes, including AD, who had an FDG-PET scan at an early disease stage and a clear clinical diagnosis at follow-up. Disease-specific regional cerebral differences in FDG uptake were found in all seven studied diseases using univariate voxel-based statistical parametric mapping (SPM) analyses comparing patient groups and healthy volunteers. In AD patients, most prominent decreases in metabolic activity were found in the angular gyrus and other parieto-temporal regions including precuneus extending to the posterior- and middle cingulate gyrus.

Multivariate techniques like the scaled subprofile model/principal component analysis (SSM/PCA) are able to show information about underlying relationships between brain regions that are not captured by univariate techniques like SPM (Eidelberg, 2009, Habeck et al. 2008). In parkinsonian syndromes, SSM/PCA is increasingly used to study pathophysiological mechanisms and to assist in the differential diagnosis (Eckert et al. 2008, Ma et al. 2007a, Poston et al. 2012, Tang et al. 2010b, Teune et al. 2013). Huang used the SSM/PCA approach to identify specific spatial covariance patterns related to cognitive function in non-demented PD patients in addition to the previously found motor-related covariance pattern (Huang et al. 2007b).

However, almost no multivariate SSM/PCA techniques in patients with dementia, including Alzheimer's disease, have been applied.

The first study that tried to apply this technique in patients with AD was presented by Scarmeas by using radiolabelled water (H₂¹⁵O)-PET scans to measure brain perfusion (Scarmeas et al. 2004).

They found sensitivities between 76-94% and specificities between 63-81% with considerable overlap in pattern expression among AD patients and controls. Therefore they concluded that the derived perfusion pattern cannot be used as a sufficient diagnostic test in clinical settings. Habeck performed univariate and multivariate discriminant analysis of brain FDG-PET scans to evaluate their ability to identify AD (Habeck, et al. 2008). They concluded that multivariate measures of AD utilize the covariance structure of imaging data and provide complementary, clinically relevant information that may be superior to univariate measures (Habeck, et al. 2008). In a parallel study by the same research group an AD-related spatial covariance pattern was identified using continuous arterial spin labelling (CASL-MRI) (Asllani et al. 2008). However, they pointed out that it was necessary to do further research regarding specificity and stability of the covariance patterns, before it can be used in clinical practice.

In this study we present and validate the Alzheimer's disease-related glucose metabolic brain pattern using the SSM/PCA analysis identified in a cohort of AD patients with a clinical diagnosis according to the the clinical research criteria for AD (McKhann et al. 1984) and scanned at an early disease stage. Furthermore, we tested this AD-related metabolic brain pattern prospectively in a second confirmation cohort of patients with memory complaints ranging from subjective complaints to probable AD and correlated it with the patients' performance on neuropsychological tests.

6.2 METHODS

6.2.1 Patients

Identification cohort

To identify AD-related metabolic brain patterns, we used data from a sample that was included in a previous study (Teune et al. 2010). This sample comprised 18 healthy controls and 15 patients with a diagnosis of AD according to the NINCDS-ADRDA clinical criteria (McKhann et al. 1984). The mean age of the 15 included AD patients was 65 ± 10 years (mean \pm SD) and disease duration at the time of the FDG-PET scan 3 ± 2 years. The diagnosis was confirmed during a follow-up time after scanning of 3 ± 2 years. These 15 AD patients and 18 healthy controls were used to identify an AD-related metabolic brain pattern.

Confirmation cohort

The AD-related metabolic brain pattern that was identified in the identification cohort was prospectively tested in an independent confirmation cohort. Inclusion criteria for the individual patients in the confirmation cohort were a referral to the UMCG Center for Geriatric Medicine with a complaint of memory loss, a formal neuropsychological examination, and a FDG-PET scan. All patients gave written informed consent. In total 15 patients could be included in the present

analysis. Of these 15 patients, 9 patients (age 71 ± 5 ; DD 3 ± 1) were diagnosed as having probable AD according to the clinical research criteria for AD (McKhann, et al. 1984) by two independent dementia specialists (GI and JV), who were blinded to the outcome of the FDG-PET scan. Six patients were classified as non-probable AD (age 63 ± 11 ; DD 3 ± 2) (one possible AD, two MCI and three subjective complaints).

6.2.2 Neuropsychological examination

Patients in the confirmation cohort suspected having dementia received an extensive neuropsychological examination, covering several cognitive domains, including Mini Mental State Examination (MMSE) (Folstein et al. 1975); Dutch version: Kok & Verhey, 2002), for general cognitive function and orientation. Verbal memory (immediate recall, delayed recall, and recognition) was assessed with the Dutch version of the Rey Verbal Learning Test (RAVLT) (Saan and Deelman. 1986). Visual memory function (recall of cue- and association cards) was assessed with Visual Association Test (Lindeboom et al. 2002). Furthermore, attention and processing speed was assessed with the Stroop Colour Word Task (Stroop. 1935) and Trailmaking Test A & B (Reitan R. 1958). Language was assessed by naming and category fluency; and visuospatial function and construction with the Clock Drawing and Visual Object and Space Perception (VOSP, subtests Incomplete Letters and Dot Counting) (Warrington and James 1991). Executive function was assessed with the Dutch version of the Frontal Assessment Battery (FAB) (Dubois et al. 2000) the Trailmaking Test part B and the Key Search task of the Behavioral Assessment of the Dysexecutive Syndrome (BADS) (Wilson et al. 1996)

6.2.3 FDG-PET scan acquisition

Patients were scanned 30 minutes after injection of approximately 200 MBq FDG in 4ml saline using a Siemens ECAT HR+ PET scanner or for some patients in the confirmation cohort, a Siemens Biograph mCT camera in a 3D mode under standard resting conditions with the eyes closed. All reconstructed FDG-PET images were spatially normalized using the PET template supplied in SPM8 and smoothed with a 10 mm full-width at half-maximum (FWHM) isotropic Gaussian kernel in the identification cohort and 12 mm for the individual patients in the confirmation cohort. (SPM8; Functional Imaging Laboratory, running in Matlab 7.10.0 (R2010a, Mathworks))

6.2.4 FDG-PET statistical analysis

Identification cohort

SSM/PCA was applied using software written in-house, based on the methods of Spetsieris and Eidelberg (Eidelberg. 2009, Spetsieris and Eidelberg. 2010). A 35% threshold of the whole-brain intensity maximum was applied to remove out-of-brain voxels which results in a mask of mainly grey matter, followed by a log transformation. After removing between-subject and between-region averages, a principal component analysis (PCA) was applied. All components that together

described at least 50% of the variance were used for further analysis. A disease-related metabolic covariance pattern was determined by a linear combination of the selected principal components with the lowest AIC (Akaike information criterion) value (Akaike, 1974) in a stepwise regression procedure. Thereafter, a leave-one-out cross validation procedure was performed, resulting in subject scores independent from the pattern identification step and providing an estimate of the disease-related metabolic brain patterns and their variances. By dividing the estimate by its variance a T-score was obtained. Resulting patterns were thresholded at $T > 3.7$ (corresponding to $p < 0.001$, assuming normality of the data) and overlaid onto a T1 MR template using MRIcron.

Subject scores were transformed into z-scores with respect to the healthy control population and displayed, for each comparison separately, in a scatter plot. Receiving-operating-characteristic (ROC) curves were determined for the probability values of AD. Optimum cut-off probability values for classifying individual patients were calculated by identifying an inflection point on each ROC curve that corresponded to the best combination of sensitivity and specificity. Patients were classified as correctly diagnosed if their probability value was higher than the cut-off value. Thereafter, we calculated sensitivity, specificity, and positive and negative predictive value (PPV and NPV respectively).

Confirmation cohort

For each of the fifteen individual patients, individual subject-scores were obtained for the expression of the AD-related metabolic brain pattern defined using cohort 1. These subject scores were transformed into z-scores with respect to the healthy control population and displayed separately for the probable and non-probable AD, in a scatter plot.

6.3 RESULTS

AD-related metabolic brain pattern calculated using the identification cohort

The first four principal components accounted for 55% of the explained variance. In a stepwise regression model the lowest AIC value was calculated. The model with the lowest AIC value and hereafter considered as disease-related was determined by principal components 1 and 3 (36%). This AD-related covariance pattern was characterized by bilateral relatively decreased metabolic activity in the bilateral temporal regions, precuneus, posterior cingulate and angular gyrus, the inferior parietal region and supramarginalis. Relatively increased metabolic activity was seen in the subcortical white matter, cerebellum and sensorimotor cortex. (See figure 1 a) Their corresponding z-scores showed an overlap between the patients and healthy controls using the AD-related metabolic pattern. A cut-off value of $z=0.65$ resulted in a sensitivity and positive predictive value of 93% and specificity and negative predictive value of 94% for correct AD classification of an individual patient. (See figure 1 b)

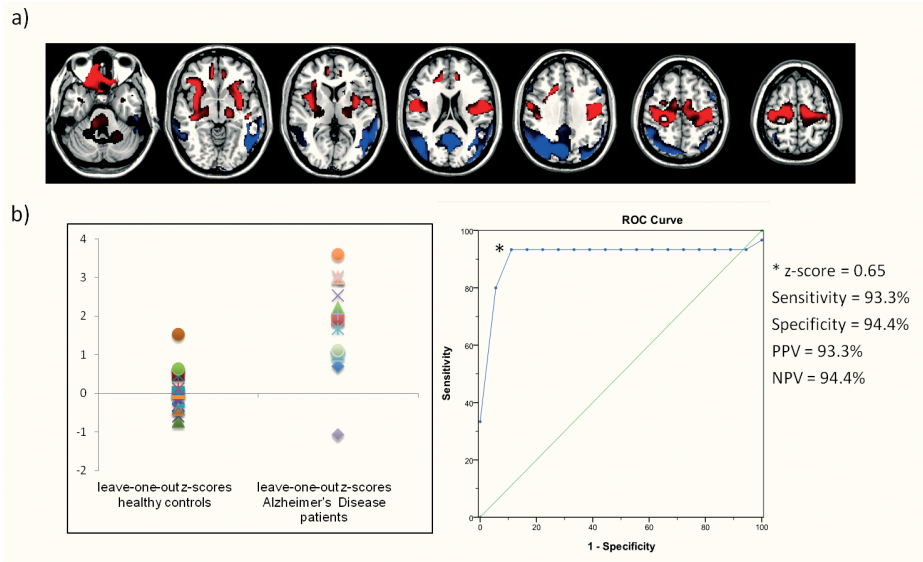


Figure 1:
 a) A (T) map of the AD-related metabolic brain pattern using cohort 1 was overlaid on a T1 MR template. Relative metabolic decreases (blue) and increases (red) compared to the control group are thresholded at $T = 3.7-6.7$ ($P < 0.001$). Seven transversal slices through the brain are shown.
 b) Scatter plot and ROC curves for the AD-related metabolic brain pattern. On the Y-axis the leave-one-out z-scores are displayed and on the X-axis the group comparison of health controls vs AD. Receiving-operating-characteristic (ROC) curves were plotted for each comparison separately. * = inflection point (z-score); Y-axis= sensitivity, X-axis= 1-specificity; PPV = positive predictive value; NPV = negative predictive value.

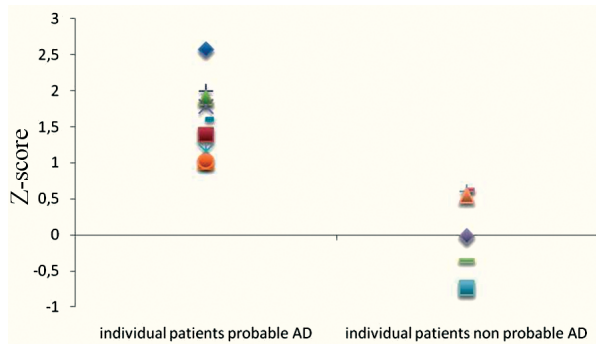


Figure 2: Scatter plot of the individual patients with probable AD and non-probable AD of cohort 2 is displayed. On the Y-axis the leave-one-out z-scores are displayed and on the X-axis the individual patients with probable AD and non-probable AD.

AD-related pattern expression in the confirmation cohort.

The Z-scores of the fifteen individual subjects representing the AD-related pattern expression are displayed in figure 2. Table 1 displays correlations with the AD pattern Z-score and the neuropsychological profiles.

MMSE and RAVLT immediate- and delayed recall showed significant negative correlations with AD pattern scores, suggesting that subjects with a low score on memory tasks had a higher Z-score for the AD-related metabolic brain pattern. In the attention and information processing speed domain, Stroop Color/Word interference task and Trailmaking Test part A & B, significant positive correlations with AD pattern expression were shown. High scores on the tasks for attention and speed reflect a worse performance.

Moderate to high, however non-significant, correlations (negative and positive) were found between AD pattern expressions and Visual Association Test, Category Fluency, Clock Drawing, Stroop Color naming, and Frontal Assessment Battery.

Differences in pattern expression between the 9 probable AD patients and the 6 non-probable AD patients were assessed using the Mann-Whitney U-test. Mean of the Z-score of the probable AD-group was 1.6 and of the non-probable group 0.11 ($p < 0.000$).

6.4 DISCUSSION

The Alzheimer disease-related metabolic brain pattern presented in this study and obtained using FDG-PET scans and SSM/PCA analysis showed high sensitivity and specificity.

We have shown that individual patients within the independent confirmation cohort with a diagnosis of non-probable AD (minimal or mild cognitive impairment) had a low Z-score for the AD-related metabolic brain pattern and patients with a diagnosis of probable AD had a high Z-score for the AD-related pattern. Moreover, there was no overlap in z-scores between the individual subjects with probable AD and subjects with non-probable AD.

Sensitivity and specificity of the identified metabolic brain pattern is higher in our study compared to the study of Scarmeas et al. This is possibly related to the lower signal-to-noise ratio of the $H_2^{15}O$ -PET scans in their study. As Scarmeas suggested already in 2004, the fact that expression of the identified pattern correlated with functional and cognitive measures in a population whose PET data were not used to derive the pattern, provides strong evidence for its validity (Scarmeas et al. 2004). This has now been confirmed by our study presented here.

Moreover, sensitivity and specificity are comparable to those found in larger studies including neuropathological confirmation (Bohnen et al. 2012). These authors concluded that even in the situations in which FDG-PET disagreed with the clinical diagnosis, the correct pathological diagnosis was more likely to be congruent with FDG-PET than with the initial clinical diagnosis.

The brain regions we found using the SSM/PCA analysis are comparable to the regions we already identified using a univariate analysis in AD patients (Teune et al. 2010). The benefit of the current approach is the ability to provide information about the way that brain areas co-vary with each other and to yield per subject a quantifiable expression (a Z-score) of the AD-related pathological pattern of neuronal degeneration. These Z-scores also correlated significantly with several neuropsychological tests. Significant negative correlations were found between the pattern and two memory subtests (RAVLT immediate and delayed recall) while significant positive

correlations were found between two tasks for attention and processing speed and the pattern. Low scores on memory tests and high scores on attention and speed tasks reflect a worse performance. This indicates that patients who performed worse on cognitive tests had a higher Z-score for the AD-related glucose metabolic brain pattern which in turn reflects a glucose metabolism distribution pattern in the brain similar to Alzheimer's disease pathological patterns.

After being taken up by the brain, glucose or its radiotracer analogue [^{18}F]fluoro-deoxyglucose, are phosphorylated by hexokinase to glucose-6- PO_4 or fluorodeoxyglucose-6- PO_4 , the first step of the glycolytic process. However, FDG being a deoxy variant of glucose is not a substrate for further metabolism and consequently trapped in brain tissue for the duration of the scanning procedure. Thus the outcome measure of regional cerebral FDG-uptake measured by PET is the first step of the glycolysis. From the early days on FDG has remained the only available radiotracer to detect accurately and reliably the cerebral glucose metabolism (Reivich, et al. 1979). As glucose is the only source of energy for the brain in normal conditions it reflects the energy needs of underlying brain neuronal systems. The detected disease-related altered metabolic brain patterns using FDG-PET is therefore reflecting the underlying pathological alterations of the affected brain regions. Since a few years FDG is commercially available and being used in many Nuclear Medicine Departments worldwide. Until recently the here presented statistical analysis techniques were not available for use in clinical practice, but can now be applied at a large scale.

Quantifying the magnitude of the expression of an AD-related metabolic covariance pattern on a single case basis may thus aid in the differential diagnosis of dementia. However, apart from confirming the diagnosis of AD in an individual patient it will also be necessary to determine the abnormal brain patterns in other dementing conditions such as in frontotemporal dementia or dementia with Lewy Bodies in order to make the differential diagnosis of dementia more powerful. It will be clear that further elaboration of dementia patterns largely depend on the correct selection of the needed reference patient groups for the identification procedure.

6.5 CONCLUSION

The Alzheimer's disease-related cerebral glucose metabolic covariance pattern identified by SSM/PCA analysis was highly sensitive and specific for Alzheimer's disease. Individual patients within the confirmation cohort with a diagnosis of probable AD had a high Z-score for the AD-related metabolic brain pattern, whereas patients with a diagnosis of non-probable AD had a low Z-score for the AD-related metabolic brain pattern. This method is expected to be helpful in the early diagnosis of Alzheimer's disease in clinical practice.

CHAPTER 7

GLUCOSE IMAGING IN PARKINSONISMS

GLIMPS

A NATIONAL DATABASE

PROVIDING ASSISTANCE IN THE CLINICAL DIAGNOSIS OF PATIENTS WITH NEURODEGENERATIVE
BRAIN DISEASES

In this chapter we present the prospective Dutch multicenter imaging project GLucose IMaging in ParkinsonismS (GLIMPS).

It involves the establishment of a database of FDG-PET scans that depicts the glucose consumption of the brain in patients with neurodegenerative brain diseases.

The project aims at testing the feasibility of a novel image-based classification algorithm for the accurate and early individual diagnosis of patients with neurodegenerative brain diseases.

7.1 FDG-PET IMAGING IN CLINICAL PRACTICE

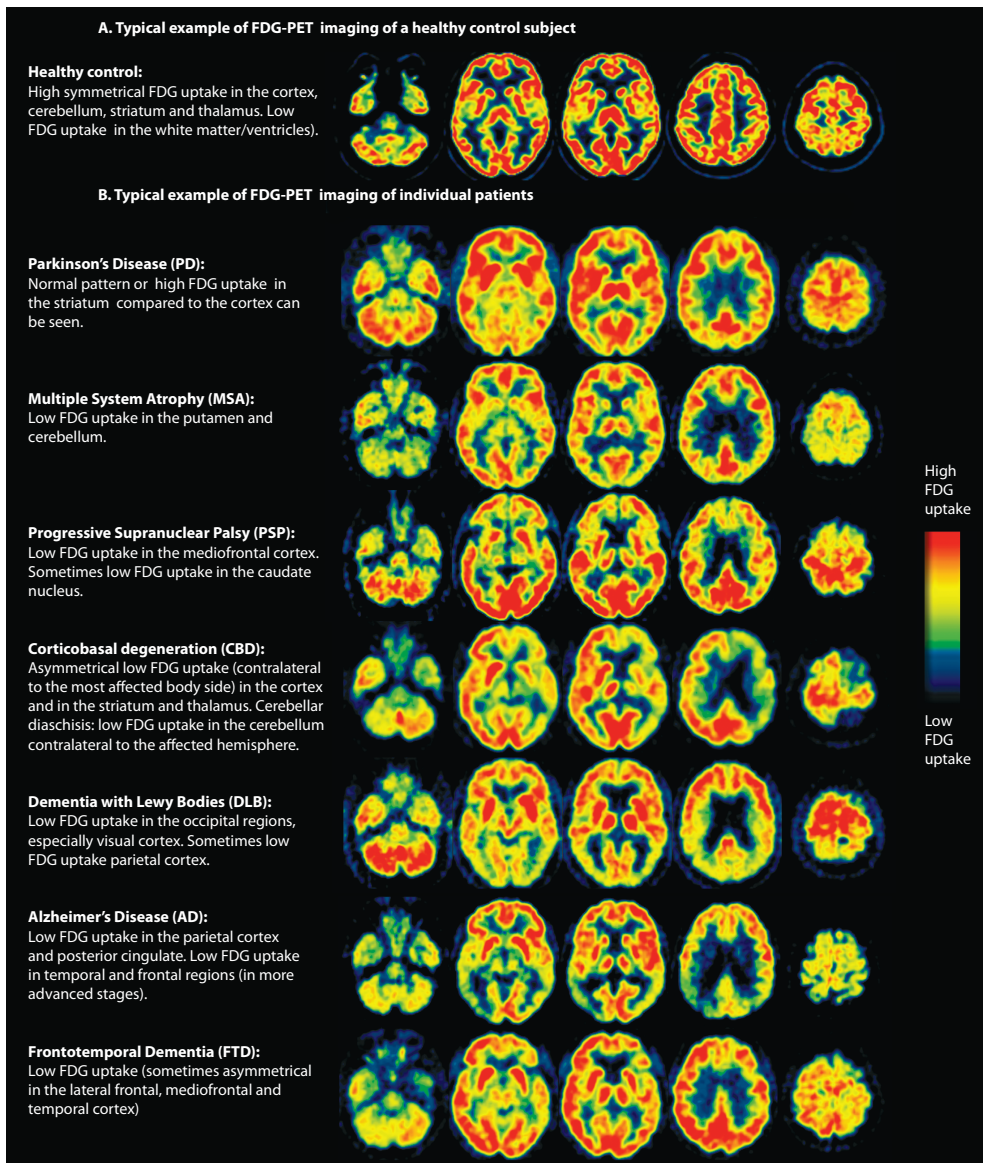
[18F]-fluoro-deoxyglucose positron emission tomography (FDG-PET) imaging is an easy and stable radiotracer method validated extensively through the years. FDG is only in recent years commercially available and being used in all the larger Nuclear Medicine Departments worldwide. FDG has remained the only available radiotracer to detect accurately and reliably the cerebral glucose metabolism. As glucose is the only source of energy for the brain it reflects the energy needs of underlying brain neuronal systems. After being taken up by the brain, glucose or its radiotracer analogue FDG, are phosphorylated by hexokinase to glucose-6-PO₄ or fluorodeoxyglucose-6-PO₄, the first step of the glycolytic process. However, FDG being a deoxy variant of glucose, is not a substrate for further metabolism and consequently trapped in brain tissue for the duration of the scanning procedure. Thus the outcome measure of regional cerebral FDG-uptake measured by FDG-PET is the first step of the glycolysis. The detected disease-specific metabolic brain patterns using FDG-PET are therefore reflecting the underlying pathological alterations of the affected brain regions. Specific brain regions degenerate and different patterns of altered glucose metabolic brain activity develop in various neurodegenerative brain diseases (**box 1**).

7.2 FDG-PET IMAGE ANALYSIS TECHNIQUES

At an early disease stage, visual interpretation of FDG-PET images can be difficult, even for experienced specialists. As already mentioned in the previous chapters, measurement of glucose consumption with FDG-PET imaging allows us to identify disease-specific cerebral metabolic brain patterns in several neurodegenerative brain diseases at an early disease stage, using the multivariate statistical analysis technique, called, Scaled Subprofile modelling/ principal component analysis (SSM/PCA).

An important question is whether an early diagnosis of neurodegenerative brain disease in one individual is possible when individual metabolic patterns are compared with a database of disease-specific metabolic brain patterns. It is possible to calculate a subject score by multiplying every voxel value in a subject scan by the corresponding voxel weight in the disease-related metabolic covariance pattern, with a subsequent summation over the whole brain volume. The obtained subject score indicates to what extent that patient expresses the disease-related pattern. In this way we can prospectively calculate subject scores of an individual patient for to date identified PD, MSA, PSP and AD disease-specific metabolic brain patterns. See **box 2** for examples of 2 patient cases.

Box 1



7.3 GLIMPS DESIGN AND GOAL

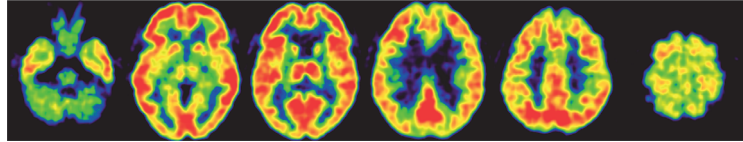
The GLIMPS project has been initiated to create a national database of FDG-PET images of patients in different disease categories together with their specific clinical information.

Starting-point of the project must be the practical clinical situation of a patient who is suspected of having a neurodegenerative brain disease and in whom the physician has a clinical reason to perform an FDG-PET scan. The FDG-PET scan must be considered as a useful diagnostic tool for

Box 2

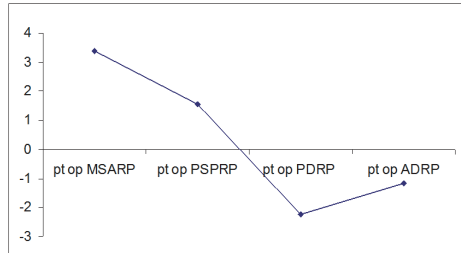
Case 1: A woman of 44 years old came for a second opinion. Since three years she was suffering from fatigue, slowness, stiffness in the limbs more left than right. At neurological examination she had a high score (40 points) on the Unified Parkinson's Disease rating scale (UPDRS) motor part 3. Under the suspicion of Parkinson's Disease her levodopa medication was increased. After several years and a moderate effect on levodopa, she had an accelerated progression of her symptoms: she had difficulty swallowing, urine incontinence and she was wheel chair bound. The physician doubted about the initial diagnosis and therefore requested an FDG-PET scan with the following question: Are there metabolic deficits compatible with MSA?

FDG-PETscan:



SSM-PCA method:

Subjectscore (Z-score) of 1 patient compared with the MSA, PSP, PD and AD disease-related glucose metabolic pattern



Outcome visual examination of the FDG-PET scan:

Low FDG uptake in putamen and cerebellum compatible with MSA

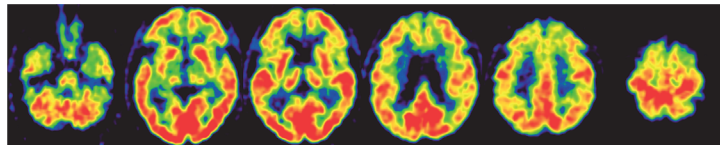
Z-scores calculated with the SSM-PCA method:

Increased expression of the MSA disease-related pattern

Conclusion: MSA

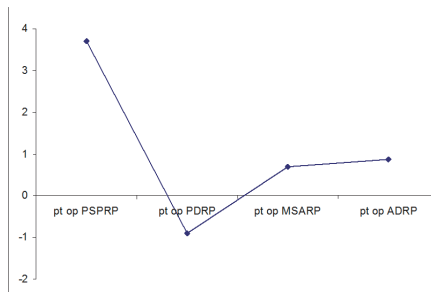
Case 2: A men of 72 years came to the outpatient department. Since 7 years he had progressive problems with memory, walking, balance and general slowness. At neurological examination he had a mask face, vertical gaze palsy, bilateral and axial rigidity, bradykinesia and frontal executive dysfunction. The physician suspected PSP. To strengthen this diagnosis he requested an FDG-PET scan with the following question: Is there mediofrontal hypometabolism compatible with PSP?

FDG-PETscan:



SSM-PCA method:

Subjectscore (Z-score) of 1 patient compared with the PSP, PD, MSA and AD disease-related glucose metabolic pattern



Outcome visual examination of the FDG-PET scan:

Mediofrontal hypometabolism compatible with PSP

Z-scores calculated with the SSM-PCA method:

Increased expression of the PSP disease-related pattern

Conclusion: PSP

doctor and patient to determine the global and regional glucose consumption in the brain.

The first goal of the project is the benefit in clinical practice by assisting in the differential diagnosis of neurodegenerative brain diseases in individual patients. The possible presence of a disease-specific metabolic brain pattern in an individual patient will be calculated by applying the image-based classification algorithm for the to date identified metabolic brain patterns. The outcome of the classification algorithm will be compared to the final clinical diagnosis to evaluate the effectiveness of the proposed new technique. A second goal is to develop further the glucose metabolic brain patterns in different disease categories in specific scientific projects. It will be clear that further elaboration of glucose metabolic brain patterns for neurodegenerative brain diseases largely depend on the correct selection of the necessary reference patient groups for the identification procedure.

Expanding the sample size will also increase sensitivity and specificity of the listed metabolic brain patterns and will enable subclassifications in for example left/right body-side affected patients. Furthermore, a large control sample consisting of enough patients within different age categories is important to study differences in for example man and women, right left handedness and to see differences in brain patterns in an aging population. In this way, patient care focused on the early differential diagnosis of patients with neurodegenerative brain diseases is expected to improve.

7.4 GLIMPS ORGANISATION

This project has been initiated by the Department of Neurology of the University Medical Center Groningen (UMCG) and is coordinated in close collaboration with the Department of Nuclear Medicine and Molecular Imaging (NGMB) in the UMCG, Neuro Imaging Center (NIC) and the Johann Bernoulli Institute for Mathematics and Computer Science (Scientific Visualisation and Computer Graphics group) at the RUG. Expertise center TARGET is involved to develop and maintain the GLIMPS database. Researchers and physicians of these departments together form the GLIMPS project group (see our website www.glimpsproject.com)

7.4.1 Department of Neurology

GLIMPS forms part of the main longstanding research topics of the department of Neurology at the UMCG i.e. clinical and pathophysiological studies of movement disorders in particular Parkinson's disease within the context of Molecular Mechanisms of Neurodegeneration. The department is playing an important role in the development of the protocol. It includes the information for patients, clinical parameters which need to be collected, clinical research criteria and the latest version of the image acquisition and scanning protocols. Selection of patients takes place at the outpatient Neurology department. Inclusion criteria for the GLIMPS project are patients who are suspected of having a neurodegenerative brain disease and in whom the physician has a clinical reason to perform an FDG-PET scan. These patients can be asked to participate in the GLIMPS project. After informed consent, clinical and scan information can be stored anonymously in the GLIMPS database.

7.4.2 Department of Nuclear Medicine and Molecular Imaging

The Department of Nuclear Medicine and Molecular Imaging at the UMCG provides daily performance of brain PET scans using radiotracers for common clinical use, like FDG ([F-18]fluoro-deoxy-glucose) and FDOPA ([F-18]fluoroDOPA), but also a range of experimental tracers. The department plays an important role in the GLIMPS project concerning image acquisition and reconstruction of the scans performed at the UMCG. Apart from that they have developed the GLIMPS image acquisition and scanning protocols in order to ensure that scans of different centers can be compared with each other.

7.4.3 Neuroimaging Center (NIC)

The NIC is a joint venture of the University Medical Center Groningen (UMCG) and the University of Groningen (RUG). Currently, it is equipped with a 3 Tesla MR-scanner, EEG and TMS equipment and data analysis facilities. Research is focused on using and improving neuroimaging techniques for behavioral and cognitive neurosciences. The NIC supervises the running of the image-based algorithms and further improves their performance as an image-analysis tool.

7.4.4 Scientific Visualisation and Computer Graphics

The Scientific Visualisation and Computer Graphics (SVCG) research group, within the Department of Computer Science, is part of the Johann Bernoulli Institute of Mathematics and Computer Science (JBI) of the University of Groningen, the Netherlands.

The group carries out research in the area of scientific visualization, information visualization, software visualization, multiscale shape analysis, illustrative computer graphics, and innovative interfaces using large displays. SVCG is participating in implementing the new versions of pattern recognition methods in the GLIMPS projects to be developed beyond the currently available image covariance techniques (Scaled Subprofile Model, SSM).

7.4.5 TARGET

The Donald Smits Center for Information Technology at the RUG, the Faculty of Mathematics and Natural Sciences together with the UMCG and other Institutions and companies have created the expertise center TARGET. Expertise center Target is building a sustainable economic cluster of intelligent sensor network information systems in the Northern part of the Netherlands, aimed at data management for very large amounts of data.

Target's role in GLIMPS is to develop and maintain the GLIMPS database, which will be hosted on the Target testbed, according to the functionality requirements of the project. All anonymous data is electronically transferred to the GLIMPS database. Target is also involved in ensuring smooth and reliable implementation of the image-based classification algorithm on its processing cluster facilities. In the end, the diagnosis based on the image-based classification algorithm will be compared to the clinical diagnosis to evaluate the effectiveness of the proposed new technique.

7.4.6. Other participating centers

Collaboration with other Dutch medical centers involved in our project will broaden our patient base and enable us to test the feasibility of this approach across different movement disorder clinics and imaging centers. At the moment more than 10 centers in the Netherlands are participating. It is the intention that the database and the classification model is developed in such a way that it should be useful in clinical practice for each participating center. Furthermore, scientific questions can be formulated by each participating center.

Internationally an important and intensive collaboration exists with the Feinstein group (Center for Neurosciences, from the Feinstein Institute for Medical Research, Manhasset, New York). This collaboration is most relevant since that group has many years of experience with the SSM/PCA method and provided the proof of principle of the method to be applied here. The Feinstein group will serve as international reference partner for our project.

7.5 GLIMPS in clinical practice

Clinical information and FDG-PET scan data will be electronically transferred in a secure and confidential manner to the GLIMPS database at TARGET of the RUG, where the image-based classification algorithm will be performed. Individual physicians of the departments of Neurology, geriatrics or nuclear medicine of each participating center will each receive a username and password which they can use to access the GLIMPS database. Each participating center has its own center number under which all patients of that center can be uploaded. Before patient information can be stored in the database, patients have to be informed about the purpose of the project and they have to sign informed consent for the anonymous storage of their patient data. After informed consent, clinical and scan information can be uploaded to the GLIMPS database. Before a referring physician can enter a new patient, he will receive a GLIMPS number which belongs to that patient. This number will need to be stored together with the medical chart of the patient, in order to inform the referring physician which patient belongs to which number. In this way the referring physician can access the own patient population so that necessary additions or repeated studies can be added. The data of patients of the other centers are not accessible. After complete upload of all necessary data, the image-based classification algorithm will be applied by the researchers of the GLIMPS project and feedback will be given within two weeks. This feedback will consist of z-scores of each of the known disease-related metabolic brain patterns (currently PD, MSA, PSP and AD, for an example of the feedback see box 2).

For the latest update of the GLIMPS protocol see our website www.glimpsproject.com.

CHAPTER 8

PARKINSON'S DISEASE-RELATED PERFUSION AND GLUCOSE METABOLIC BRAIN PATTERNS IDENTIFIED WITH PCASL-MRI AND FDG-PET IMAGING

L.K. TEUNE¹, R.J. RENKEN¹, B.M. DE JONG¹, A.T.M. WILLEMSSEN³, M.J.P. VAN OSCH⁴,
J.B.T.M. ROERDINK⁵, R.A. DIERCKX³ AND K.L. LEENDERS¹

¹Department of Neurology, University Medical Center Groningen, ²NeuroImaging Center, University Medical Center Groningen, ³Nuclear Medicine & Molecular Imaging, University Medical Center Groningen, ⁴Department of Radiology, Leiden University Medical Center, ⁵Johann Bernoulli Institute for Mathematics and Computer Science, University of Groningen, the Netherlands

Submitted

ABSTRACT

Under normal conditions, the spatial distribution of resting cerebral blood flow and cerebral metabolic rate of glucose are closely related. A relatively new magnetic resonance (MR) technique, pseudo-continuous arterial spin labeling (PCASL), was used to measure regional brain perfusion. Fourteen Parkinson's disease patients and seventeen healthy controls underwent [^{18}F]-fluorodeoxyglucose positron emission tomography (FDG-PET) imaging and PCASL-MRI to assess (dis)similarities between perfusion and glucose metabolism. Data were analyzed using scaled subprofile model/principal component analysis (SSM/PCA).

Unique Parkinson's disease-related perfusion and metabolic covariance patterns were identified, indicating that both methods contribute to the diagnosis of individual parkinsonian patients.

8.1 INTRODUCTION

For many years, nuclear imaging techniques have been used to visualize disease-related changes in brain perfusion and glucose metabolism in neurodegenerative brain diseases.

Sokoloff et al. were the first to report that under physiological steady state conditions, cerebral blood flow (CBF) is coupled to the level of cerebral oxygen ($CMRO_2$) and glucose consumption (Sokoloff, 1977). Leenders et al measured rCBF and r $CMRO_2$ in patients with Parkinson's disease (PD). They showed an increase of regional blood flow and oxygen metabolism in the basal ganglia of the affected hemisphere in PD patients with predominantly unilateral disease (Leenders et al. 1984a). In the 1980's, a SPECT tracer, ^{99m}Tc -hexamethylpropyleneamine oxime (^{99m}Tc -HM-PAO), was developed to detect cerebral blood flow with SPECT-imaging. The PET tracer [^{18}F]-fluorodeoxyglucose (FDG) allows the measurement of cerebral metabolic rate of glucose (CMR_{glc}). Regional differences in cerebral glucose metabolism have been reported in parkinsonian syndromes using univariate methods (Teune et al. 2010). Data-driven multivariate methods are increasingly used to examine disease-specific metabolic covariance patterns in parkinsonian syndromes (Ma et al. 2007a). This has improved our understanding of the pathophysiology of these diseases as well as our ability to diagnose patients at an earlier disease stage (Tang et al. 2010a, Teune et al. 2013). Ma reproduced this PD-related metabolic covariance pattern, using $H_2^{15}O$ PET scanning, indeed suggesting that cerebral blood flow and glucose metabolism are tightly coupled in PD patients (Ma et al. 2007a). However, in clinical practice, blood flow measurements with PET are not widely used because it is a demanding and time-consuming procedure, while spatial resolution of SPECT is less optimal. Recently, it has become possible to measure brain perfusion with a relatively new MR technique, pseudo-continuous Arterial Spin Labeling (PCASL). It permits the noninvasive measurement of perfusion with MRI by using a train of radio frequency (RF) pulses and magnetic field gradient pulses to achieve labeling of spins in flowing blood (Dai et al. 2008, van Osch et al. 2009). Ma et al analyzed the expression of the existing PD- related metabolic covariance pattern in a small number of parkinsonian patients using perfusion MRI (continuous arterial spin labeling) and concluded that perfusion MRI can be used for accurate quantification of disease-related covariance patterns (Ma et al. 2010a). Melzer et al were the first to identify a PD-related perfusion covariance pattern (Melzer et al. 2011). In this study we identified a PD-related perfusion and metabolic covariance pattern in the same patients using PCASL and FDG-PET imaging and assessed (dis)similarities in the disease-related pattern between perfusion and metabolism in PD patients.

8.2 PATIENTS & METHODS

8.2.1 Subjects

The study was approved by the medical ethics committee of the University Medical Center Groningen. Voluntary written informed consent was obtained from each subject after verbal and written explanation of the study, in accordance with the declaration of Helsinki. This study is part

of a larger study: in this part 14 PD patients (4 female, 10 male; mean age 63.8 years) and 17 gender and age-matched healthy controls (HC) (5 female, 12 male; mean age 61.5 years) participated. PD patients had to fulfill the UK brain Bank criteria for PD (Litvan et al. 2003). Healthy controls were not allowed to have first-degree family members with parkinsonism or dementia. All subjects underwent MRI and within 8 weeks an FDG-PET scan and two neuropsychological tests (Mini Mental State Examination (MMSE) and Frontal Assessment Battery (FAB)) and PD patients underwent the Unified Parkinson's Disease Rating Scale (UPDRS) part 3: motor symptoms. Neuropsychological scores did not differ between groups (mean HC: MMSE 29, FAB 17; mean PD: MMSE 28, FAB 16) indicating that PD patients were non-demented. PD patients had mild to moderate motor symptoms with Hoehn&Yahr stage: mean 1.3; standard deviation (SD) 0.5 and a UPDRS part 3: mean 18; SD 7. Antiparkinsonian medication was withheld for at least 12 hours and benzodiazepines 24 hours before MRI and FDG-PET scanning.

8.2.2 Image acquisition and preprocessing

MR imaging was performed on a 3T MRI scanner (Achieva 3 Tesla, Philips healthcare, Best, The Netherlands) using a standard 8-channel SENSE head coil. Subjects were wearing ear protection and instructed to lie still with their eyes closed, and to avoid falling asleep.

To enable PCASL imaging, the scanner was equipped with locally developed software. Pseudo-continuous labeling was performed by employing a train of Hanning-shaped RF pulses (tip angle 18° , duration 0.5ms) with an interpulse pause of 0.5 ms in combination with a balanced gradient scheme. PCASL images were obtained in a dynamic mode of 2x30 volumes (labeled and control) with an echo time of 14 ms, repetition time (TR) of 4200 ms, 23 axial slices, field of view (FOV) 240 mm with an 80x80 matrix and an isotropic voxel size of 3x3x6 mm. All 30 labeled and control volumes were first motion-corrected in SPM8 (Functional Imaging Laboratory, running in Matlab 7.10.0 (R2010a, Mathworks)). Volumes were smoothed with an 8 mm full-width-at-half-maximum isotropic Gaussian kernel (FWHM). Analogue to van Dijk (Van Dijk, et al. 2010), volumes were filtered against a time-course extracted from a ROI in white matter and liquor in order to diminish physiological noise. Thereafter, labeled perfusion-weighted images were subtracted from control images, creating one mean PCASL image per subject. These steps were performed using Matlab scripts developed in-house. Normalization with respect to the global mean is intrinsic in the used statistical analysis method (see below).

FDG-PET imaging was performed in a 3D mode using a Siemens Biograph mCT-64. Image acquisition was performed in a resting state with the subject's eyes closed in a dimly lighted room with minimal auditory stimulation. A 6-minute static frame was acquired starting 30 minutes after the injection of 200 MBq FDG in 4ml saline.

The FDG-PET images were iteratively reconstructed using the OSEM algorithm with 3 iterations and 24 subsets on a matrix of 400x400 and smoothed with 5 mm FWHM. No zoom was applied, resulting in images with an isotropic voxel-size of 2 mm with a specified resolution of 5 mm in the center of

the field of view. Scatter and attenuation correction were applied based on the acquired low dose CT.

A study-specific template of all mean PCASL images was spatially normalized to a standard brain PET template (Montreal Neurological Institute; MNI) using SPM8 and then used to spatially normalize the individual mean PCASL images. An example of the mean PCASL images of seventeen healthy controls is shown in Figure 1 a. FDG-PET images were directly spatially normalized to a PET template and then both were smoothed with 10 mm FWHM.

8.2.3 Statistical analysis

SSM/PCA was applied using software written in-house, based on methods of the Eidelberg research group (Spetsieris and Eidelberg, 2010). A 35% threshold of the whole-brain maximum was applied for FDG-PET images to remove out-of-brain voxels, which results in a mask of mainly grey matter, followed by a log transformation. This grey matter mask was then applied to the PCASL images without subsequent log transformation. After removing between-subject and between-region averages, a principal component analysis (PCA) was applied. All components that together described at least 50% of the variance were used for further analysis. A disease-related metabolic covariance pattern was determined by a linear combination of the selected principal components with the lowest AIC (Akaike information criterion) value in a stepwise regression procedure. Thereafter, a leave-one-out cross validation procedure was performed, resulting in subject scores independent from the pattern identification step. This provides an estimate of the disease-related metabolic brain patterns and their variances. By dividing the estimate by its variance a T-score was obtained. Resulting disease-specific metabolic and perfusion brain patterns were thresholded at $T=2.5$ (corresponding to $p<0.02$) and overlaid onto a T1 MR template using MRICron. Subject scores for the PD-related metabolic and perfusion patterns were transformed into z-scores with respect to the healthy control population. Moreover, z-scores of the PCASL images were calculated using the glucose metabolic covariance pattern as a reference. A correlation analysis was performed between z-scores of the PCASL- and FDG images on the PD-related glucose metabolic brain pattern.

8.3 RESULTS

The PD-related perfusion covariance pattern was characterized by relatively decreased cortical metabolic activity bilaterally in the temporal, insular, posterior parietal, inferior parietal, lateral occipital and prefrontal association cortex. Relative increases were seen in the cerebellum and pons, right thalamus and pallidum, sensorimotor cortex, paracentral lobule and supplementary motor area (SMA) (Figure 1 b).

The PD-related metabolic covariance pattern was characterized by relatively decreased cortical metabolic activity in the temporal, posterior parietal, inferior parietal, lateral occipital, prefrontal association cortex and SMA. Relative increases were seen in the cerebellum and pons, thalamus and pallidum, sensorimotor cortex, limbic association cortex, paracentral lobule and left SMA (Figure 1 b).

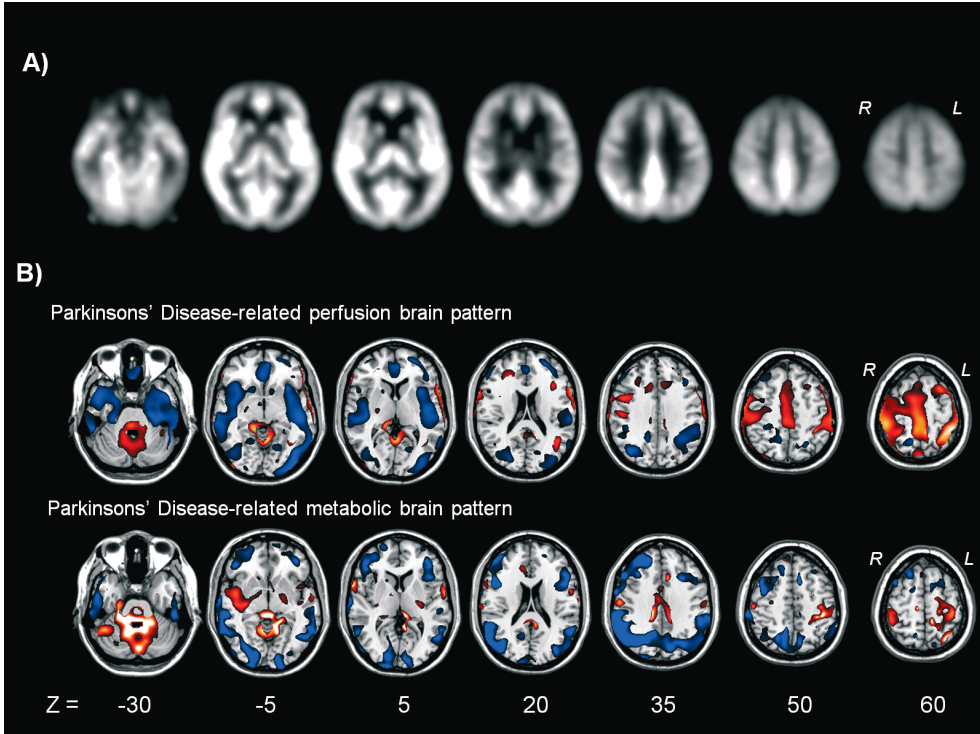


Figure 1: A) Example of the mean PCASL images of all healthy controls. Seven transversal slices through the brain are shown. B) (T) maps of the PD-related perfusion (upper row) and metabolic covariance brain patterns were overlaid on a T1 MR template. Relative perfusion and metabolic decreases (blue) and increases (red) compared to the control group are thresholded at $T = 2.5-5.0$ ($P < 0.02$). Seven transversal slices through the brain are shown.

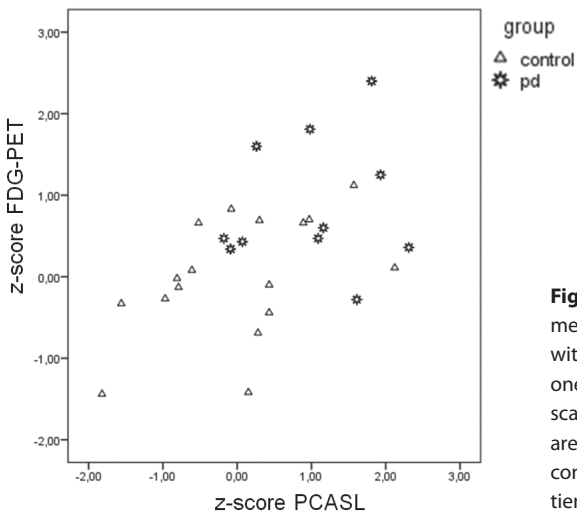


Figure 2: Correlation between the PD-related metabolic brain pattern expression measured with FDG and PCASL. On the X-axis the leave-one-out z-scores are displayed from the PCASL scans. On the Y-axis the leave-one-out z-scores are displayed from the FDG-PET scans. Healthy controls are denoted by open triangles; PD patients by open circles.

We computed the z-scores of FDG and PCASL images on the PD-related metabolic brain pattern and performed a correlation analysis. The Pearson correlation coefficient was 0.498 ($p < 0.007$) (Figure 2).

8.4 DISCUSSION

In this study we identified PD-related perfusion and glucose metabolic brain patterns measured in the same patients. The PD-related metabolic covariance brain pattern is in high accordance with previously described disease-related metabolic brain patterns in different cohorts in PD patients using standard clinical FDG-PET imaging (Ma et al. 2007a, Teune et al. 2013). Furthermore, we obtained a disease-specific perfusion brain pattern using PCASL-MR imaging. Our disease-related pattern is comparable to the PD-related perfusion brain pattern described by Melzer, characterized by decreased perfusion in posterior parieto-occipital cortex, middle frontal gyri and preserved perfusion in globus pallidus, putamen, anterior cingulate and post/precentral gyri with decreased perfusion activity in the posterior parieto-occipital cortex, posterior medial cortex and middle frontal gyrus and increased activity in bilateral globus pallidus, putamen en primary sensorimotor cortex and SMA (Melzer et al. 2011). The most characteristic difference between our perfusion brain pattern and previous reports (Fernández-Seara et al. 2012, Melzer et al. 2011), is the decrease of cerebral perfusion in the insular cortex on both sides in our data. However, Helmich et al have shown that PD patients had decreased connectivity between the posterior putamen and various cortical regions contributing to the corticostriatal loop, including the insula using resting-state functional MRI data (Helmich et al. 2010).

Performing PCASL and FDG-PET imaging in the same patients enabled a comparison between both patterns. Z-scores of PCASL datasets onto the metabolic pattern correlated positively (0.498) with the z-scores of FDG datasets onto the metabolic pattern. This value indicates there is substantial overlap, however, not complete. As discussed above, the larger perfusion decrease in the PD-related pattern in cortical regions including the insula than in the metabolic brain pattern, is suggesting that PCASL, is indeed adding relevant information to the PD-related pattern.

Another difference is the less pronounced increased perfusion in the basal ganglia in the perfusion-related pattern compared to the metabolic brain pattern. This is probably related to a lower signal-to-noise ratio. It is known that MRI head coils with multiple receive channels result in better signal to noise ratio in the cortex than in deeper brain structures.

Our data shows that PCASL is a promising technique, which gives supplementary information to FDG-PET and could thus be used as an additional measurement to improve image-based diagnosis of parkinsonian syndromes.

8.5 Conclusion

We identified PD-related perfusion and metabolic brain patterns using PCASL and FDG-PET in the same patients which were comparable with results of existing research. In this respect, PCASL appears to be a promising addition in the early diagnosis of individual parkinsonian patients.

Acknowledgments

We would like to thank M.F. Masman for assistance with PCASL image reconstruction and M. Segbers for assistance with FDG-PET image reconstruction.

CHAPTER 9

DISCUSSION

The main aim of this thesis was to investigate differences in glucose metabolism in various neurodegenerative brain diseases using [^{18}F]-fluorodeoxyglucose (FDG)-PET imaging. Furthermore, specific analysis techniques which can assist in the applicability of these brain patterns in clinical practice were investigated. In the following paragraphs specific findings and results will be highlighted. In the second part of this chapter, possibilities to extend to other image modalities and new methods that are currently subject of further study will be discussed.

9.1 BRAIN IMAGING IN THE DIFFERENTIAL DIAGNOSIS OF PARKINSONIAN SYNDROMES

The differential diagnosis of neurodegenerative brain diseases may be difficult on clinical grounds only. Parkinson's disease (PD) is the second most common neurodegenerative brain disease after Alzheimer's disease (AD). PD is manifested clinically by bradykinesia, muscular rigidity and sometimes rest tremor. Supportive features of the diagnosis are a unilateral onset of motor symptoms, progressive disorder and a good and consistent levodopa response (Litvan, et al. 2003). Especially at early disease stages, it can be difficult to distinguish PD from other neurodegenerative parkinsonian syndromes such as multiple system atrophy (MSA), progressive supranuclear palsy (PSP), corticobasal degeneration (CBD) or dementia with Lewy Bodies (DLB). In general neurological practice, diagnostic accuracy of parkinsonian syndromes is around 76% (Hughes, et al. 1992). In **chapter 2**, radiotracer neuroimaging techniques using positron emission tomography (PET) or single photon emission computed tomography (SPECT) are discussed which can be helpful to differentiate PD from other diseases. Presynaptic dopaminergic imaging either with [^{18}F]-DOPA PET or [^{123}I]FP-CIT SPECT is used to differentiate between patients with parkinsonian features associated with a presynaptic dopaminergic deficit such as PD, (but also MSA, PSP, CBD and DLB) and without a presynaptic dopaminergic deficit such as essential tremor, drug-induced parkinsonism or vascular parkinsonism. In a recent study of Hellwig (Hellwig, et al. 2012), the diagnostic accuracy of FDG-PET compared to [^{123}I] iodobenzamide (IBZM) for SPECT imaging was investigated. They concluded that the diagnostic accuracy of FDG-PET for discriminating Lewy Body Dementia from other parkinsonian syndromes is considerably higher than for IBZM-SPECT. This suggests that FDG-PET should replace IBZM-SPECT in clinical routine examinations of parkinsonian patients. In order to differentiate within the group of before mentioned neurodegenerative parkinsonian syndromes, disease-related metabolic brain patterns identified with FDG-PET imaging could be of great assistance in the individual clinical diagnosis (see below).

9.2 FDG-PET IMAGING IN THE DIFFERENTIAL DIAGNOSIS OF NEURODEGENERATIVE BRAIN DISEASES

FDG-PET imaging is increasingly available for routine clinical practice and has remained the only available radiotracer to detect accurately and reliably the cerebral glucose metabolism. As glucose is the only source of energy for the brain, it reflects the energy needs of underlying brain neuronal systems. After being taken up by the brain, glucose or its radiotracer analogue [^{18}F]

FDG, are phosphorylated by hexokinase to glucose-6-PO₄ or fluorodeoxyglucose-6-PO₄, the first step of the glycolytic process. However, FDG being a deoxy variant of glucose, is not a substrate for further metabolism and consequently trapped in brain tissue for the duration of the scanning procedure. The outcome measure of regional cerebral FDG-uptake measured by PET is the first step of the glycolysis. The detected specific metabolic brain patterns using FDG-PET are therefore reflecting the underlying pathological alterations of the affected brain regions. Specific brain regions degenerate and different patterns of altered glucose metabolic brain activity develop in various neurodegenerative brain diseases, before structural (atrophy) changes can be detected with imaging techniques.

9.2.1 Univariate analysis method

In **chapter 3**, we have performed a retrospective study selecting typical patients with PD, MSA, PSP, CBD DLB, AD and frontotemporal dementia (FTD). At the time of referral for imaging, the clinical diagnosis of most patients was uncertain. The final clinical diagnoses according to established clinical research criteria (Gilman et al. 2008, Litvan et al. 1996, Litvan et al. 2003, Mahapatra et al. 2004, McKeith. 2006, McKhann et al. 1984, McKhann et al. 2001) were made after a follow up time after scanning of PD 4 ± 3 (mean \pm SD in years), MSA (2 ± 1), PSP (3 ± 2), CBD (3 ± 1), DLB (2 ± 1), AD (3 ± 2) and FTD (3 ± 1).

To identify differences between patients and controls we used a univariate voxel-based analysis technique called statistical parametric mapping (SPM). Images of each of the seven patient groups were separately compared to 18 healthy controls using this SPM procedure and a two-sample t-test. Disease-specific patterns of relatively decreased metabolic activity were found in PD (contralateral parieto-occipital and frontal regions), MSA (bilateral putamen and cerebellar hemispheres), PSP (prefrontal cortex and nucleus caudatus, thalamus and mesencephalon), CBD (contralateral cortical regions), DLB (occipital and parieto-temporal regions), AD (parieto-temporal regions), and FTD (fronto-temporal regions). In these patients, scanned at an early disease stage, typical differences between patient groups and healthy controls were found for each disease. In **chapter 4**, an overview of the literature of disease-specific metabolic brain patterns in several neurodegenerative brain diseases is given. Furthermore, advances of using multivariate analysis methods compared to univariate methods are outlined. In a multivariate statistical analysis technique, called Scaled Subprofile Modelling/Principal Component Analysis (SSM/PCA), not only group differences between patients and controls can be identified like in univariate methods, but it is also possible to identify relationships in relatively increased and decreased metabolic activity between different brain regions in combined samples of patients and control scans (Eidelberg. 2009, Moeller, et al. 1987).

9.2.2 Multivariate analysis method

In **chapter 5** we validated disease-related metabolic brain patterns for PD, MSA and PSP using SSM/PCA in the same patients and controls that were used in the univariate analysis of **chapter**

3. Validation showed that the disease-related metabolic brain patterns were highly similar to the earlier described group differences in **chapter 3** and discriminative of the three disorders. The findings are consistent with previous studies. However, some interesting differences can be noted. In our study the PD-related metabolic covariance pattern was characterized by an asymmetrical relatively decreased metabolic activity, contralateral to the affected body side in 14 out of 20 patients, comprising the (posterior) parietal association cortex, visual cortex, lateral premotor and prefrontal association cortex. To our knowledge, an asymmetrical PD pattern has not been described before (Huang et al. 2007c, Ma et al. 2007a).

Moreover, Tang studied longitudinal changes in network activity in each cerebral hemisphere, focusing specifically on the “presymptomatic” hemisphere, ipsilateral to the initially involved body side, to see whether the network changes appear at or before symptom onset. In the context of PD, the cerebral hemisphere ipsilateral to the initially affected limbs can be considered “presymptomatic” at least until symptoms appear on the opposite body side. They found that elevations at the network level of the PD motor-related pattern (PDRP) were already present at baseline in both hemispheres. This contrasts with hemispheric expression of the PD cognition-related pattern 4 years after the appearance of the motor network abnormality which was characterized by decreased metabolic activity in the contralateral precuneus (Tang, et al. 2010a). This localized metabolic change may reflect the earliest stages of early cognitive decline in Parkinson disease as defined by mild cognitive impairment (Huang, et al. 2007a).

We included PD patients at an early disease stage even before the clinical diagnosis was clear. However we did not differentiate between PD specific motor and cognitive related changes and we have not studied this cohort over time. Nonetheless, we hypothesize that the appearance of cortical metabolic decreased activity contralateral to the most affected body side in our cohort could be an early marker of advancing disease including the development of neuropsychological deficits. Future studies should be carried out to predict onset and progression of specific PD-related symptoms. Further data inclusion will increase sensitivity and specificity of the listed metabolic brain patterns. Application of this SSM/PCA method may also be useful for other parkinsonian and dementia syndromes to enhance diagnostic precision.

We extended the SSM/PCA approach in **chapter 6** to identify an Alzheimer’s Disease-related glucose metabolic brain pattern. Group differences in regional cerebral glucose utilisation of patients with dementia compared to healthy controls are well-known. However, multivariate analysis techniques aiming at identifying diagnostic neural networks in diseases, have been applied less frequently. The aim of this study was to present and validate an AD-related glucose metabolic brain pattern and to apply it prospectively in a second cohort of individual patients with memory complaints. The identification cohort consisted of the same AD patients and controls already described in **chapter 3**. The AD-related glucose metabolic brain pattern was characterized by relatively decreased metabolic activity in the temporal and parietal regions and relatively increased metabolic activity in the subcortical white matter, cerebellum and sensorimotor cortex.

The metabolic brain pattern we found using the SSM/PCA analysis was comparable to the regions we already identified using a univariate analysis in AD patients (see **chapter 3**) with a sensitivity of 93% and a specificity of 94% for the AD-related metabolic brain pattern. Furthermore, we applied this method to investigate the ability of the identified AD-related metabolic covariance pattern to discriminate between individual patients with probable AD and non-probable AD (possible AD, mild cognitive impairment (MCI) or subjective complaints) and the association of the metabolic patterns with neuropsychological tests. This part of the study was done in an independent cohort of 15 patients referred to our memory clinic (confirmation cohort). In the confirmation cohort, all the subjects with clinically probable AD diagnosis showed a high expression of the AD-related metabolic brain pattern whereas in all the subjects with a non-probable AD diagnosis a low expression was found.

9.3 FDG-PET IMAGING AND THE SSM/PCA METHOD IN CLINICAL PRACTICE

Since a few years FDG is commercially available and being used in many Nuclear Medicine Departments worldwide. Now we have the possibility, based on the disease-related patterns for PD, MSA, PSP and AD, to obtain a score for an individual subject. This score is calculated by multiplying every voxel value in a subject scan by the corresponding voxel weight in the disease-related metabolic covariance pattern, with a subsequent summation over the whole brain volume. The obtained subject score indicates to what extent that patient expresses the disease-related pattern. In **chapter 5** we showed that the “simple” comparison between healthy controls and patient groups already yielded a high sensitivity and specificity for correctly classifying PD, MSA or PSP patients. Tang et al have already demonstrated an image-based classification routine with high specificity to distinguish between PD and MSA/PSP and in a second step between MSA and PSP compared to controls. (Tang et al. 2010b). We performed another analysis in **chapter 5** by directly comparing PD and MSA instead of a comparison against healthy controls and demonstrated that especially specificity increased. This is relevant for applying this method in clinical practice because the clinical motivation for a FDG-PET originates from doubts between PD or MSA, not between healthy or PD. In a recent study of Hellwig (Hellwig, et al. 2012), the diagnostic accuracy of FDG-PET in discriminating parkinsonian patients was investigated. FDG-PET scans were analyzed by visual assessment including individual voxel based statistical maps (a 3D stereotactic surface projection technique (3D-SSP)). First, a differentiation between MSA, PSP and CBD from DLB was made, followed by a subclassification in MSA, PSP and CBD. Sensitivity and specificity of FDG-PET was 77/97% for MSA, 74/95% for PSP and 75/92% for CBD respectively. These studies compared only two classes at a time or in two levels (healthy and patient group, or two patient groups). This puts forward a research challenge to improve the SSM/PCA method, to be able to distinguish different neurodegenerative brain diseases from each other in one analysis. One might consider machine learning approaches like decision-tree methods to be able to compare more than two patient groups at the same time and possibly detect subclassifications within patient groups (see future perspectives).

Rather than demonstrating pattern specificity in group comparisons, it is important to know whether an early diagnosis of neurodegenerative brain disease of one individual is possible when individual metabolic patterns are compared with a database of disease-specific metabolic brain patterns.

In **chapter 7** we present the prospective Dutch multicenter imaging project GLucose IMaging in ParkinsonismS (GLIMPS) which aims at testing the feasibility of a novel image-based classification algorithm for the accurate and early individual diagnosis of patients with neurodegenerative brain diseases. However, apart from confirming the diagnosis of a neurodegenerative brain disease in an individual patient, it will also be necessary to determine abnormal glucose metabolic brain patterns in other parkinsonian and dementia syndromes such as in CBD, DLB and FTD in order to make the differential diagnosis of dementia more reliable. It is clear that further elaboration of glucose metabolic brain patterns largely depend on the correct selection of the needed reference patient groups for the identification procedure. Expanding sample size will increase sensitivity and specificity of the listed metabolic brain patterns and will enable subclassifications in for example left/right body-side affected patients. Furthermore, a large control sample consisting of sufficient patients within different age categories is important to study differences in brain patterns in an aging population and for example in man and women or right and left handedness.

9.4 PARKINSON'S DISEASE-RELATED METABOLIC BRAIN PATTERNS COMPARED TO OTHER IMAGE MODALITIES.

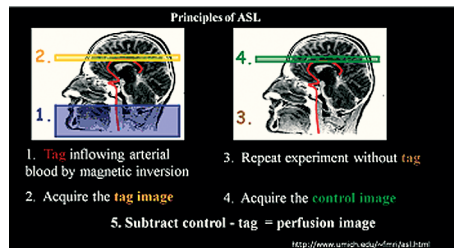
It is increasingly recognized that combining information derived from different image modalities can be used for improvements in the sensitivity and specificity of disease-related patterns for parkinsonian disorders. A prospective study was carried out in 20 PD patients and 17 healthy controls to test whether FDG-PET scanned on high resolution camera combined with magnetic resonance imaging (MRI)-based techniques such as arterial spin labeling (ASL), resting state fMRI images and diffusion tensor imaging (DTI) will provide an even more distinguished disease-related pattern for Parkinson's disease. Under normal conditions, the spatial distribution of resting cerebral blood flow and cerebral metabolic rate of glucose are closely related.

A relatively new magnetic resonance (MR) technique, pseudo-continuous arterial spin labeling (PCASL), (**see box 1**) was used to measure regional brain perfusion.

In **chapter 8** fourteen Parkinson's disease patients and seventeen healthy controls could be included and underwent FDG-PET imaging and PCASL-MRI. Data were analyzed using scaled subprofile model/principal component analysis (SSM/PCA). We identified a PD-related metabolic and perfusion covariance pattern in the same patients using PCASL and FDG-PET imaging and assessed (dis)similarities in the disease-related pattern between perfusion and metabolism in PD patients. The PD-related metabolic covariance brain pattern is in high accordance with previously described disease-related metabolic brain patterns in different cohorts in PD patients. Furthermore, we obtained a disease-specific perfusion brain pattern using PCASL-MR imaging. The PD-related

Box 1: pseudo-continuous arterial spin labeling

Pseudo-continuous Arterial Spin Labeling (PCASL) permits the noninvasive measurement of perfusion with MRI by using a train of radio frequency (RF) pulses and magnetic field gradient pulses to achieve labeling of spins in flowing blood (Dai et al. 2008, van Osch et al. 2009). The arterial blood in the feeding artery is magnetically and non-invasively labeled (tagged) and an image is acquired after a time delay (i.e. labeled image). The labeled protons in blood act as endogenous tracers. They are exchanged with the water protons in brain tissue as the blood flows into the capillary. At a steady-state of this exchange, the concentration of the labeled protons in brain tissue reflects the amount of blood perfusion which is weighted by regional T1 relaxation. A second image (i.e. control image) can be acquired in the same manner except that the incoming blood is not magnetically labeled and all the spins in the brain are aligned with static magnetic field. The subtraction of label from control image provides an image that is proportional to the cerebral blood flow, also called the perfusion image (see figure below).



perfusion covariance pattern was characterized by relatively decreased cortical metabolic activity bilaterally in the temporal, insular, posterior parietal, inferior parietal, lateral occipital and prefrontal association cortex. Relative increases were seen in the cerebellum and pons, right thalamus and pallidum, sensorimotor cortex, paracentral lobule and supplementary motor area (SMA). Performing PCASL and FDG-PET imaging in the same patients enabled a comparison between both patterns. The earlier described decreased perfusion in the insular cortex was not present in the glucose metabolic brain pattern, which is suggesting that PCASL is indeed adding relevant information to the PD-related pattern. Our perfusion brain pattern is comparable to the earlier described PD-related perfusion brain pattern (Melzer et al. 2011). The most characteristic difference between our perfusion brain pattern and previous reports (Fernández-Seara et al. 2012, Melzer et al. 2011) is the decrease of cerebral perfusion in the insular cortex on both sides in our data. In support of our findings, Helmich used resting-state functional MRI data to test the effect of striatal dopamine depletion on cortico-striatal network properties. (see **box 2** for an explanation of resting state fMRI). They showed that PD patients had decreased connectivity between the posterior putamen, which is early affected in PD (see **chapter 2**) and various cortical regions contributing to the corticostriatal loop, including the insula (Helmich, et al. 2010). Preliminary findings of our own PD patient cohort showed that it is possible to adapt the SSM/PCA method to be used for resting state fMRI studies. Meaningful patterns of positive and negative correlations were identified when the left pallidum

Box 2: Resting state fMRI

In functional magnetic resonance imaging (fMRI), changes in the Blood Level Oxygenation Dependent (BOLD) effect are measured and visualized in brain tissue. fMRI using task-based or stimulus-driven paradigms has been critical to our current understanding of brain function. Using the relative signal changes (0.5-5%) from baseline in the BOLD signal during the performance of a task or in response to a stimulus, one infers that certain areas of the brain are activated or deactivated. In recent years, there has been increasing interest in the application of the technique at rest, termed resting-state fMRI or functional connectivity MR imaging. In resting state fMRI, subjects are scanned without external stimulus to derive brain connectivity patterns which are assumed to represent a default-mode network. A seed-based approach is commonly used to identify brain regions that are functionally connected (Lee et al. 2012).

was used as a seed region. Interestingly, a positive correlation was found between the left pallidum and the insular cortex on both sides. Future investigations are needed to further optimize the technique and use different seed regions to determine resting state connectivity between this region and the rest of the brain.

Another way of looking at abnormal connectivity patterns between brain regions is diffusion tensor imaging (DTI)-tractography. It can be used to visualize nerve fiber tracts or compute various anisotropy measures (**see box 3**). In our research group we are currently working on optimizing protocols for our own PD patient cohort, to be able to answer questions related to changed thalamo-cortico-striatal connections in PD patients compared to controls. Earlier studies did investigate diffusion coefficients and found promising results.

Box 3: Diffusion Tensor Imaging

Diffusion magnetic resonance imaging is increasingly used to investigate white matter structures in patients with neurodegenerative brain diseases. In Diffusion Weighted Imaging the direction of diffusion in each voxel can be determined. This will be used to estimate both the presence and orientation of white matter tracts. Diffusion tensor imaging (DTI) calculates a tensor in each voxel, taking into account parameters of the rate of diffusion and the preferred direction of diffusion. In an isotropic medium (liquor), water molecules naturally move randomly and isotropically. In biological tissues however, the diffusion may be anisotropic. Fractional anisotropy (FA) can be calculated for each voxel and contains combined information in multiple directions. Highly organized white matter tracts have high FA because diffusion is highly constrained by the tract's cellular organization. As white matter is damaged, FA decreases due to decreased anisotropic diffusion. Apparent diffusion coefficient (ADC) values measure the average water diffusion, and increasing ADC values indicate damaged white matter. In addition, DTI-tractography can be used to visualize nerve fiber tracts and study abnormal connectivity patterns between brain regions. Depending on the goal one can use either a voxel-based or skeleton-based approach. In voxel-based approaches one cannot be certain that the same regions of white matter tracts correspond across subjects. The tract-based spatial statistics (TBSS) method aims to solve this problem. (Rae et al. 2012)

Ito compared ADC and FA values in the pons, cerebellum and putamen in patients with PD, MSA and controls and detected early pathological involvement prior to magnetic resonance signal changes in MSA. In particular, low FA values in the pons showed high specificity in discriminating MSA from PD (Ito et al. 2007).

Although DTI has typically been used to study white matter tracts, it also holds promise to study grey matter areas. Vaillancourt demonstrated that the FA values were reduced in the SN of early stage, unmedicated patients with PD. The difference between *de novo* patients with PD and healthy control subjects was greatest in the caudal ROI of the SN compared with the middle and rostral SN ROI. By using this technique, all *de novo* patients with PD were distinguished from all healthy individuals with 100% sensitivity and specificity (Vaillancourt et al. 2009).

9.5 FUTURE DIRECTIONS

We know now that disease-related metabolic and perfusion brain patterns can be derived in patients with neurodegenerative brain diseases. As already suggested in **chapter 8**, it is increasingly recognized that combining information derived from different image modalities including FDG-PET and PCASL can be used for improvements in the sensitivity and specificity of biomarkers for parkinsonian disorders. However, complexity regarding analysis techniques increases.

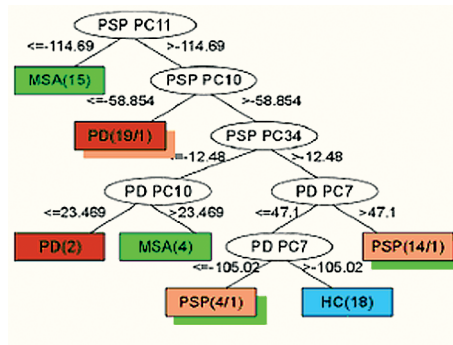
9.6 DECISION TREE CLASSIFICATION OF FDG-PET DATA TO PREDICT NEURODEGENERATIVE BRAIN DISEASES

As described above, different image modalities can be used to extract disease-related metabolic brain patterns in neurodegenerative brain diseases. However, the above described SSM/PCA method can only deal with one image modality, and comparison of two classes (healthy and patient group, or two patient groups) at a time. This puts forward a research challenge to improve the SSM/PCA method. Regarding previous suggestions to select components used for creating a disease-related metabolic pattern (Spetsieris and Eidelberg. 2010), one might consider machine learning approaches like decision-tree methods to improve sensitivity and specificity (Quinlan. 1993). (see **box 4** for an explanation and example of the decision tree method). The objective for future research will be to explore the first examples of the decision tree method by carefully looking at each step in the tree, identify misclassified patients and get validated results. Furthermore, besides being able to classify patients of different patient groups in one analysis, it is possible to use characteristic image features derived from multimodal brain data (FDG-PET, DTI, PCASL and resting state fMRI images). From these data, image features and network patterns can be extracted, which can be used as input for the decision tree method. Another advantage of this method is that non-linear combinations of image features can be used. This will result in a supervised classification method for associating brain patterns to various stages of neurodegenerative diseases.

Box 4: Decision tree

Decision tree method is an approach for analytically making decisions and uses graphical representation of decision tree(s) to present several decision classes. Decision trees have been known for their capability in classification of objects and they can be modified as new cases or more information from different image modalities is presented.

In this example carried out by the Visualization and Computer Graphics group (RUG), a decision tree program (c4.5 by Quinlan (Quinlan, 1993)) was adapted to be used as a machine learning technique to classify neurodegenerative brain diseases. The decision tree program has been used to classify subjects as healthy, PD, MSA or PSP together in one analysis with respect to their individual subject score calculated for each principal component of each patient group instead of one score for the disease-related combination pattern. The data consists of 76 subjects (18 healthy controls, 20 PD, 21 MSA and 17 PSP) (see chapter 5) and in total 112 principal components (38 PD, 39 MSA and 35 PSP) (see chapter 5) and in total 112 principal components (38 PD, 39 MSA and 35 PSP). The decision tree shows in oval shapes the features (principal components used in the process of classification), the conditions on which decisions are made, and the resulting classes (decisions) are presented in rectangles. Below an example of an output of the decision tree method is shown.



Interestingly, the first 15 of the MSA patients are classified by using a component which belongs to PSP. When looking at the metabolic pattern of PSP PC11, it consists mainly of increased metabolic activity in the putamen. MSA patients have decreased metabolism in the putamen and this is probably the reason why patients with a low subject score for this component can be classified. Another key component in this example is PD PC 7. The pattern in this component consists of decreased metabolism in thalamus, caudate nucleus, mesencephalon and prefrontal areas. These regions are typically decreased in PSP patients and 14/17 PSP patients could be classified.

9.7 CONCLUSION

FDG-PET imaging is increasingly available for routine clinical practice and has remained the only available radiotracer to detect accurately and reliably the cerebral glucose metabolism. The SSM/PCA method can identify relationships in relatively increased and decreased metabolic activity between different brain regions in combined samples of patients and controls. The expression of a covariance pattern can be quantified in an individual patient. The obtained subject score indicates to

what extent that patient expresses the disease-related pattern. These metabolic brain patterns can therefore be a valuable aid in the differential diagnosis of individual patients with neurodegenerative brain diseases. Furthermore, we propose that a disease biomarker can be identified by using decision tree methods to combine network patterns from different image modalities derived from patients with parkinsonian and dementia syndromes. This disease biomarker is expected to help in diagnosing patients at an early stage of the disease and can be used to track disease progression when follow-up scans are performed.

SUMMARY

SUMMARY

The main aim of this thesis was to investigate differences in glucose metabolism in various neurodegenerative brain diseases using [¹⁸F]-fluorodeoxyglucose (FDG)-PET imaging. Furthermore, specific analysis techniques which can assist in the applicability of these brain patterns in clinical practice were investigated. In the following paragraphs specific findings will be summarized and discussed.

The differential diagnosis of neurodegenerative brain diseases may be difficult on clinical grounds only. Parkinson's disease (PD) is the second most common neurodegenerative brain disease after Alzheimer's disease (AD). It can be difficult to distinguish PD from other neurodegenerative parkinsonian syndromes such as multiple system atrophy (MSA), progressive supranuclear palsy (PSP), corticobasal degeneration (CBD) or dementia with Lewy Bodies (DLB). In **chapter 2**, radiotracer neuroimaging techniques using positron emission tomography (PET) or single photon emission computed tomography (SPECT) are discussed which can be helpful to differentiate PD from other diseases. In order to differentiate between neurodegenerative brain diseases, disease-related metabolic brain patterns identified with FDG-PET imaging could be of great assistance in the individual clinical diagnosis.

FDG-PET imaging is increasingly available for routine clinical practice and has remained the only available radiotracer to detect the cerebral glucose metabolism accurately and reliably. As glucose is the only source of energy for the brain, it reflects the energy needs of underlying brain neuronal systems. After being taken up by the brain, glucose or its radiotracer analogue [¹⁸F]FDG, are phosphorylated by hexokinase to glucose-6-PO₄ or fluorodeoxyglucose-6-PO₄, the first step of the glycolytic process. However, FDG being a deoxy variant of glucose, is not a substrate for further metabolism and is consequently trapped in brain tissue for the duration of the scanning procedure. The outcome measure of regional cerebral FDG-uptake measured by PET, therefore, is the first step of the glycolysis. The detected disease-related metabolic brain patterns using FDG-PET reflect the underlying pathological alterations of the affected brain regions.

In **chapter 3** we have performed a retrospective study selecting typical patients with PD, MSA, PSP, CBD DLB, AD and frontotemporal dementia (FTD). At the time of referral for imaging, the clinical diagnosis of most patients was uncertain.

To identify differences between patients and healthy controls we used a univariate voxel-based analysis technique called statistical parametric mapping (SPM). Images of each of the 7 patient groups were separately compared to 18 healthy controls using this SPM procedure and a two-sample t-test. Disease-specific patterns of relatively decreased metabolic activity were found in PD (contralateral parieto-occipital and frontal regions), MSA (bilateral putamen and cerebellar hemispheres), PSP (prefrontal cortex and nucleus caudatus, thalamus and mesencephalon), CBD (contralateral cortical regions), DLB (occipital and parieto-temporal regions), AD (parieto-temporal regions), and FTD (fronto-temporal regions). In these patients, scanned at an early disease stage, typical differences between patient groups healthy control were found for each

disease. In **chapter 4** an overview of the literature of disease-specific metabolic brain patterns in several neurodegenerative brain diseases is given. Furthermore, advances of using multivariate analysis methods compared to univariate methods are outlined. In a multivariate statistical analysis technique, called Scaled Subprofile Modelling/Principal Component Analysis (SSM/PCA), not only group differences between patients and controls can be identified like in univariate methods, but it is also possible to identify relationships in relatively increased and decreased metabolic activity between different brain regions in combined samples of patients and control scans.

Multivariate analysis method

In **chapter 5** we validated disease-related metabolic brain patterns for PD, MSA and PSP using SSM/PCA in the same patients and controls that were used in the univariate analysis of **chapter 3**. Results showed that the disease-related metabolic brain patterns were highly similar to the earlier described group differences and discriminative of the three disorders.

In **chapter 6** we identified an Alzheimer's Disease-related glucose metabolic brain pattern using the SSM-PCA methods. Group differences in regional cerebral glucose utilisation of patients with dementia compared to healthy controls are well-known. However, multivariate analysis techniques aiming at identifying diagnostic neural networks in diseases, have been applied less frequently. The aim of this study was to present and validate an AD-related glucose metabolic brain pattern and to apply it prospectively in a second cohort of individual patients with memory complaints. The identification cohort consists of the same AD patients and controls as described in **chapter 3**. The AD-related glucose metabolic brain pattern was characterized by relatively decreased metabolic activity in the temporal and parietal regions and relatively increased metabolic activity in the subcortical white matter, cerebellum and sensorimotor cortex with a sensitivity of 93% and a specificity of 94%. Furthermore, we applied this method to investigate the ability of the identified AD-related metabolic covariance pattern to discriminate between individual patients with probable AD and non-probable AD (possible AD, mild cognitive impairment (MCI) or subjective complaints) and the association of the metabolic patterns with neuropsychological tests. In the confirmation cohort, all the subjects with clinically probable AD diagnosis showed a high expression of the AD-related metabolic brain pattern whereas in all the subjects with a non-probable AD diagnosis a low expression was found.

In **chapter 7** we present the prospective Dutch multicenter imaging project GLucose IMaging in ParkinsonismS (GLIMPS) which aims at testing the feasibility of a novel image-based classification algorithm for the accurate and early individual diagnosis of patients with neurodegenerative brain diseases. It is increasingly recognized that combining information derived from different image modalities can be used for improvements in the sensitivity and specificity of disease-related patterns for parkinsonian disorders.

Extending to other image modalities

A prospective study was carried out in 20 PD patients and 17 healthy controls to test whether FDG-PET scanned on a high resolution camera combined with magnetic resonance imaging (MRI)-based techniques such as arterial spin labeling (ASL), resting state fMRI images and diffusion tensor imaging (DTI) will provide an even more distinguished disease-related pattern for Parkinson's disease.

Besides studying glucose metabolism, it is possible to study brain perfusion with a relatively new magnetic resonance based technique called pseudocontinuous arterial spin labeling (PCASL). In **chapter 8** we identified a PD-related metabolic and perfusion covariance pattern in the same patients using PCASL and FDG-PET imaging and assessed (dis)similarities in the disease-related pattern between perfusion and metabolism in PD patients.

The PD-related metabolic covariance brain pattern is in high accordance with disease-related metabolic brain patterns in different cohorts in PD patients previously described, showing bilaterally decreased metabolic activity in the (posterior) parietal association cortex, inferior parietal cortex, lateral occipital cortex, prefrontal association cortex and SMA. Relative increases were seen in the cerebellum and pons, thalamus and pallidum, sensorimotor cortex, limbic association cortex, paracentral lobule and left SMA. (see also **chapter 5**).

Furthermore, we obtained a disease-specific perfusion brain pattern using PCASL-MR imaging. Our perfusion brain pattern is comparable to the previously described PD-related perfusion brain patterns. We know now that disease-related metabolic and perfusion brain patterns can be derived in patients with neurodegenerative brain diseases. As suggested in **chapter 8**, it is increasingly recognized that combining information derived from different image modalities including FDG-PET and PCASL can be used for improvements in the sensitivity and specificity of biomarkers for parkinsonian disorders. However, complexity regarding analysis techniques increases.

As described above different image modalities can be used to extract disease-related metabolic brain patterns in neurodegenerative brain diseases. However, the above described SSM/PCA method can only deal with one image modality, and comparison of two classes (healthy and patient group, or two patient groups) at a time. This puts forward a research challenge to improve the SSM/PCA method. One might consider machine learning approaches like decision-tree methods to improve sensitivity and specificity.

CONCLUSION

FDG-PET imaging is increasingly available for routine clinical practice and has remained the only available radiotracer to detect the cerebral glucose metabolism accurately and reliably. The SSM/PCA method can identify relationships in relatively increased and decreased metabolic activity between different brain regions in patients and controls. The expression of a covariance pattern can be quantified in an individual patient. The obtained subject score indicated to what extent that individual patient expresses the disease-related pattern. These metabolic brain patterns can therefore be a valuable aid in the differential diagnosis of individual patients with neurodegenerative brain diseases.

REFERENCES

References

- Akaike H. A New Look at the Statistical Model Identification *IEEE Trans. Automat. Contr* 1974; 716-23.
- Alexander GE, DeLong MR, Strick PL. Parallel organization of functionally segregated circuits linking basal ganglia and cortex. *Annu Rev Neurosci* 1986; 9: 357-81.
- Antonini A, Leenders KL, Spiegel R, Meier D, Vontobel P, Weigell-Weber M, et al. Striatal glucose metabolism and dopamine D2 receptor binding in asymptomatic gene carriers and patients with Huntington's disease. *Brain* 1996; 119(Pt6):2085-95.
- Antonini A, Schwarz J, Oertel WH, Pogarell O, Leenders KL. Long-term changes of striatal dopamine D2 receptors in patients with parkinson's disease: A study with positron emission tomography and [¹¹C]raclopride. *Mov Disord* 1997; 12: 33-8.
- Asanuma K, Carbon-Correll M, Eidelberg D. Neuroimaging in human dystonia. *J Med Invest* 2005; 52 (suppl):272-9.
- Asanuma K, Tang C, Ma Y, Dhawan V, Mattis P, Edwards C, et al. Network modulation in the treatment of parkinson's disease. *Brain* 2006; 129: 2667-78.
- Asanuma K, Ma Y, Huang C, Carbon-Correll M, Edwards C, Raymond D, et al. The metabolic pathology of dopa-responsive dystonia. *Ann Neurol* 2005; 57(4):596-600.
- Asllani I, Habeck C, Scarmeas N, Borogovac A, Brown TR, Stern Y. Multivariate and univariate analysis of continuous arterial spin labeling perfusion MRI in Alzheimer's Disease. *J Cereb Blood Flow Metab* 2008; 28: 725-36.
- Au WL, Adams JR, Troiano AR, Stoessl AJ. Parkinson's disease: In vivo assessment of disease progression using positron emission tomography. *Brain Res Mol Brain Res* 2005; 134: 24-33.
- Bartels AL, Leenders KL. Parkinson's disease: The syndrome, the pathogenesis and pathophysiology. *Cortex* 2009; 45: 915-21.
- Bartels AL, Willemsen AT, Doorduyn J, de Vries EF, Dierckx RA, Leenders KL. [¹¹C]-PK11195 PET: Quantification of neuroinflammation and a monitor of anti-inflammatory treatment in parkinson's disease? *Parkinsonism Relat Disord* 2010; 16: 57-9.
- Boecker H, Ceballos-Baumann AO, Volk D, Conrad B, Forstl H, Haussermann P. Metabolic alterations in patients with parkinson disease and visual hallucinations. *Arch Neurol* 2007; 64: 984-8.
- Bohnen NI, Djang DSW, Herholz K, Anzai Y, Minoshima S. Effectiveness and safety of 18F-FDG PET in the evaluation of dementia: A review of the recent literature. *J Nucl Med* 2012; 53: 59-71.
- Booij J, Tissingh G, Boer GJ, Speelman JD, Stoof JC, Janssen AG, et al. [¹²³I]FP-CIT SPECT shows a pronounced decline of striatal dopamine transporter labelling in early and advanced Parkinson's Disease. *J Neurol Neurosurg Psychiatry* 1997; 62: 133-40.
- Borghammer P, Aanerud J, Gjedde A. Data-driven intensity normalization of PET group comparison studies is superior to global mean normalization. *Neuroimage* 2009a;46(4):981-8.
- Borghammer P, Cumming P, Aanerud J, Gjedde A. Artefactual subcortical hyperperfusion in PET studies normalized to global mean: Lessons from parkinson's disease. *Neuroimage* 2009b; 45(2): 249-57.
- Braune S, Reinhardt M, Schnitzer R, Riedel A, Lucking CH. Cardiac uptake of [¹²³I]MIBG separates parkinson's

- disease from multiple system atrophy. *Neurology* 1999; 53: 1020-5.
- Brooks DJ, Frey KA, Marek KL, Oakes D, Paty D, Prentice R, et al. Assessment of neuroimaging techniques as biomarkers of the progression of parkinson's disease. *Exp Neurol* 2003; 184 Suppl 1: S68-79.
- Brooks DJ, Ibanez V, Sawle GV, Playford ED, Quinn N, Mathias CJ, et al. Striatal D2 receptor status in patients with parkinson's disease, striatonigral degeneration, and progressive supranuclear palsy, measured with 11C-raclopride and positron emission tomography. *Ann Neurol* 1992; 31:184-92.
- Cairns NJ, Bigio EH, Mackenzie IR, Neumann M, Lee VM, Hatanpaa KJ, et al. Neuropathologic diagnostic and nosologic criteria for frontotemporal lobar degeneration: Consensus of the consortium for frontotemporal lobar degeneration. *Acta Neuropathol* 2007; 114: 5-22.
- Carbon M., Trost M., Ghilardi MF., Eidelberg D. Abnormal brain networks in primary torsion dystonia. *Adv Neurol* 2004;94:155-61.
- Chung EJ, Lee WY, Yoon WT, Kim BJ, Lee GH. MIBG scintigraphy for differentiating parkinson's disease with autonomic dysfunction from parkinsonism-predominant multiple system atrophy. *Mov Disord* 2009; 24: 1650-5.
- Ciarmiello A., Giovacchini G, Orobello S, Bruselli L, Elifani F, Squitieri F. 18F-FDG PET uptake in the pre-huntington disease caudate affects the time-to-onset independently of CAG expansion size. *Eur J Nucl Med Mol Imaging* 2012;39(6):1030-6.
- Cummings JL. Behavioral and psychiatric symptoms associated with huntington's disease. *Adv Neurol* 1995;65:179-186.
- Dai W, Garcia D, de Bazelaire C, Alsop DC. Continuous flow-driven inversion for arterial spin labeling using pulsed radio frequency and gradient fields. *Magn Reson Med* 2008; 60: 1488-97.
- de Lau LM, Breteler MM. Epidemiology of parkinson's disease. *Lancet Neurol* 2006; 5: 525-35.
- DeLong M, Wichmann T. Update on models of basal ganglia function and dysfunction. *Parkinsonism Relat Disord* 2009; 15 Suppl 3: S237-40.
- DeLong MR, Wichmann T. Circuits and circuit disorders of the basal ganglia. *Arch Neurol* 2007; 64: 20-4.
- Dickson DW, Bergeron C, Chin SS, Duyckaerts C, Horoupian D, Ikeda K, et al. Office of rare diseases neuropathologic criteria for corticobasal degeneration. *J Neuropathol Exp Neurol* 2002; 61: 935-46.
- Diehl-Schmid J, Grimmer T, Drzezga A, Bornschein S, Riemenschneider M, Forstl H, et al. Decline of cerebral glucose metabolism in frontotemporal dementia: A longitudinal 18F-FDG-PET-study. *Neurobiol Aging* 2007; 28: 42-50.
- Dubois B, Slachevsky A, Litvan I, Pillon B. The FAB: A frontal assessment battery at bedside. *Neurology* 2000; 55: 1621-6.
- Eckert T, Eidelberg D. The role of functional neuroimaging in the differential diagnosis of idiopathic parkinson's disease and multiple system atrophy. *Clin Auton Res* 2004; 14: 84-91.
- Eckert T, Barnes A, Dhawan V, Frucht S, Gordon MF, Feigin AS, et al. FDG PET in the differential diagnosis of parkinsonian disorders. *Neuroimage* 2005; 26: 912-21.

- Eckert T, Tang C, Ma Y, Brown N, Lin T, Frucht S, et al. Abnormal metabolic networks in atypical parkinsonism. *Mov Disord* 2008; 23(5): 727-33.
- Eggers C, Hilker R, Burghaus L, Schumacher B, Heiss WD. High resolution positron emission tomography demonstrates basal ganglia dysfunction in early parkinson's disease. *J Neurol Sci* 2009; 276: 27-30.
- Ehrt U, Broich K, Larsen JP, Ballard C, Aarsland D. Use of drugs with anticholinergic effect and impact on cognition in parkinson's disease: A cohort study. *J Neurol Neurosurg Psychiatry* 2010; 81: 160-5.
- Eidelberg D. Abnormal brain networks in DYT1 dystonia. *Adv Neurol* 1998;78:127-33.
- Eidelberg D. Metabolic brain networks in neurodegenerative disorders: A functional imaging approach. *Trends Neurosci* 2009; 32: 548-57.
- Eidelberg D, Moeller JR, Dhawan V, Spetsieris P, Takikawa S, Ishikawa T, et al. The metabolic topography of parkinsonism. *J Cereb Blood Flow Metab* 1994; 14: 783-801.
- Emre M, Cummings JL, Lane RM. Rivastigmine in dementia associated with Parkinson's Disease and Alzheimer's Disease: Similarities and differences. *J Alzheimers Dis* 2007; 11: 509-19.
- Eshuis SA, Jager PL, Maguire RP, Jonkman S, Dierckx RA, Leenders KL. Direct comparison of FP-CIT SPECT and F-DOPA PET in patients with parkinson's disease and healthy controls. *Eur J Nucl Med Mol Imaging* 2009; 36: 454-62.
- Fahn S. Does levodopa slow or hasten the rate of progression of parkinson's disease? *J Neurol* 2005; 252 Suppl 4: IV37-42.
- Farde L, Ehrin E, Eriksson L, Greitz T, Hall H, Hedstrom CG, et al. Substituted benzamides as ligands for visualization of dopamine receptor binding in the human brain by positron emission tomography. *Proc Natl Acad Sci U S A* 1985; 82: 3863-7.
- Feigin A, Leenders KL, Moeller JR, Missimer J, Kuenig G, Spetsieris P, et al. Metabolic network abnormalities in early huntington's disease: An [(18)F]FDG PET study. *J Nucl Med* 2001; 42: 1591-5.
- Fernández-Seara MA, Mengual E, Vidorreta M, Aznárez-Sanado M, Loayza FR, Villagra F, et al. Cortical hypoperfusion in parkinson's disease assessed using arterial spin labeled perfusion MRI. *Neuroimage* 2012; 59: 2743-50.
- Folstein M, Folstein S, McHugh P. "Mini-mental state". A practical method for grading the cognitive state of patients for the clinician. *Journal of psychiatric research* 1975; 12: 189-98.
- Foster NL, Heidebrink JL, Clark CM, Jagust WJ, Arnold SE, Barbas NR, et al. FDG-PET improves accuracy in distinguishing frontotemporal dementia and alzheimer's disease. *Brain* 2007; 130: 2616-35.
- Frackowiak RS, Lenzi GL, Jones T, Heather JD. Quantitative measurement of regional cerebral blood flow and oxygen metabolism in man using ¹⁵O and positron emission tomography: Theory, procedure, and normal values. *J Comput Assist Tomogr* 1980; 4: 727-36.
- Fredholm BB, Svenningsson P. Adenosine-dopamine interactions: Development of a concept and some comments on therapeutic possibilities. *Neurology* 2003; 61: 55-9.
- Galpern WR, Lang AE. Interface between tauopathies and synucleinopathies: A tale of two proteins. *Ann Neurol* 2006; 59: 449-58.

- Garnett ES, Firnau G, Nahmias C. Dopamine visualized in the basal ganglia of living man. *Nature* 1983; 305: 137-8.
- Gauthier S, Reisberg B, Zaudig M, Petersen RC, Ritchie K, Broich K, et al. Mild cognitive impairment. *Lancet* 2006; 367: 1262-70.
- Gerhard A, Pavese N, Hotton G, Turkheimer F, Es M, Hammers A, et al. In vivo imaging of microglial activation with [11C](R)-PK11195 PET in idiopathic parkinson's disease. *Neurobiol Dis* 2006; 21: 404-12.
- Gerschlagner W, Bencsits G, Pirker W, Bloem BR, Asenbaum S, Prayer D, et al. [¹²³I]beta-CIT SPECT distinguishes vascular parkinsonism from parkinson's disease. *Mov Disord* 2002; 17: 518-23.
- Gilman S, Wenning GK, Low PA, Brooks DJ, Mathias CJ, Trojanowski JQ, et al. Second consensus statement on the diagnosis of multiple system atrophy. *Neurology* 2008; 71: 670-6.
- Grafton ST, Mazziotta JC, Pahl JJ, St George-Hyslop P, Haines JL, Gusella J, et al. Serial changes of cerebral glucose metabolism and caudate size in persons at risk for huntington's disease. *Arch Neurol* 1992;49(11):1161-7.
- Groenewegen HJ. The basal ganglia and motor control. *Neural Plast* 2003; 10: 107-20.
- Groenewegen HJ, van Dongen Y.C. Role of the basal ganglia. In: E.Ch.Wolters, T.van Laar, H.W.Berendse, editors. *Parkinsonism Relat Disord*. : VU University press; 2008.
- Grunder G. "Absolute" or "relative": Choosing the right outcome measure in neuroimaging. *Neuroimage* 2009; 45: 258-9.
- Habeck C, Foster NL, Perneczky R, Kurz A, Alexopoulos P, Koeppe RA, et al. Multivariate and univariate neuroimaging biomarkers of Alzheimer's disease. *Neuroimage* 2008; 40: 1503-15.
- Hauw JJ, Daniel SE, Dickson D, Horoupian DS, Jellinger K, Lantos PL, et al. Preliminary NINDS neuropathologic criteria for steele-richardson-olszewski syndrome (progressive supranuclear palsy). *Neurology* 1994; 44: 2015-9.
- Hellwig S, Amtage F, Kreft A, Buchert R, Winz OH, Vach W, et al. [¹⁸F]FDG-PET is superior to [¹²³I]IBZM-SPECT for the differential diagnosis of parkinsonism. *Neurology* 2012; 79: 1314-22.
- Helmich RC, Derikx LC, Bakker M, Scheeringa R, Bloem BR, Toni I. Spatial remapping of cortico-striatal connectivity in parkinson's disease. *Cerebral cortex* 2010; 20: 1175-86.
- Herholz K, Salmon E, Perani D, Baron JC, Holthoff V, Frolich L, et al. Discrimination between alzheimer dementia and controls by automated analysis of multicenter FDG PET. *Neuroimage* 2002; 17: 302-16.
- Hilker R, Voges J, Weber T, Kracht LW, Roggendorf J, Baudrexel S, et al. STN-DBS activates the target area in Parkinson Disease: An FDG-PET study. *Neurology* 2008; 71: 708-13.
- Hilker R, Thomas AV, Klein JC, Weisenbach S, Kalbe E, Burghaus L, et al. Dementia in parkinson disease: Functional imaging of cholinergic and dopaminergic pathways. *Neurology* 2005; 65: 1716-22.
- Hilker R, Voges J, Weisenbach S, Kalbe E, Burghaus L, Ghaemi M, et al. Subthalamic nucleus stimulation restores glucose metabolism in associative and limbic cortices and in cerebellum: Evidence from a FDG-PET study in advanced parkinson's disease. *J Cereb Blood Flow Metab* 2004; 24: 7-16.
- Hilker R, Portman AT, Voges J, Staal MJ, Burghaus L, van Laar T, et al. Disease progression continues in patients with advanced parkinson's disease and effective subthalamic nucleus stimulation. *J Neurol Neurosurg*

- Psychiatry* 2005; 76: 1217-21.
- Holmes RA, Chaplin SB, Royston KG, Hoffman TJ, Volkert WA, Nowotnik DP, et al. Cerebral uptake and retention of 99Tcm-hexamethylpropyleneamine oxime (99Tcm-HM-PAO). *Nucl Med Commun* 1985; 6: 443-7.
- Horstink M, Tolosa E, Bonuccelli U, Deuschl G, Friedman A, Kanovsky P, et al. Review of the therapeutic management of parkinson's disease. report of a joint task force of the european federation of neurological societies and the movement disorder society-european section. part I: Early (uncomplicated) parkinson's disease. *Eur J Neurol* 2006; 13: 1170-85.
- Huang C, Mattis P, Tang C, Perrine K, Carbon M, Eidelberg D. Metabolic brain networks associated with cognitive function in parkinson's disease. *Neuroimage* 2007a; 34: 714-23.
- Huang C, Eidelberg D, Habeck C, Moeller J, Svensson L, Tarabula T, et al. Imaging markers of mild cognitive impairment: Multivariate analysis of CBF SPECT. *Neurobiol Aging* 2007b; 28: 1062-9.
- Huang C, Tang C, Feigin A, Lesser M, Ma Y, Pourfar M, et al. Changes in network activity with the progression of parkinson's disease. *Brain* 2007c; 130: 1834-46.
- Hughes A, Daniel S, Kilford L, Lees A. Accuracy of clinical diagnosis of idiopathic parkinson's disease: A clinico-pathological study of 100 cases. *J Neurol Neurosurg Psychiatry* 1992; 55(3):181-4.
- Hughes AJ, Daniel SE, Ben-Shlomo Y, Lees AJ. The accuracy of diagnosis of parkinsonian syndromes in a specialist movement disorder service. *Brain* 2002; 125: 861-70.
- Innis RB, Seibyl JP, Scanley BE, Laruelle M, Abi-Dargham A, Wallace E, et al. Single photon emission computed tomographic imaging demonstrates loss of striatal dopamine transporters in parkinson disease. *Proc Natl Acad Sci U S A* 1993; 90: 11965-9.
- Ishibashi K, Saito Y, Murayama S, Kanemaru K, Oda K, Ishiwata K, et al. Validation of cardiac (123I)-MIBG scintigraphy in patients with parkinson's disease who were diagnosed with dopamine PET. *Eur J Nucl Med Mol Imaging* 2010; 37: 3-11.
- Ito M, Watanabe H, Kawai Y, Atsuta N, Tanaka F, Naganawa S, et al. Usefulness of combined fractional anisotropy and apparent diffusion coefficient values for detection of involvement in multiple system atrophy. *J Neurol Neurosurg Psychiatry* 2007; 78: 722-8.
- Jarvis MF, Schulz R, Hutchison AJ, Do UH, Sills MA, Williams M. [3H]CGS 21680, a selective A2 adenosine receptor agonist directly labels A2 receptors in rat brain. *J Pharmacol Exp Ther* 1989; 251: 888-93.
- Jenner P, Mori A, Hauser R, Morelli M, Fredholm BB, Chen JF. Adenosine, adenosine A2A antagonists, and parkinson's disease. *Parkinsonism Relat Disord* 2009; 15: 406-13.
- Jeong Y, Cho SS, Park JM, Kang SJ, Lee JS, Kang E, et al. 18F-FDG PET findings in frontotemporal dementia: An SPM analysis of 29 patients. *J Nucl Med* 2005; 46: 233-9.
- Josephs KA, Petersen RC, Knopman DS, Boeve BF, Whitwell JL, Duffy JR, et al. Clinicopathologic analysis of frontotemporal and corticobasal degenerations and PSP. *Neurology* 2006; 66: 41-8.
- Juh R, Kim J, Moon D, Choe B, Suh T. Different metabolic patterns analysis of parkinsonism on the 18F-FDG PET. *Eur J Radiol* 2004; 51: 223-33.
- Kalbe E, Voges J, Weber T, Haarer M, Baudrexel S, Klein JC, et al. Frontal FDG-PET activity correlates with cognitive

- outcome after STN-DBS in parkinson disease. *Neurology* 2009; 72: 42-9.
- Kikuchi T, Okamura T, Zhang MR, Fukushi K, Irie T. In vivo evaluation of N-[18F]fluoroethylpiperidin-4ylmethyl acetate in rats compared with MP4A as a probe for measuring cerebral acetylcholinesterase activity. *Synapse* 2010; 64: 209-15.
- Klein JC, Eggers C, Kalbe E, Weisenbach S, Hohmann C, Vollmar S, et al. Neurotransmitter changes in dementia with lewy bodies and parkinson disease dementia in vivo. *Neurology* 2010; 74: 885-92.
- Klein RC, de Jong BM, de Vries JJ, Leenders KL. Direct comparison between regional cerebral metabolism in progressive supranuclear palsy and parkinson's disease. *Mov Disord* 2005; 20: 1021-30.
- Kung HF, Alavi A, Chang W, Kung MP, Keyes JW, Jr., Velchik MG, et al. In vivo SPECT imaging of CNS D-2 dopamine receptors: Initial studies with iodine-123-IBZM in humans. *J Nucl Med* 1990; 31: 573-9.
- Kwong KK, Belliveau JW, Chesler DA, Goldberg IE, Weisskoff RM, Poncelet BP, et al. Dynamic magnetic resonance imaging of human brain activity during primary sensory stimulation. *Proc Natl Acad Sci U S A* 1992; 89: 5675-9.
- Lebowitz ER, Motlagh MG, Katsovich L, King RA, Lombroso PJ, Grantz H, et al. Tourette syndrome in youth with and without obsessive compulsive disorder and attention deficit hyperactivity disorder. *Eur Child Adolesc Psychiatry* 2012.
- Lee CS, Samii A, Sossi V, Ruth TJ, Schulzer M, Holden JE, et al. In vivo positron emission tomographic evidence for compensatory changes in presynaptic dopaminergic nerve terminals in parkinson's disease. *Ann Neurol* 2000; 47: 493-503.
- Leenders KL, Wolfson L, Jones T. Cerebral blood flow and oxygen metabolism measurement with positron emission tomography in parkinson's disease. *Monogr Neural Sci* 1984a; 11: 180-6.
- Leenders KL, Gibbs JM, Frackowiak RS, Lammertsma AA, Jones T. Positron emission tomography of the brain: New possibilities for the investigation of human cerebral pathophysiology. *Prog Neurobiol* 1984b; 23: 1-38.
- Leenders KL, Wolfson L, Gibbs JM, Wise RJ, Causon R, Jones T, et al. The effects of L-DOPA on regional cerebral blood flow and oxygen metabolism in patients with parkinson's disease. *Brain* 1985; 108 (Pt 1): 171-91.
- Leenders KL, Salmon EP, Tyrrell P, Perani D, Brooks DJ, Sager H, et al. The nigrostriatal dopaminergic system assessed in vivo by positron emission tomography in healthy volunteer subjects and patients with parkinson's disease. *Arch Neurol* 1990; 47: 1290-8.
- Leenders KL, Palmer AJ, Quinn N, Clark JC, Firnau G, Garnett ES, et al. Brain dopamine metabolism in patients with parkinson's disease measured with positron emission tomography. *J Neurol Neurosurg Psychiatry* 1986; 49: 853-60.
- Leonard JP, Nowotnik DP, Neirinckx RD. Technetium-99m-d, 1-HM-PAO: A new radiopharmaceutical for imaging regional brain perfusion using SPECT--a comparison with iodine-123 HIPDM. *J Nucl Med* 1986; 27: 1819-23.
- Limousin P, Krack P, Pollak P, Benazzouz A, Ardouin C, Hoffmann D, et al. Electrical stimulation of the subthalamic nucleus in advanced parkinson's disease. *N Engl J Med* 1998; 339: 1105-11.
- Lindeboom J, Schmand B, Tulner L, Walstra G, Jonker C. Visual association test to detect early dementia of the alzheimer type. *J Neurol Neurosurg Psychiatry* 2002; 73: 126-33.

- Litvan I, Bhatia KP, Burn DJ, Goetz CG, Lang AE, McKeith I, et al. Movement disorders society scientific issues committee report: SIC task force appraisal of clinical diagnostic criteria for parkinsonian disorders. *Mov Disord* 2003; 18: 467-86.
- Litvan I, Agid Y, Calne D, Campbell G, Dubois B, Duvoisin RC, et al. Clinical research criteria for the diagnosis of progressive supranuclear palsy (steele-richardson-olszewski syndrome): Report of the NINDS-SPSP international workshop. *Neurology* 1996; 47: 1-9.
- Lobotesis K, Fenwick JD, Phipps A, Ryman A, Swann A, Ballard C, et al. Occipital hypoperfusion on SPECT in dementia with lewy bodies but not AD. *Neurology* 2001; 56: 643-9.
- Ma Y, Tang C, Moeller JR, Eidelberg D. Abnormal regional brain function in parkinson's disease: Truth or fiction? *Neuroimage* 2009; 45: 260-6.
- Ma Y, Tang C, Spetsieris PG, Dhawan V, Eidelberg D. Abnormal metabolic network activity in parkinson's disease: Test-retest reproducibility. *J Cereb Blood Flow Metab* 2007a; 27: 597-605.
- Ma Y, Tang C, Spetsieris PG, Dhawan V, Eidelberg D. Abnormal metabolic network activity in parkinson's disease: Test-retest reproducibility. *J Cereb Blood Flow Metab* 2007b; 27: 597-605.
- Ma Y, Huang C, Dyke JP, Pan H, Alsop D, Feigin A, et al. Parkinson's disease spatial covariance pattern: Noninvasive quantification with perfusion MRI. *J Cereb Blood Flow Metab* 2010a; 30: 505-9.
- Ma Y, Tang C, Chaly T, Greene P, Breeze R, Fahn S, et al. Dopamine cell implantation in parkinson's disease: Long-term clinical and (18)F-FDOPA PET outcomes. *J Nucl Med* 2010b; 51: 7-15.
- Mahapatra RK, Edwards MJ, Schott JM, Bhatia KP. Corticobasal degeneration. *Lancet Neurol* 2004; 3: 736-43.
- Marshall VL, Patterson J, Hadley DM, Grosset KA, Grosset DG. Two-year follow-up in 150 consecutive cases with normal dopamine transporter imaging. *Nucl Med Commun* 2006; 27: 933-7.
- Mayberg HS. Frontal lobe dysfunction in secondary depression. *J Neuropsychiatry Clin Neurosci* 1994;6(4):428-42.
- McKeith IG. Consensus guidelines for the clinical and pathologic diagnosis of dementia with lewy bodies (DLB): Report of the consortium on DLB international workshop. *J Alzheimers Dis* 2006; 9: 417-23.
- McKeith IG, Dickson DW, Lowe J, Emre M, O'Brien JT, Feldman H, et al. Diagnosis and management of dementia with lewy bodies: Third report of the DLB consortium. *Neurology* 2005; 65: 1863-72.
- McKhann G, Drachman D, Folstein M, Katzman R, Price D, Stadlan EM. Clinical diagnosis of Alzheimer's disease: Report of the NINCDS-ADRDA work group under the auspices of department of health and human services task force on Alzheimer's disease 35. *Neurology* 1984; 34: 939-44.
- McKhann GM, Albert MS, Grossman M, Miller B, Dickson D, Trojanowski JQ. Clinical and pathological diagnosis of frontotemporal dementia: Report of the work group on frontotemporal dementia and pick's disease. *Arch Neurol* 2001; 58: 1803-9.
- Melzer TR, Watts R, Macaskill MR, Pearson JF, Rueger S, Pitcher TL, et al. Arterial spin labelling reveals an abnormal cerebral perfusion pattern in Parkinson's disease. *Brain* 2011; 134: 845-55.
- Minoshima S, Foster NL, Sima AA, Frey KA, Albin RL, Kuhl DE. Alzheimer's disease versus dementia with lewy bodies: Cerebral metabolic distinction with autopsy confirmation. *Ann Neurol* 2001; 50: 358-65.

- Mishina M, Ishiwata K, Kimura Y, Naganawa M, Oda K, Kobayashi S, et al. Evaluation of distribution of adenosine A(2A) receptors in normal human brain measured with [C-11]TMSX PET. *Synapse* 2007; 61: 778-84.
- Moeller JR, Strother SC. A regional covariance approach to the analysis of functional patterns in positron emission tomographic data. *J Cereb Blood Flow Metab* 1991; 11: A121-35.
- Moeller JR, Strother SC, Sidtis JJ, Rottenberg DA. Scaled subprofile model: A statistical approach to the analysis of functional patterns in positron emission tomographic data. *J Cereb Blood Flow Metab* 1987; 7: 649-58.
- Moeller JR, Nakamura T, Mentis MJ, Dhawan V, Spetsieris P, Antonini A, et al. Reproducibility of regional metabolic covariance patterns: Comparison of four populations. *J Nucl Med* 1999; 40: 1264-9.
- Morrish PK, Rakshi JS, Bailey DL, Sawle GV, Brooks DJ. Measuring the rate of progression and estimating the preclinical period of parkinson's disease with [18F]dopa PET. *J Neurol Neurosurg Psychiatry* 1998; 64: 314-9.
- Mosconi L, Tsui WH, Herholz K, Pupi A, Drzezga A, Lucignani G, et al. Multicenter standardized 18F-FDG PET diagnosis of mild cognitive impairment, alzheimer's disease, and other dementias. *J Nucl Med* 2008; 49: 390-8.
- Mure H, Hirano S, Tang CC, Isaias IU, Antonini A, Ma Y, et al. Parkinson's disease tremor-related metabolic network: Characterization, progression, and treatment effects. *Neuroimage* 2011; 54: 1244-53.
- Nagano-Saito A, Washimi Y, Arahata Y, Iwai K, Kawatsu S, Ito K, et al. Visual hallucination in parkinson's disease with FDG PET. *Mov Disord* 2004; 19: 801-6.
- Nakajima K, Yoshita M, Matsuo S, Taki J, Kinuya S. Iodine-123-MIBG sympathetic imaging in lewy-body diseases and related movement disorders. *Q J Nucl Med Mol Imaging* 2008; 52: 378-87.
- Otsuka M, Kuwabara Y, Ichiya Y, Hosokawa S, Sasaki M, Yoshida T, et al. Differentiating between multiple system atrophy and parkinson's disease by positron emission tomography with 18F-dopa and 18F-FDG. *Ann Nucl Med* 1997; 11: 251-7.
- Otsuka M, Ichiya Y, Kuwabara Y, Hosokawa S, Sasaki M, Yoshida T, et al. Differences in the reduced 18F-dopa uptakes of the caudate and the putamen in parkinson's disease: Correlations with the three main symptoms. *J Neurol Sci* 1996; 136: 169-73.
- Ouchi Y, Yoshikawa E, Sekine Y, Futatsubashi M, Kanno T, Ogosu T, et al. Microglial activation and dopamine terminal loss in early parkinson's disease. *Ann Neurol* 2005; 57: 168-75.
- Parkinson Study Group. Pramipexole vs levodopa as initial treatment for parkinson disease: A randomized controlled trial. *JAMA* 2000; 284: 1931-8.
- Patwardhan MB, McCrory DC, Matchar DB, Samsa GP, Rutschmann OT. Alzheimer disease: Operating characteristics of PET--a meta-analysis. *Radiology* 2004; 231: 73-80.
- Pavese N, Kiferle L, Piccini P. Neuroprotection and imaging studies in parkinson's disease. *Parkinsonism Relat Disord* 2009; 15 Suppl 4: S33-7.
- Pavese N, Evans AH, Tai YF, Hotton G, Brooks DJ, Lees AJ, et al. Clinical correlates of levodopa-induced dopamine release in parkinson disease: A PET study. *Neurology* 2006; 67: 1612-7.
- Piccini P, Whone A. Functional brain imaging in the differential diagnosis of parkinson's disease. *Lancet Neurol* 2004; 3: 284-90.

- Pirker W, Holler I, Gerschlager W, Asenbaum S, Zetting G, Brucke T. Measuring the rate of progression of parkinson's disease over a 5-year period with beta-CIT SPECT. *Mov Disord* 2003; 18: 1266-72.
- Poston KL, Eidelberg D. Network biomarkers for the diagnosis and treatment of movement disorders. *Neurobiol Dis* 2009; 35: 141-7.
- Poston KL, Tang CC, Eckert T, Dhawan V, Frucht S, Vonsattel J-, et al. Network correlates of disease severity in multiple system atrophy. *Neurology* 2012; 78: 1237-44.
- Pourfar M, Feigin A, Tang CC, Carbon-Correll M, Bussa M, Budman C, et al. Abnormal metabolic brain networks in tourette syndrome. *Neurology* 2011; 76: 944-52.
- Quinlan JR. C4.5: Programs for machine learning. *Morgan Kaufmann Publishers*; 1993.
- Reitan. R. Validity of the trail making test as an indicator of organic brain damage. *Perceptual and motor skills* 1958; 8: 271-276.
- Reivich M, Kuhl D, Wolf A, Greenberg J, Phelps M, Ido T, et al. The [18F]fluorodeoxyglucose method for the measurement of local cerebral glucose utilization in man. *Circ Res* 1979; 44: 127-37.
- Rinne JO, Kuikka JT, Bergstrom KA, Rinne UK. Striatal dopamine transporter in different disability stages of parkinson's disease studied with [(123I)]beta-CIT SPECT. *Parkinsonism Relat Disord* 1995; 1: 47-51.
- Rinne JO, Bergman J, Ruottinen H, Haaparanta M, Eronen E, Oikonen V, et al. Striatal uptake of a novel PET ligand, [18F]beta-CFT, is reduced in early parkinson's disease. *Synapse* 1999; 31: 119-24.
- Saan RJ, Deelman BG. De 15 woorden tests A en B. (een voorlopige handleiding). Groningen afd neuropsychologie, *UMCG* 1986.
- Scarmeas N, Habeck CG, Zarahn E, Anderson KE, Park A, Hilton J, et al. Covariance PET patterns in early alzheimer's disease and subjects with cognitive impairment but no dementia: Utility in group discrimination and correlations with functional performance. *Neuroimage* 2004; 23: 35-45.
- Schwarz J, Antonini A, Tatsch K, Kirsch CM, Oertel WH, Leenders KL. Comparison of 123I-IBZM SPECT and 11C-raclopride PET findings in patients with parkinsonism. *Nucl Med Commun* 1994; 15: 806-13.
- Schwarz J, Tatsch K, Arnold G, Ott M, Trenkwalder C, Kirsch CM, et al. 123I-iodobenzamide-SPECT in 83 patients with de novo parkinsonism. *Neurology* 1993; 43: 517-20.
- Silverman DH, Small GW, Chang CY, Lu CS, Aburto KD, Chen W, et al. Positron emission tomography in evaluation of dementia: Regional brain metabolism and long-term outcome. *JAMA* 2001; 286: 2120-7.
- Sokoloff L. Relation between physiological function and energy metabolism in the central nervous system. *J Neurochem* 1977; 29: 13-26.
- Sokoloff L, Reivich M, Kennedy C, Des Rosiers MH, Patlak CS, Pettigrew KD, et al. The [14C]deoxyglucose method for the measurement of local cerebral glucose utilization: Theory, procedure, and normal values in the conscious and anesthetized albino rat. *J Neurochem* 1977; 28: 897-916.
- Spetsieris PG, Eidelberg D. Scaled subprofile modeling of resting state imaging data in parkinson's disease: Methodological issues. *Neuroimage* 2011; 54(4):2899-914.
- Spetsieris PG, Dhawan V, Eidelberg D. Three-fold cross-validation of parkinsonian brain patterns. *Conf Proc IEEE*

- Eng Med Biol Soc* 2010; 2010: 2906-9.
- Spetsieris PG, Ma Y, Dhawan V, Eidelberg D. Differential diagnosis of parkinsonian syndromes using PCA-based functional imaging features. *Neuroimage* 2009; 45: 1241-52.
- Stacy M, Jankovic J. Differential diagnosis of parkinson's disease and the parkinsonism plus syndromes. *Neurol Clin* 1992; 10: 341-59.
- Steele JC, Richardson J, Olszewski J. Progressive supranuclear palsy: A heterogeneous degeneration involving the brain stem, basal ganglia and cerebellum with vertical gaze and pseudobulbar palsy, nuchal dystonia and dementia. *Arch Neurol* 1964; 10: 333-59.
- Stroop J. Studies of interference in serial verbal reactions. *J Exp Psychology* 1935; 18: 643-662.
- Tang CC, Poston KL, Dhawan V, Eidelberg D. Abnormalities in metabolic network activity precede the onset of motor symptoms in parkinson's disease. *J Neurosci* 2010a; 30: 1049-56.
- Tang CC, Poston KL, Eckert T, Feigin A, Frucht S, Gudesblatt M, et al. Differential diagnosis of parkinsonism: A metabolic imaging study using pattern analysis. *Lancet Neurol* 2010b; 9: 149-58.
- Teismann P, Tieu K, Cohen O, Choi DK, Wu DC, Marks D, et al. Pathogenic role of glial cells in parkinson's disease. *Mov Disord* 2003; 18: 121-9.
- Teune LK, Renken RJ, Mudali D, de Jong BM, Dierckx RA, Roerdink JBTM, et al. Validation of parkinsonian disease-related metabolic brain patterns. *Mov Disord, Epub ahead of print: 2013 Mar 11*.
- Teune LK, Bartels AL, de Jong BM, Willemsen AT, Eshuis SA, de Vries JJ, et al. Typical cerebral metabolic patterns in neurodegenerative brain diseases. *Mov Disord* 2010; 25: 2395-404.
- Tissingh G, Booij J, Bergmans P, Winogrodzka A, Janssen AG, van Royen EA, et al. Iodine-123-N-omega-fluoropropyl-2beta-carbomethoxy-3beta-(4-iodophenyl)tropane SPECT in healthy controls and early-stage, drug-naive parkinson's disease. *J Nucl Med* 1998; 39: 1143-8.
- Trost M., Carbon M., Edwards C., Ma Y., Raymond D., Mentis MJ., et al. Primary dystonia: Is abnormal functional brain architecture linked to genotype? *Ann Neurol* 2002; 52(6):853-6.
- Vaillancourt DE, Spraker MB, Prodoehl J, Abraham I, Corcos DM, Zhou XJ, et al. High-resolution diffusion tensor imaging in the substantia nigra of de novo parkinson disease. *Neurology* 2009; 72: 1378-84.
- Van Dijk KR, Hedden T, Venkataraman A, Evans KC, Lazar SW, Buckner RL. Intrinsic functional connectivity as a tool for human connectomics: Theory, properties, and optimization. *J Neurophysiol* 2010; 103(1):297-321.
- van Osch MJ, Teeuwisse WM, van Walderveen MA, Hendrikse J, Kies DA, van Buchem MA. Can arterial spin labeling detect white matter perfusion signal? *Magn Reson Med* 2009; 62: 165-73.
- Volkow ND, Ding YS, Fowler JS, Wang GJ, Logan J, Gatley SJ, et al. A new PET ligand for the dopamine transporter: Studies in the human brain. *J Nucl Med* 1995; 36: 2162-8.
- Volkow ND, Gur RC, Wang GJ, Fowler JS, Moberg PJ, Ding YS, et al. Association between decline in brain dopamine activity with age and cognitive and motor impairment in healthy individuals. *Am J Psychiatry* 1998; 155: 344-9.
- Warrington EK, James M. The visual object and space perception battery (VOSP). In: Anonymous Bury st

- Edmunds: *Thames Valley test company*. England; 1991.
- Wenning GK, Tison F, Ben Shlomo Y, Daniel SE, Quinn NP. Multiple system atrophy: A review of 203 pathologically proven cases. *Mov Disord* 1997; 12: 133-47.
- Whone AL, Watts RL, Stoessl AJ, Davis M, Reske S, Nahmias C, et al. Slower progression of parkinson's disease with ropinirole versus levodopa: The REAL-PET study. *Ann Neurol* 2003; 54: 93-101.
- Wilson B, Alderman N, Burgess P, Emslie H, Hodges J. Behavioural assessment of the dysexecutive syndrome (BADs). In: Anonymous Bury st Edmund: *Thames Valley test company*. England; 1996.
- Yakushev I, Hammers A, Fellgiebel A, Schmidtman I, Scheurich A, Buchholz HG, et al. SPM-based count normalization provides excellent discrimination of mild alzheimer's disease and amnesic mild cognitive impairment from healthy aging. *Neuroimage* 2009; 44: 43-50.
- Yakushev I, Landvogt C, Buchholz HG, Fellgiebel A, Hammers A, Scheurich A, et al. Choice of reference area in studies of alzheimer's disease using positron emission tomography with fluorodeoxyglucose-F18. *Psychiatry Res* 2008; 164: 143-53.
- Yong SW, Yoon JK, An YS, Lee PH. A comparison of cerebral glucose metabolism in parkinson's disease, parkinson's disease dementia and dementia with lewy bodies. *Eur J Neurol* 2007; 14: 1357-62.

SAMENVATTING

Neurodegeneratieve hersenziekten zijn hersenaandoeningen waarbij langzamerhand – over vele jaren - de zenuwcellen in bepaalde gebieden verloren gaan. Vaak is de oorzaak van deze hersenziekten onbekend en zijn de behandelingsmogelijkheden beperkt. De laatste tientallen jaren wordt echter veel onderzoek naar deze aandoeningen gedaan met de verwachting dat dit zal resulteren in beter inzicht en betere behandelingsmogelijkheden. Voorbeelden van neurodegeneratieve ziekten zijn onder andere Ziekte van Parkinson (PD), multisysteem atrofie (MSA), progressieve supranucleaire parese (PSP), Corticobasale degeneratie (CBD) en Dementie met Lewy Bodies (DLB). Deze ziekten hebben gemeenschappelijk dat ze allemaal in meer of mindere mate parkinsonistische verschijnselen hebben (stijfheid, traagheid, rusttremor, balansproblemen). Daarnaast kunnen bij sommige aandoeningen op een bepaald moment in de ziekte geheugenklachten, problemen met het uitvoeren van complexe taken en visuele hallucinaties optreden. Bij de ziekte van Alzheimer (AD) staan vooral geheugenproblemen op de voorgrond en bij frontotemporale dementie (FTD) kunnen gedragsverandering en problemen met taal voorkomen. Alle bovenstaande aandoeningen vallen onder de categorie neurodegeneratieve hersenziekten.

Een precieze diagnose stellen kan vooral in een vroeg ziektestadium lastig zijn omdat de symptomen van patiënten op elkaar lijken. Het beloop van de ziekte in de tijd (welke symptomen precies, snelheid, ernst) leiden uiteindelijk naar de juiste diagnose. Hier kan soms jaren overheen gaan. Het is echter wel van belang voor de patiënt voor de prognose, en soms ook voor de behandeling om in een vroeg ziektestadium een precieze diagnose te kunnen stellen.

Een aantal nieuwe beeldvormende technieken kunnen medisch specialisten, zoals de neuroloog, helpen om in een beginstadium van een ziekte een beter onderscheid tussen de verschillende neurodegeneratieve hersenziekten te maken. In **hoofdstuk 2** worden verschillende radiotracer neuroimagingtechnieken besproken die kunnen helpen bij het onderscheid tussen PD en overige neurodegeneratieve hersenziekten.

Om een onderscheid binnen de groep neurodegeneratieve hersenziekten te maken kan een [¹⁸F]-fluorodeoxyglucose (FDG)-PET scan behulpzaam zijn. Bij dit onderzoek wordt de radiotracer FDG (dit is een vorm van glucose (suiker)) ingezet. Glucose is normaal gesproken de enige energiebron van hersenweefsel. Door een FDG-PET scan van de hersenen te maken wordt zichtbaar welke hersengebieden meer of minder energie gebruiken en dus goed of minder goed functioneren volgens een bepaald patroon. Deze patronen van verminderde en soms verhoogd energieverbruik oftewel het glucosemetabolisme zijn verschillend voor de genoemde neurodegeneratieve hersenziekten en kunnen ook al aanwezig zijn in het begin van deze hersenziekten.

Het doel van dit proefschrift was om met behulp van een FDG-PET scan het glucose metabolisme in de hersenen bij neurodegeneratieve hersenziekten in beeld te brengen. Daarnaast werden verschillende analysetechnieken en ook andere beeldvormende MRI technieken onderzocht om de ziekte-specifieke metabole patronen weer te geven.

In **hoofdstuk 3** hebben wij retrospectief FDG-PET scans geanalyseerd van patiënten in een vroeg ziektestadium met verschillende neurodegeneratieve hersenziekten.

In totaal werden 96 patiënten geïncludeerd die een klinische FDG-PET scan ondergingen en voldeden aan klinische onderzoekscriteria waarvan 20 met de ziekte van Parkinson (PD), 21 multisysteem atrofie (MSA), 17 progressieve supranucleaire parese (PSP), 10 corticobasale degeneratie (CBD), 6 dementie met lewy bodies (DLB), 15 ziekte van Alzheimer (AD) en 7 frontotemporale dementie (FTD). De FDG-PET beelden werden geanalyseerd en vergeleken met 18 gezonden via Statistical Parametric Mapping (SPM5). Verlaagde metabole activiteit in bepaalde hersengebieden ten opzichte van gezonde controles werd gevonden in PD (contralateraal parieto-occipitaal, frontaal), MSA (bilateraal putamen, cerebellum), PSP (prefrontale cortex, nucleus caudatus, thalamus, mesencephalon), CBD (contralaterale corticale regio's), DLB (occipitaal, parieto-temporaal), AD (parieto-temporaal) en FTD (fronto-temporaal). In deze patiënten die gescand waren in een vroeg ziektestadium waren dus typische verschillen tussen patiënten groepen en gezonden te zien.

In **hoofdstuk 4** wordt een literatuur overzicht gegeven van ziekte-specifieke metabole patronen bij verschillende neurodegeneratieve hersenziekten. Daarnaast wordt in dit hoofdstuk een bepaalde wiskundige techniek uitgelegd, de zogenoemde scaled subprofile model/principal component analyse (SSM-PCA). Dit is een multivariaat methode gebaseerd op principal component analyse waarmee het verschil in hersenpatronen in een gecombineerde groep gezonden en patiënten gevonden kan worden en weergegeven in een ziekte-specifiek metabool patroon. Het laat relaties zien welke men niet zo direct op het oog kan zien en het bepaalt de kans dat veranderingen in het glucosemetabolisme in verschillende hersengebieden bij elkaar horen in een patroon.

Het grote voordeel van deze analyse methode is dat niet alleen twee groepen onderling vergeleken kunnen worden, maar dat ook de bijdrage van elk individu ten opzichte van het patroon berekend kan worden. Dit betekent dat voor elke nieuwe patiënt met behulp van deze methode een score (de zogenaamde z-score) berekend kan worden die weergeeft hoeveel het metabole hersenpatroon van die patiënt lijkt op het ziekte-specifieke metabole groeps patroon van die ziekte. Hoe hoger de z-score, (hoge expressie van het ziekte-specifieke patroon bij dat individu), hoe groter de kans (hogere waarschijnlijkheid) dat die patiënt ook die bepaalde ziekte heeft. Deze scores kunnen berekend worden voor elk beschikbaar en gevalideerd ziekte-specifiek metabool patroon.

In **hoofdstuk 5** valideerden wij het ziekte-specifieke metabole patroon voor PD, MSA en PSP met behulp van deze SSM/PCA analyse waarbij bleek dat met behulp van deze patronen een goed onderscheid tussen de verschillende ziektebeelden gemaakt kon worden. In **hoofdstuk 6** identificeerden wij het Alzheimer-gerelateerde metabole patroon en pasten het daarnaast toe in een prospectieve groep patiënten onderverdeeld in een waarschijnlijk en niet- waarschijnlijk ziekte van Alzheimergroep. Voor elke patiënt werd een z-score berekend voor het AD-gerelateerde patroon die weergeeft hoeveel die patiënt lijkt op het ziekte-specifieke AD groeps patroon. Het bleek dat de

patiënten uit de “waarschijnlijke”AD-groep inderdaad een hoge score hadden voor het AD-patroon en patiënten met “niet-waarschijnlijke” AD een lage score hadden.

In **hoofdstuk 7** presenteren wij het GLIMPS project (GLIMPS is een acroniem voor GLucose IMaging in ParkinsonismS). Dit is een landelijk project, gecoördineerd vanuit het UMC Groningen, waaraan verschillende ziekenhuizen in Nederland meedoen. Het doel van dit project is om de diagnostiek bij patiënten in een vroege fase van een neurodegeneratieve hersenziekte te verbeteren door systematisch de het glucose metabolisme in de hersenen bij patiënten met neurodegeneratieve hersenziekten te onderzoeken met behulp van een FDG-PET scan.

Bij het beoordelen van een patroon bij een individuele patiënt is het van belang een krachtige referentiegroep van bekende ziekte-specifieke metabole patronen van bepaalde patiëntengroepen ter vergelijking te hebben. Het landelijk verzamelen van deze metabolepatronen bij patiënten slechts sinds kort mogelijk aangezien thans FDG-PET in de meeste grote regionale centra in Nederland beschikbaar is.

Daarnaast wordt het steeds duidelijker dat een combinatie van verschillende beeldvormende technieken zoals verschillende MRI scans kunnen bijdragen aan een verbeterde omschrijving van ziekte-specifieke metabole patronen van de hersenen. Een prospectieve studie werd uitgevoerd bij 20 Parkinsonpatiënten en 17 gezonde vrijwilligers om te onderzoeken of FDG-PET gescand met een hoge resolutie camera gecombineerd met verschillende MRI scans zoals Arterial Spin Labeling (ASL), resting state fMRI en diffusion tensor imaging (DTI) een nog beter en duidelijker ziekte-specifiek patroon voor de ziekte van Parkinson zou opleveren.

In **hoofdstuk 8** werd het ziekte-specifieke Parkinsonpatroon gemeten met de hoge resolutie FDG-PET scan vergeleken met het patroon gevonden met ASL, een techniek om de doorbloeding (perfusie) in de hersenen te meten. Het metabole patroon voor PD gemeten met FDG-PET komt overeen met het eerder beschreven PD-patroon in hoofdstuk 5 en eerdere literatuur. Daarnaast is het mogelijk gebleken om een ziekte-specifiek metabool- en perfusie-patroon bij dezelfde Parkinsonpatiënten te vinden. Beide patroon lijken veel op elkaar, maar er zijn ook enkele verschillen. We concludeerden dat het combineren van verschillende soorten scans, PET en MRI, meer inzicht kan geven in de onderliggende pathologische processen, maar dat de complexiteit van de data-analyse toeneemt. Ook worden de analysemethoden zelf verder ontwikkeld om voor de toekomst de technieken nog gevoeliger te maken voor de verschillen tussen de neurodegeneratieve hersenziekten.

CONCLUSIE

FDG-PET is steeds meer beschikbaar voor de klinische praktijk en is nog steeds de meest betrouwbare techniek die nauwkeurig het energieverbruik in de hersenen laat zien. De wiskunde rekentechniek SSM/PCA kan verbanden tussen verhoogde en verlaagde glucose metabolisme in verschillende hersengebieden in 1 patroon voor elke neurodegeneratieve apart laten zien. Vervolgens kan met

behulp van een rekenmethode een score berekend worden die weergeeft hoeveel het metabole hersenpatroon van een individuele patiënt lijkt op het ziekte-specifieke metabole groeps patroon van bv PD, MSA of PSP. Hoe hoger deze score, hoe meer het hersenpatroon van de individuele patiënt lijkt op het groeps patroon en des te waarschijnlijker het is dat de patiënt deze ziekte heeft. Daarom kunnen bij patiënten met neurodegeneratieve hersenziekten deze ziekte-specifieke metabole patronen in de hersenen een waardevol hulpmiddel zijn in de klinische praktijk bij het stellen van de juiste diagnose.

DANKWOORD

DANKWOORD

Last but not least, het dankwoord: waarschijnlijk het meest gelezen onderdeel van dit proefschrift;-). Allereerst wil ik graag de patiënten en gezonde vrijwilligers bedanken die aan dit proefschrift hebben meegewerkt door de scans te ondergaan en de collega's voor het aanmelden van patiënten. Zonder jullie medewerking was dit niet gelukt.

Daarnaast wil ik een aantal mensen in het bijzonder noemen die direct of indirect van belang geweest zijn voor dit proefschrift.

Om te beginnen wil ik mijn promotor, Prof. dr. K.L. Leenders bedanken. Nico, ik heb veel van je geleerd de afgelopen jaren, bij jou ligt de basis voor dit proefschrift. Ik vond de uitstapjes naar het Hammersmith Hospital in Londen en het Feinstein Institute in New York erg interessant en leerzaam. Ik vond het daarnaast erg leuk om alle verhalen over vroeger, hoe het allemaal begonnen is in de PET wereld, te horen. Ook waren de vele bezoeken aan de verschillende ziekenhuizen in Nederland voor het GLIMPS project erg inspirerend. Ik hoop dat we nog lang kunnen blijven samenwerken in het GLIMPS project.

Verder wil ik mijn 2^e promotor, Prof. dr. R.A. Dierckx, bedanken voor het mede mogelijk maken van de verschillende onderzoeken en het beoordelen van de artikelen. Daarnaast ook mijn copromotor Dr. R.J. Renken; Beste Remco, ik heb veel van je geleerd in het analyseren van de MRI beelden en de ontwikkeling van de SSM/PCA. Onze besprekingen waren altijd zeer verhelderend. Wanneer ik later toch nog vragen had of bugs in de scripts ontdekte, kon ik gelukkig altijd bij je aankloppen.

Verder vind ik het een grote eer dat Prof. dr. D. Eidelberg, Prof dr. J. Booij en Prof. dr. J.B.T.M. Roerdink in de leescommissie zitting wilden nemen. Ik wil jullie van harte bedanken voor het lezen en beoordelen van het proefschrift. Dear professor Eidelberg, it is a great honour for me to have you in the reading committee. I do appreciate this very much and I would like to thank you for reading this thesis. I found the visit to your lab interesting and inspiring.

Alle mede-auteurs, bedankt voor de prettige samenwerking bij de totstandkoming van de artikelen.

Bauke de Jong bedankt voor je directe en concrete hulp bij de verschillende studies en het opschrijven ervan. Je was altijd goed voor een kritische blik en het inkorten van de tekst om aan de woordlimiet te voldoen.

Collega onderzoekers Carolien, Anne Marthe, Martijn, Anna Bartels, Janneke, Esther Smits, Marja, Madelein, Anouk, Meike, Maarten, Arnoud en Jelmer bedankt voor de gezelligheid tijdens het werk maar ook daarbuiten tijdens borrels en congressen.

Martje en Teus, en overige betrokkenen bij de polikliniek bewegingsstoornissen bedankt voor de

prettige samenwerking tijdens de afgelopen jaren.

Deborah Sival, bedankt dat ik mijn 1^e ervaring met wetenschappelijk onderzoek op heb kunnen doen bij jou. Ik heb er veel van geleerd!

De afdeling Nucleaire geneeskunde, in het bijzonder de mnw-ers bedankt voor het scannen, opzoeken en soms diverse malen reconstrueren van de FDG-PET scans.

Silvia bedankt voor je altijd vrolijke aanwezigheid, ik wens je alle geluk in het voor jou vertrouwde Friesland!

Het Neuroimaging center (NIC): Remco en Jan-Bernard bedankt voor de participatie in het GLIMPS project en Judith en Anita voor de inzet bij het maken van de MRI scans.

Deborah Mudali en Jos Roerdink van de afdeling wetenschappelijke visualisatie en computergrafiek van de RUG. Ik heb veel geleerd van de besprekingen waarbij het erg leuk was om het eens van een geheel andere kant te bekijken, wat soms tot nieuwe inzichten kan leiden. Bedankt hiervoor and Deborah, good luck with your thesis!

Andrey and Rees from TARGET: many thanks for the design and building of the GLIMPS database.

Lisette en Henny bedankt voor het overnemen van de praktische gang van zaken van het GLIMPS project. Ik hoop dat het project succesvol blijft en dat we nog lang mogen blijven samenwerken.

Tijdens mijn promotie-onderzoek was ik ook betrokken bij de parel neurodegeneratieve ziekten van het Parelsnoer Initiatief. Truus, Stephen, Bas, René van bureau onderzoek en de TCC en overige leden van de stuurgroep biobanking bedankt voor de prettige samenwerking. Gerbrand, Jeroen, Fijanne, Rita en Elske-Marije van het UCO bedankt voor de prettige samenwerking en het mogen bijwonen van de nabespreking van het multidisciplinaire dementie spreekuur. Ik heb er veel van geleerd!

Mijn nieuwe AIOS-collega's, staf neurologie, en overige neurologie collega's bedankt voor de fijne werksfeer wat maakte dat ik mij al snel thuis voelde op mijn nieuwe werkplek!

Lieve vrienden zijn absoluut onmisbaar: Nina en Dirk, Niels en Mirelle, Jo en Jelle, Stefanie en Frank, Floris en Loes, Arjen en Nienke, Daan en Irene, Elvera, Marcelle en Janneke: bedankt voor de altijd gezellige etentjes en bezoeken.

De R(H)ijkskampers bedankt voor de vele gezellige borrels, hopelijk volgen er nog genoeg, ondanks dat we nu geen officiële burens meer zijn.

Carolien: onderzoekscollega vanaf het begin, bedankt voor alle gezelligheid en de inspirerende, relativerende en opbeurende gesprekken die wij hadden. Ook vond ik het erg leuk om met jou en Riko in Argentinië rond te toeren. Fijn dat je het nu zo naar je zin hebt in Amsterdam. Ik vind het een hele eer dat jij mijn paranimf wilt zijn. Ik hoop dat we elkaar nog vaak blijven zien, daar proosten we op;-).

Mijn schoonfamilie, Jannie en Jitze, Heleen, Mark en Stan, Jeroen en Dirk-Geert bedankt voor jullie betrokkenheid en interesse voor mijn onderzoek en werk.

Dennis, broertje, we zijn erg verschillend, maar ik ben er trots op je zus te zijn. Veel succes met klussen in je huis en veel geluk samen met Angela.

Jenny, bedankt voor de gezellige 'zussie avondjes', je humor en je vrolijke lach. Daarnaast ben je er altijd goed in om mij te helpen een knoop door te hakken. Ik vind het erg leuk en een hele eer dat jij mijn paranimf wilt zijn. Jaap, bedankt voor de noodzakelijke laptopupdates en de interesse in mijn onderzoek. Ik wens jullie veel geluk, samen met jullie schattige konijntjes Pila en Chouffie.

Papa en mama, heel erg bedankt voor jullie onvoorwaardelijke steun in mijn keuzes. Jullie hebben altijd geholpen om mijn dromen waar te maken op studie- en onderzoeksgebied.

Mama ik vind het erg stoer dat je de sprong hebt gewaagd en je eigen bedrijf Mentorschap Noord-Oost bent gestart. Daarnaast ben je ook nog druk met verschillende terrazzo projecten. Onze keuken wordt daardoor prachtig!

Papa, jij bent altijd in voor een origineel idee of creatieve oplossing, met vervolgens de uitdrukking 'dat ken'k zelf wel mokn!' Ik ben wel benieuwd wanneer de moerasboot eindelijk gaat aanmeren. Daarnaast is ook op klusgebied jullie steun onmisbaar en bedankt voor jullie vele hulp op ieder moment!

Lieve Wouter, heel erg bedankt voor je extra liefde, steun, geduld en rust in drukke perioden. Dit was absoluut onmisbaar voor de totstandkoming van dit proefschrift. Vooral het afgelopen half jaar, toen de start van de opleiding en de bouw van ons huis voor nog meer drukte en stress heeft gezorgd. Inmiddels hebben wij onze intrek genomen in ons huis, wat nog een beetje een bouwproject is. Ik ben heel erg gelukkig bij jou en hopelijk hebben we binnenkort meer tijd om samen van ons nieuwe huis op deze mooie plek te genieten!

CURRICULUM VITAE

Over de auteur:

Laura Teune werd geboren op 29-12-1981 te Amersfoort. In 2001 behaalde zij haar atheneum diploma aan het Fivelcollege te Delfzijl. In datzelfde jaar startte zij met de studie geneeskunde aan de Rijksuniversiteit Groningen. In 2004 raakte zij verder geïnteresseerd in de Neurologie en verrichtte zij onderzoek naar epilepsie bij kinderen onder begeleiding van Dr. D.A. Sival. In 2007, na afloop van het keuze-coschap Neurologie op de afdeling Neurologie in het UMCG, liep zij haar wetenschappelijke stage bij de afdeling bewegingsstoornissen onder leiding van Prof. dr. K.L. Leenders. Dit was het begin van een langdurige samenwerking wat resulteerde in dit proefschrift. In augustus 2007 behaalde zij haar artsexamen om vervolgens eerst een jaar als AGNIO Neurologie in de Isala Klinieken in Zwolle te werken. Na een succesvolle subsidie-aanvraag bij het IPF kon zij in oktober 2008 starten met het promotietraject naar metabole patroonherkenning bij neurodegeneratieve hersenziekten. Gedurende haar promotietraject had zij naast het opzetten en uitvoeren van wetenschappelijk onderzoek 1 dagdeel per week haar eigen bewegingsstoornissenpoli in het UMCG. Daarnaast was zij werkzaam bij de parel neurodegeneratieve ziekten van het parelsnoer initiatief (PSI). Zij was nauw betrokken bij het opzetten van de parel neurodegeneratieve ziekten in het UMCG in samenwerking met bureau onderzoek en het Universitair Centrum Ouderengeneeskunde. Zij is tot juni 2012 parelondersteuner gebleven. Daarnaast had zij vanaf 2010 een coördinerende rol in de voorbereiding en start van het GLIMPS project (GLucose IMaging in ParkinsonismS). Sinds oktober 2012 is zij in opleiding tot neuroloog in het UMCG.

Articles:

Joost Nicolai, Albert P. Aldenkamp, Johannes R. Huizenga, **Laura K. Teune** and Oebele F. Brouwer. Cognitive side effects of valproic acid-induced hyperammonemia in children with epilepsy. *Journal of Clinical Psychopharmacology*. 2007 Apr; 27(2):221-4

L.K. Teune, J.H. vd Hoeven, N.M. Maurits, A.F. Bos, J.W.C. Alffenaar, D.J.Reijngoud, O.F. Brouwer and D.A. Sival. Pyridoxine induces non-specific EEG alterations in infants with therapy resistant seizures. *Seizure*. 2007 Jul;16(5):459-64

Koopman K, **Teune L.K.**, Ter Laan M, Uyttenboogaart M, Vroomen P.C, De Keyser J, Luijckx G.J. An often unrecognized cause of thunderclap headache: reversible cerebral vasoconstriction syndrome. *J Headache Pain*. 2008 Dec ;9(6):389-91.

Laura K. Teune, Anna L. Bartels, Bauke M. de Jong, Antoon T.M. Willemsen, Silvia A. Eshuis, Jeroen J. de Vries, Joost C.H. van Oostrom, and Klaus L. Leenders. Typical cerebral metabolic patterns in neurodegenerative brain diseases. *Mov Disord*. 2010 Oct 30;25(14):2395-404

Bok LA, Maurits NM, Willemsen MA, Jakobs C, **Teune LK**, Poll-The BT, de Coo IF, Toet C, Hagebeuk EE, Brouwer OF, Van der Hoeven JH, Sival DA. The EEG-response to pyridoxine-IV neither identifies nor excludes pyridoxine-dependent epilepsy. *Epilepsia*. 2010 Dec;51(12):2406-11

A.M. Meppelink, B.M. de Jong, **L.K. Teune**, T. van Laar. Regional cortical grey matter loss in Parkinson's Disease without dementia is independent from visual hallucinations. *Mov Disord*. 2011 Jan;26(1):142-7

J. Booi, **L.K. Teune** and H.J. Verberne. The role of molecular imaging in the differential diagnosis of parkinsonism. *Q J nucl med mol imaging* 2012 Feb;56(1):17-26 review

L.K. Teune, R.J. Renken, D. Mudali, B.M. de Jong, R.A. Dierckx, J.B.T.M. Roerdink and K.L. Leenders. Validation of Parkinsonian disease-related metabolic brain patterns. *Movement Disorders*, Epub ahead of print: 2013 Mar 11

L.K. Teune, F. Strijkert, R.J. Renken, G.J. Izaks, J.J. de Vries, M. Segbers, J.B.T.M. Roerdink, R.A. Dierckx and K.L. Leenders. The Alzheimer's disease-related glucose metabolic brain pattern. *submitted*

L.K. Teune, R.J. Renken, B.M. de Jong, A.T.M. Willemsen, M.J.P. van Osch, J.B.T.M. Roerdink, R.A. Dierckx and K.L. Leenders. Parkinson's disease-related perfusion and glucose metabolic brain patterns identified with PCASL-MRI and FDG-PET imaging. *submitted*

C.C. Tang, A. Feigin, Y. Ma, C. Habeck, J.S. Paulsen, K.L. Leenders, **L. K. Teune**, J.C.H. van Oostrom, M. Guttman, V. Dhawan and D. Eidelberg. Metabolic Network as a Progression Biomarker of Premanifest Huntington's Disease. *submitted*

Book contributions

L.K. Teune and K.L. Leenders. Molecular Imaging in Parkinson's Disease. *Neuromethods* (2012): Molecular Imaging in the Neurosciences. Chapter 18 Parkinson's Disease.

L.K. Teune, A.L. Bartels and K.L. Leenders. FDG-PET imaging in the differential diagnosis of neurodegenerative brain diseases. *submitted*

